# ENTANGLEMENT MANIPULATIONS AND APPLICATIONS

By

Sougato Bose

A thesis submitted to the University of London

for the degree of Doctor of Philosophy

The Blackett Laboratory

Imperial College

August 1999

BRITISH LIBRARY HSITIB

IMAGING SERVICES NORTH
Boston Spa, Wetherby
West Yorkshire, LS23 7BQ
www.bl.uk

# PAGINATED BLANK PAGES ARE SCANNED AS FOUND IN ORIGINAL THESIS

# NO INFORMATION IS MISSING

Except where acknowledged in the customary manner, the material presented in this thesis is, to the best of my knowledge, original and has not been submitted in whole or part for a degree in any university.

# Acknowledgements

I would like to thank Prof. P. L. Knight for his supervision, patience and encouragement during the entire length of my PhD research, and for providing helpful comments and suggestions on my thesis drafts. Working in the quantum optics group at Imperial College has been both challenging and enjoyable. I would like to specially thank three colleagues with whom I have collaborated extensively during my time here, namely, Vlatko Vedral, Martin Plenio and Kurt Jacobs. Working with them has been a great pleasure and a privilege. I would also like to thank other group members during my stay at Imperial, to whom I owe a lot of wisdom, namely, Daniel Jonathan, Emmanuel Paspalakis, Akshay Patel, Steve Parker, Shash Virmani, Dimitris Angelakis, Polykarpos Papadopoulos, Almut Beige, Susanna Huelga, Mio Murao, Jörg Steinbach, Marcos Protopapas and Vladimir Buzek. Suggestions of Dipankar Home and Miles Blencowe from outside the group were greatly appreciated.

There are many friends who have contributed to my time here in ways incalculable. In particular I would like to thank Anupam, David Chiew, Vivek, David and Daniel Phan, Wei Mun, Chirag, Manu, Janelle, Sud, Brendan and Gemma. Very special thanks go to my parents and sister for always being there.

I would also like to thank the Inlaks Foundation, which allowed me to study in England.

## List of Publications

In the following list, those on which this thesis is based are asterisked.

1. *S. Bose, P. L. Knight, M. B. Plenio and V. Vedral, *Teleportation of an atomic state via cavity decay*, LANL eprint: quant-ph/9908004 (submitted to Phys. Rev. Lett.).

2. S. Parker, S. Bose and M. B. Plenio, *Entanglement quantification and purification in continuous variable systems*, LANL eprint: quant-ph/9906098 (accepted in Phys. Rev. A).

3. *S. Bose, V. Vedral and P. L. Knight, *Purification via entanglement swapping and conserved entanglement*, Phys. Rev. A **60**, 194 (1999).

4. *S. Bose, M. B. Plenio and V. Vedral, *Mixed state dense coding and its relation to entanglement measures*, LANL eprint: quant-ph/9810025 (To appear in J. Mod. Optics, special issue on quantum information, 1999).

5. *S. Bose, K. Jacobs, and P. L. Knight, *A scheme to probe the decoherence of a macroscopic object*, Phys. Rev. A **59**, 3204 (1999).

6. S. Bose, P. L. Knight, M. Murao, M. B. Plenio and V. Vedral, *Implementations of quantum logic: fundamental and experimental limits*, Phil. Trans. R. Soc. Lond. A **356**, 1823 (1998).

7. *S. Bose, V. Vedral, and P. L. Knight, *Multiparticle generalization of entanglement swapping*, Phys. Rev. A **57**, 822 (1998).

8. *S. Bose, K. Jacobs, and P. L. Knight, *Preparation of nonclassical states in cavities with a moving mirror*, Phys. Rev. A **56**, 4175 (1997).

9. D. Home and S. Bose, *Standard quantum mechanics with environment induced decoherence and wavefunction collapse: Possibility of an empirical discrimination using neutron interferometry*, Phys. Lett. A **217**, 209 (1996).

# Abstract

In this thesis we describe some manipulations and applications of entanglement and a few physical implementations of these processes. First, we describe some applications of entanglement to state preparation in quantum optics. For this, we concentrate on a specific system of a cavity mode coupled to a macroscopic movable mirror. Next, we use the same system to propose an experiment to probe the decoherence of a macroscopic object. Our proposal is a quantum optical version of Schrödinger's cat thought experiment (entanglement between a microscopic and a macroscopic system). After this, we describe how to entangle many spatially separated particles by operations at a central exchange. This is done by generalizing the scheme of entanglement swapping to the multiparticle case. Next, we show how entanglement swapping can also be used for concentrating shared entanglement and how a measure of pure state entanglement remains conserved in this process. After this, we connect dense coding (an application of entanglement) to the apparently unrelated process of entanglement distillation. In this context, we obtain bounds on the capacity of dense coding with mixed states in terms of the entanglement of these states. Finally, we propose a physical implementation of teleportation that uses cavity decays. This is a rare example of a decay mechanism being made to play a constructive role in quantum information processing.

# Contents

**Acknowledgements** 3

**List of Publications** 4

**Abstract** 5

**1 Introduction** 11

1.1 The concept of entanglement . . . . . 11

1.2 A brief history of entanglement . . . . . 12

1.2.1 Entanglement and quantum nonlocality . . . . . 12

1.2.2 Entanglement in description of quantum measurement . . . . . 15

1.2.3 Entanglement as an invaluable practical resource . . . . . 17

1.3 Overview of the thesis . . . . . 18

**2 Entanglement between a microscopic and a macroscopic system I: applications in state preparation.** 21

2.1 Introduction . . . . . 21

2.2 A brief history of the model . . . . . 22

2.3 The system Hamiltonian and the time evolution operator . . . . . 23

2.4 The entanglement between the states of the cavity field and the movable mirror 26

2.5 Entangling cavity modes that do not interact directly . . . . . 28

2.6 Conditional state preparation of the cavity mode by measurements on the movable mirror . . . . . 33
2.7 Inducing unconventional decoherence of the cavity field . . . . . 37
2.8 Relevant parameter domains . . . . . 42
2.9 Conclusions . . . . . 43

**3 Entanglement between a microscopic and a macroscopic system II: applications in probing macroscopic decoherence** **45**
3.1 Introduction . . . . . 45
3.2 Schrödinger's method for creating macroscopic superpositions . . . . . 47
3.3 The system under consideration . . . . . 50
3.4 The proposed scheme . . . . . 50
3.5 A heuristic formula for the average decoherence rate . . . . . 54
3.6 Constraints on the parameters . . . . . 55
3.7 Experimental parameter regimes satisfying the constraints . . . . . 56
3.8 Parameter regime required to test gravitationally induced collapse theories . 60
3.9 Conclusions . . . . . 61

**4 Multiparticle entanglement swapping** **63**
4.1 Introduction . . . . . 63
4.2 The entanglement swapping scheme of Zukowski et al . . . . . 64
4.3 A multiparticle generalization of entanglement swapping . . . . . 66
4.4 Establishing multiparticle entanglement between particles located at different nodes of a communication network . . . . . 68
4.5 Communication schemes using distributed multiparticle entanglement . . . 71
4.5.1 Cryptographic conferencing . . . . . 71
4.5.2 A multiparticle generalization of superdense coding . . . . . 72
4.6 Entangled states of higher number of particles from entangled states of lower number of particles . . . . . 76
4.7 Comparison with the method of Zeilinger et al. . . . . 77

4.8 Conclusion . . . . . 80

**5 Entanglement concentration via entanglement swapping and conserved entanglement** **81**

5.1 Introduction . . . . . 81

5.2 The scheme of entanglement concentration via entanglement swapping . . . 82

5.3 A conserved measure of entanglement in concentration via swapping . . . . 85

5.4 The scheme viewed as a generalization of entanglement swapping . . . . . 87

5.5 Conclusions . . . . . 89

**6 Mixed state dense coding and entanglement measures** **91**

6.1 Introduction . . . . . 91

6.2 The Holevo function as a measure of C . . . . . 93

6.3 Capacity of SDC with pure letter states . . . . . 95

6.4 Nature of the ensemble used in SDC . . . . . 98

6.5 The relative entropy of entanglement as a lower bound on C . . . . . 99

6.6 Average distinguishability as an upper bound on C . . . . . 100

6.7 An upper bound on C in terms of the entanglement of formation . . . . . 101

6.8 An upper bound on C in terms of the relative entropy of entanglement . . . 104

6.9 SDC and purification . . . . . 110

6.10 Conclusion . . . . . 118

**7 Teleportation of an atomic state via cavity decay** **121**

7.1 Introduction . . . . . 121

7.2 The basic idea . . . . . 122

7.3 The scheme in detail . . . . . 123

7.4 Estimates of efficiency and success . . . . . 128

7.5 A reliable state transfer protocol . . . . . 131

7.6 Conclusions . . . . . 131

**8 Conclusions** **133**

A The time evolution operator for a cavity mode interacting with a movable mirror 135

B Solution to the master equation for the system when the mirror's motion is damped 137

Bibliography 140

# Chapter 1

# Introduction

## 1.1 The concept of entanglement

Consider two distant parties Alice and Bob. Each of them have an unlimited supply of particles. States of each of Alice's particles span the Hilbert space $H_A$, while the states of each of Bob's particles span the Hilbert space $H_B$. Alice's and Bob's particles are drawn from two completely independent sources and are not correlated in any way. Suppose Alice and Bob are now given the task of constructing states in their joint Hilbert space $H_A \otimes H_B$. While Alice and Bob are allowed to communicate classically with each other to any extent, neither of them are allowed to send a quantum state across to the other party. There are some quantum states in $H_A \otimes H_B$ which Alice and Bob, working according to the above constraints, will never be able to produce. These states are called *entangled* states. The property which makes these states differ from those which Alice and Bob *can* produce is called *entanglement*. Without sending a quantum state to the other party, Alice and Bob can only construct states of the type

$$\rho_{AB} = \sum_i P_i (|\psi_i\rangle\langle\psi_i|)_A \otimes (|\phi_i\rangle\langle\phi_i|)_B \tag{1.1}$$

where $|\psi_i\rangle_A$ and $|\phi_i\rangle_B$ are arbitrary members of $H_A$ and $H_B$ respectively and $P_i$ is a probability distribution (each $P_i \geq 0$ and $\sum_i P_i = 1$). Thus, any state $\rho_{AB}$ in $H_A \otimes H_B$

that cannot be written in the above way is an entangled state (or is said to posses entanglement). More than two systems $A, B, C, ..., N$ can also exist in an entangled state. They would be said to be entangled if their joint state cannot be written as $\rho_{ABC...N} = \sum_i P_i(|\psi_i\rangle\langle\psi_i|)_A \otimes (|\phi_i\rangle\langle\phi_i|)_B \otimes (|\chi_i\rangle\langle\chi_i|)_C \otimes ...(|\gamma_i\rangle\langle\gamma_i|)_N$.

The simplest example of an entangled state is a non-factorizable pure state of two quantum systems. This is any state of the form

$$|\Psi\rangle_{AB} = \sum_i c_i|\psi_i\rangle_A \otimes |\phi_i\rangle_B, \tag{1.2}$$

where more than one of the amplitudes $c_i$ are nonzero. The existence of states of this kind is probably the most striking difference between the quantum world and the classical world. These types of states have appeared again and again in the history of quantum mechanics, predominantly for three types of purposes: (1) in elucidating the non-local nature of quantum mechanics, (2) in discussions of the measurement process in quantum mechanics, and (3) as an invaluable practical resource. The last way of looking at entangled states is relatively recent (a nineties outlook) and inspires the study of the nature of entanglement and its manipulations on their own right. In what follows, we will describe a brief history of entanglement studies since the advent of quantum mechanics. Of course, it is rather a very small part of all that has been done to date on entanglement, and we apologise in advance for any omissions.

## 1.2 A brief history of entanglement

### 1.2.1 Entanglement and quantum nonlocality

The story of quantum nonlocality started in 1935 when Einstein, Podolsky and Rosen (EPR) presented a thought experiment to assert that the quantum mechanical description of physical reality was incomplete [1]. They defined an element of reality to be associated with an observable of a quantum system if the value of that observable could be predicted without disturbing the system in any way. They also assumed that measuring the state of a system at one spatial location does not affect the state of another system separated from it

by a large distance (the locality condition). Then they considered the entangled state (not normalized)

$$\begin{aligned} |\Psi\rangle_{AB} &= \int_{-\infty}^{+\infty} |p\rangle_A \otimes |-p\rangle_B \, dp \\ &= \int_{-\infty}^{+\infty} |x\rangle_A \otimes |x+x_0\rangle_B \, dx, \end{aligned} \tag{1.3}$$

of spatially separated systems $A$ and $B$, where $|p\rangle_A$ and $|-p\rangle_B$ are momentum kets and $|x\rangle_A$ and $|x+x_0\rangle_B$ are position kets. By measuring either the momentum or the position of system $A$ one can immediately deduce the momentum or the position of system $B$ accurately. The locality condition then implies that both the position and momentum of system $B$ have simultaneous elements of reality. On the other hand, if quantum description of reality was complete, then position and momentum could not have elements of reality corresponding to the same quantum state. EPR thus concluded that the quantum description of reality was incomplete. However, from what became clearer later on, the EPR example actually illustrates the nonlocal nature of quantum mechanics and the locality assumption of EPR fails. In 1952, David Bohm constructed a simpler analogue of the EPR example using a maximally entangled state

$$|\Psi\rangle_{AB} = |\uparrow\rangle_A|\downarrow\rangle_B - |\downarrow\rangle_A|\uparrow\rangle_B \tag{1.4}$$

of two spin half particles [2]. In 1964, John Bell used the above entangled state of two spin half particles for the first quantitative demonstration of quantum nonlocality [3]. He derived an inequality from the assumption that the outcome of a spin measurement on system $B$ should not depend on the alignment of an apparatus measuring the spin of system $A$. This is the locality condition. Now consider that we have the choice to measure the spin of particle $A$ along axes $\mathbf{a}$ and $\mathbf{a}'$ and the spin of particle $B$ along axes $\mathbf{b}$ and $\mathbf{b}'$. In general, if the locality condition wasn't required, then the outcomes of these possible measurements would depend on the apparatus setting on the other side. We label eight such distinct outcomes by $a(\mathbf{b}), a(\mathbf{b}'), a'(\mathbf{b}), a'(\mathbf{b}'), b(\mathbf{a}), b(\mathbf{a}'), b'(\mathbf{a})$ and $b'(\mathbf{a}')$. Each of these outcomes can have a value $\pm 1$. Now consider the expression

$$S = a(\mathbf{b})b(\mathbf{a}) + a(\mathbf{b}')b'(\mathbf{a}) + a'(\mathbf{b})b(\mathbf{a}') - a'(\mathbf{b}')b'(\mathbf{a}'). \tag{1.5}$$

This quantity can have values 0,$\pm 2$ and $\pm 4$. However, if we impose the locality condition, then $a(\mathbf{b}) = a(\mathbf{b}') = a, a'(\mathbf{b}) = a'(\mathbf{b}') = a', b(\mathbf{a}) = b(\mathbf{a}') = b$ and $b'(\mathbf{a}) = b'(\mathbf{a}') = b'$. Then we have

$$S = ab + ab' + a'b - a'b', \tag{1.6}$$

which can only take values $\pm 2$. Thus an average of $S$ over measurement on several pairs of particles obeys

$$-2 \leq \langle S \rangle \leq 2. \tag{1.7}$$

This is the Bell's inequality (more precisely, the CHSH version of the Bell's inequality [4]). If the spin measurement directions $\mathbf{a}$, $\mathbf{b}$, $\mathbf{a}'$ and $\mathbf{b}'$ are each separated from the adjacent ones by $\pi/8$, we have the expectation value of $S$ in the state $|\uparrow\rangle_A|\downarrow\rangle_B - |\downarrow\rangle_A|\uparrow\rangle_B$ to be $2\sqrt{2}$ which clearly violates the Bell's inequality Eq.(1.7). This demonstrates the nonlocal nature of quantum theory in a concrete way. More recently, Gisin [5] and Popescu and Rohrlich [6] have shown that every entangled pure state violated some Bell's inequality.

Bell's inequalities have been tested in various ways ( See for example, Ref.[7]), though there are still worries about loopholes in these experiments [8]. More recently, in 1989, Greenberger, Horne and Zeilinger (GHZ) gave an interesting demonstration of quantum nonlocality using the entangled state of four particles [9]. We will describe a simplified version of this (due to Mermin [10]) that uses the entangled state $|\uparrow\rangle_A|\uparrow\rangle_B|\uparrow\rangle_C - |\downarrow\rangle_A|\downarrow\rangle_B|\downarrow\rangle_C$ of three spin half particles $A$, $B$ and $C$. This state is an eigenstate of the operator $\sigma_x^A\sigma_x^B\sigma_x^C$ with an eigenvalue $-1$ and also an eigenstate of the operators $\sigma_x^A\sigma_y^B\sigma_y^C$, $\sigma_y^A\sigma_y^B\sigma_x^C$ and $\sigma_y^A\sigma_x^B\sigma_y^C$ with an eigenvalue $+1$. Locality demands that the outcome of a measurement of $\sigma_x^A$ (we label it by $m_x^A$), should not depend on the alignment of the apparatus measuring the spins of $B$ and $C$. Thus, we assign real values for spins in each direction to each of the particles. These real values are labelled by replacing the $\sigma$ of the operators by $m$. Thus we have $m_x^A m_y^B m_y^C = m_y^A m_x^B m_y^C = m_y^A m_y^B m_x^C = 1$. As the square of any of the real spin values is unity, we have

$$(m_x^A m_y^B m_y^C)(m_y^A m_x^B m_y^C)(m_y^A m_y^B m_x^C) = m_x^A m_x^B m_x^C = 1, \tag{1.8}$$

which contradicts $\sigma_x^A \sigma_x^B \sigma_x^C$ having an eigenvalue of $-1$. Similar types of contradictions of the locality condition can be shown for bi-partite entanglement as well (as shown by Hardy [11]). Next, we briefly describe the role which entangled states have played in description of the measurement process in quantum mechanics.

### 1.2.2 Entanglement in description of quantum measurement

In 1932, von Neumann used entangled states in description of the measurement process in quantum mechanics [12]. This was, probably one of the very first occasions (three years before EPR) in which the entangled nature of the state of two quantum systems was exploited. He described measurement as the following type of interaction of a macroscopic apparatus $M$ with a measured system $S$

$$(|1\rangle_S + |2\rangle_S)|\phi_0\rangle_M \rightarrow |1\rangle_S|\phi_1\rangle_M + |2\rangle_S|\phi_2\rangle_M, \tag{1.9}$$

where $|1\rangle_S$ and $|2\rangle_S$ are orthogonal states of the system $S$ and $|\phi_1\rangle_M$ and $|\phi_2\rangle_M$ are orthogonal states of the apparatus. von Neumann's approach of treating a macroscopic apparatus quantum mechanically, was a marked departure from the existing (Bohr) interpretation of that time in which a measurement apparatus was to be strictly regarded as a classical device. In a famous paper in 1935, Schrödinger exposed the apparent absurdity of a superposition such as that of Eq.(1.9) [13]. In his thought example $|1\rangle_S$ and $|2\rangle_S$ corresponded to the occurence and the nonoccurence of a radioactive decay and $|\phi_1\rangle_M$ and $|\phi_2\rangle_M$ corresponded to dead and alive states of a cat. He also introduced the term *entanglement* for the first time in this paper. To quote him in this context (while introducing the concept of entanglement), he said that *the best possible knowledge of a whole does not necessarily include the same of its parts.* What von Neumann's and Schödinger's work showed was that *the existence of entanglement leads to the a serious interpretational problem of quantum measurement.* The measured system and the measuring apparatus are in an entangled state after measurement in which the apparatus fails to be in a definite state. This contrasts what is seen in all quantum measurements. At the end of any quantum measurement an apparatus is always observed to be in a definite state. Even if the apparatus is observed by another apparatus,

which is observed by another apparatus and so on, we only end up with a many system entangled state in which the final apparatus is still in an indefinite state. As a desperate remedy to breaking the chain of more and more apparatus getting entangled with the system (known as the von Neumann chain), Wigner (1961) suggested that the final apparatus, namely the human consciousness, does not get entangled, but causes the entire chain of apparatus to *collapse* to a definite state [14].

So far, entanglement has sounded like the creator of the major foundational problem of quantum mechanics. Strangely, it has also been viewed by some as the solution to all foundational problems of quantum mechanics. In 1957, Everett proposed his relative state formulation of quantum mechanics [15]. According to this interpretation, the system-observer entangled state $|1\rangle_S|\phi_1\rangle_O + |2\rangle_S|\phi_2\rangle_O$ (where $|\phi_1\rangle_O$ and $|\phi_2\rangle_O$ are states of the observer) has a special physical meaning. It means that observer's consciousness is split into two components: the component $|\phi_1\rangle_O$ perceiving the system to be in the definite state $|1\rangle_S$ and the component $|\phi_2\rangle_O$ perceiving the system to be in the specific state $|2\rangle_S$. This was his way of explaining the perception of a single outcome in a quantum measurement. More recently, entanglement has been used to explain the instability of superpositions of distinct states of a macroscopic object. Consider a macroscopic system $A$ (which may be an apparatus), to be in the state $c_1|\psi_1\rangle_A + c_2|\psi_2\rangle_A$. As it interacts strongly with its environment, it gets rapidly entangled with it. The system-environment state is then of the form $c_1|\psi_1\rangle_A|\zeta_1(t)\rangle_E + c_2|\psi_2\rangle_A|\zeta_2(t)\rangle_E$, where $|\zeta_1(t)\rangle_E$ and $|\zeta_2(t)\rangle_E$ are states of the environment whose overlap decreases with time. This causes the coherence between the components $|\psi_1\rangle_A$ and $|\psi_2\rangle_A$ of system $A$ to decrease with time provided one traces out the unobserved environmental states. Thus for a macroscopic system (one that would strongly interact with its environment), superpositions of distinct states are unstable. This general theme is known as the environment induced decoherence programme (See for example, Ref.[16]).

### 1.2.3 Entanglement as an invaluable practical resource

In 1991, Ekert showed that entanglement could be used for generating a secret random key between distant parties. The non-local correlations of quantum theory are used to generate the secret random key. An eavesdropper's presence could be recognized by the destruction of the non-local correlations as can be revealed by testing Bell's inequalities. In the following year Bennett and Wiesner showed how prior shared entanglement could double the classical capacity of a quantum channel, a scheme called superdense coding [18]. To top it all, in 1993, Bennett and co-workers showed that shared entanglement could be used for teleportation of a quantum state to a distant location [19]. This is very interesting because you cannot simply copy a quantum state (due to the quantum the no-cloning theorem [20]) and send that copy to a remote location. It is also worthwhile to mention that many regard the power of quantum computation [21] (which can accomplish some tasks much faster than known classical methods of computation) to be stemming from entanglement [22].

These amazing practical applications of entanglement have triggered off extensive fundamental research into the nature of entanglement and its manipulations. Firstly, people have realized that the type of entanglement shared between distant users will not, in general, be pure and maximal to start with. It will, in fact, be a mixed entangled state. This happens due to noise in the channels used for the distribution of entanglement between distant parties. However, as was first shown by Werner in 1989, for mixed entangled states, Bell's inequalities need not be violated [23]. Yet, as Popescu pointed out in 1994, such states could still be used for teleportation (which is another aspect of nonlocality distinct from Bell's inequalities) [24]. Popescu's work steered research into finding out the conditions under which a mixed entangled state violated Bell's inequality or permitted teleportation [25]. But more importantly, it made people think about locating the fundamental signature of entanglement (which would then be more fundamental than the violation of Bell's inequality). Would it be the ability to teleport or to accomplish some other task? Peres and the Horodecki family discovered that a mixed state of a $2 \times 2$ and $2 \times 3$ systems is entangled if and only if its partial transpose is not a positive operator [26]. This was a mathematical

signature of the existence of entanglement. A physical signature was also found out soon afterwards. Already in 1995, Popescu had shown that a mixed entangled state that did not violate Bell's inequalities, could be converted to one that did, simply by local actions on either part of the entangled state [27]. This eventually led to the process of entanglement distillation by local actions and classical communication [28, 29, 30]. In this process, local actions on a large number of shared pair of particles in a less entangled state are used to produce a smaller number of more entangled shared pairs. Practically, this process has the greatest significance, because it allows the sharing of pure maximal entanglement despite of the noisy channels used for sharing it. This pure maximal entanglement can then be used for the optimal implementation of the applications described in the last paragraph. But even from a fundamental point of view, this process of entanglement distillation has inspired work in *quantifying* the amount of entanglement in a given mixed state [30, 31, 32, 33].

## 1.3 Overview of the thesis

In this thesis, we shall be primarily concerned with the practical applications of entanglement, and manipulations which assist in the implementation of these applications. For example, in chapter 7 we shall present a scheme to physically implement the teleportation of an atomic state over large distances. Strangely, that scheme utilizes cavity decays (normally regarded harmful to entanglement applications) in a profitable way. In chapter 4, we present a scheme of multiparticle entanglement manipulation which would find practical application in the distribution of entanglement (multipartite) in a many user network. In the chapter following that (chapter 5) we show that a similar type of procedure can be used for a simple demonstration of entanglement distillation by local actions for polarization entangled photons. The theme of chapter 6 is to try to link an application of entanglement (superdense coding) with the apparently disconnected notion of entanglement distillation. This can be regarded as the very starting step towards a unification of all entanglement applications by relating their efficiency to the amount of entanglement being used. Chapters 2 and 3 are a little different in spirit from the rest of the thesis in that they are neither applications

nor manipulations of *distributed* entanglement. But nonetheless, chapter 2 describes applications of entanglement in various types of state preparation in quantum optics. These are *genuine* applications of entanglement in the sense that they would not have been possible *without* the presence of entanglement. In chapter 3, we go back to the original context in which Schrödinger introduced the term entanglement for the first time, namely to describe the entanglement of a microscopic and a macroscopic object. In this chapter, we propose a scheme to use the entangled state of a cavity field and a macroscopic movable mirror to test the rate at which the macroscopic mirror becomes entangled with its environment. The flavour of that chapter, is then, more like that of section 1.2.2 in which the role played by entanglement in quantum measurement was described.

# Chapter 2

# Entanglement between a microscopic and a macroscopic system I: applications in state preparation.

## 2.1 Introduction

In this chapter, we will study a specific quantum optical system to highlight some applications of entanglement in state preparation. The system to be considered is a cavity with one fixed and one movable mirror, the movable mirror being regarded as a harmonic oscillator (see Fig. 2.1). If there is an electromagnetic field mode inside the cavity, it will exert a pressure on the movable mirror. The effect of this pressure can be written in terms of an interaction Hamiltonian between the cavity field mode and the movable mirror, *when both are treated quantum mechanically.* This interaction can entangle the state of the cavity field (a microscopic system) with the state of the movable mirror (a macroscopic system). In this chapter, we show how this entanglement can be utilised for:

(a) Entangling the states of two cavity modes that do not interact directly,

(b) Conditional state preparation of the cavity mode by measurements on the movable mirror,

(c) Inducing decoherence of a rather unconventional form (as we shall see) of the cavity field.

We will also justify why none of these applications would be possible *without* the entanglement between the cavity field and the movable mirror. These would thus *genuinely* be *applications of entanglement.* Our general approach would be to regard the system as a toy model which illustrates the applications of entanglement to issues related to state preparation. But in section 2.8 we will also describe some potentially achievable experimental regimes in which these applications can be implemented.

## 2.2 A brief history of the model

We will briefly digress in this section to describe why the model of a quantum cavity field interacting with a quantum movable mirror arose. The necessity to treat a macroscopic harmonic oscillator in a quantum mechanical fashion was first realized in efforts to detect gravitational waves. To detect gravitational waves, one may require to observe position displacements of a macroscopic oscillator with a precision smaller than the spread of its ground state wavefunction. For measurements of such precision, the oscillator's state gets significantly affected by the measurement and this can be a source of noise in a subsequent measurement. This was realized by Braginsky and coworkers in the 1970's [34]. In 1979, Hollenhorst [35] showed that placing gravitational wave detectors (which were macroscopic oscillators) in squeezed states led to better sensitivity. In 1980, Caves and coworkers also needed to treat macroscopic oscillators quantum mechanically to formulate back action evading measurement schemes for massive gravitational wave sensors [36]. Around the

same time, laser interferometric detectors for gravitational waves were becoming popular [37]. Treating only the optical field in these interferometers quantum mechanically, a lot of estimates on the ultimate sensitivity of such detectors were carried out [38]. However, in all analysis till 1993 (to our knowledge), either only the optical field in the interferometers or only the macroscopic oscillator were being treated quantum mechanically. In other words, no interaction Hamiltonian of an optical field with a movable mirror was known. In 1993, to make a self consistent Hamiltonian model for an entire laser interferometric gravitational wave detector, Pace *et al.* introduced such an interaction Hamiltonian for the first time [39]. This is how the model to be considered in this section arose in the first place. Subsequently, it was also considered for setting limits to atomic force microscopy [40] and for quantum nondemolition measurements of photon number in a cavity[41].

But in recent years, it has evolved a long way from the initial motivation to an interesting system for cavity quantum electrodynamics (CQED) *with an empty cavity.* In CQED, one generally makes nonlinear crystals or single atoms interact with a single mode of a cavity field in a controlled way and can prepare arbitrary quantum states of the atom, the cavity field and even entangled states of the atom and the cavity field. It has gradually become clear that a movable mirror can mimic a nonlinear crystal from the facts that it can produce squeezing of the cavity field [42, 43], and prepare the cavity field in a Schrödinger cat state [44]. In this chapter, we take a step further and try to treat the movable mirror as a replacement of the atom in the cavity. In a manner analogous to entangled states of an atom and a cavity field, we will consider entangled states of the movable mirror and the cavity field. We will then show the applications of this entanglement in preparation of states of the cavity field.

## 2.3 The system Hamiltonian and the time evolution operator

We will only consider the case when the mirror moves *adiabatically.* In other words, the mirror moves so slowly that photons of a given frequency do not get Doppler shifted to another frequency on scattering off the moving mirror. Mathematically this is equivalent

to demanding that the mirror displacement $x$ due to the cavity radiation pressure is much smaller than the length $L$ of the cavity. Under such circumstances, a single mode of the electromagnetic field inside the cavity couples *only* to the movable mirror and not with any other cavity mode. We now follow the treatment of Pace *et. al.* [39] to derive a Hamiltonian for this coupling from phenomenological considerations.

Let $\omega_0$ be the frequency of the single cavity mode under consideration. As this is chosen to be resonant inside the cavity, we have

$$\omega_0 = (n + \frac{1}{2})\frac{2\pi c}{L}, \tag{2.1}$$

where $c$ is the speed of light. The Hamiltonian for this mode is thus

$$H = \hbar(n + \frac{1}{2})\frac{2\pi c}{L}\, a^\dagger a, \tag{2.2}$$

where $a$ and $a^\dagger$ are annihilation and creation operators of the mode. Now, if the mirror slowly moves so that the cavity length increases from $L$ to $L+x$, the fundamental frequency of the cavity decreases to $2\pi c/(L+x)$ and the Hamiltonian for the mode under consideration changes to

$$\begin{aligned} H &= \hbar(n + \frac{1}{2})\frac{2\pi c}{L + x}\, a^\dagger a \\ &\approx \hbar\frac{2\pi c}{L}\, a^\dagger a(1 - \frac{x}{L}) \\ &= \hbar\omega_0\, a^\dagger a - \hbar\frac{\omega_0}{L}\, a^\dagger a x. \end{aligned} \tag{2.3}$$

The decrease in energy of the mode under consideration is thus $(\hbar\omega_0 x/L)\, a^\dagger a$, which is also the increase in the energy of the movable mirror (assuming the cavity and the moving mirror to be a closed system). We now quantize the mirror's position $x$ as $\sqrt{\hbar/2m\omega_m}(b+b^\dagger)$ (where $m$ and $\omega_m$ are the mass and the frequency of the movable mirror respectively) in the last term of Eq.(2.3) and get the following interaction Hamiltonian of the cavity mode and the movable mirror

$$H_{\text{int}} = -\hbar\frac{\omega_0}{L}\sqrt{\frac{\hbar}{2m\omega_m}}a^\dagger a(b + b^\dagger). \tag{2.4}$$

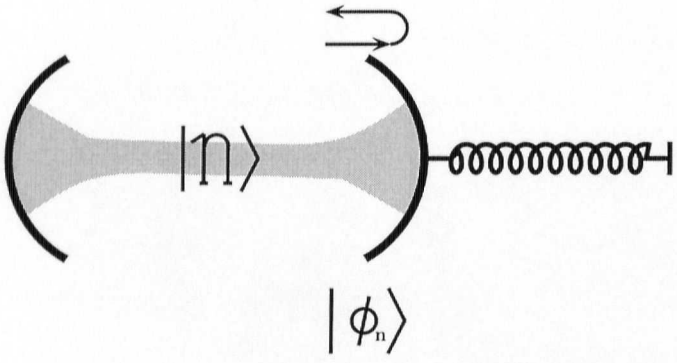



Figure 2.1: The quantum optical system under consideration: a cavity field interacting with a movable mirror. The figure shows the case when the cavity field is in a Fock state $|n\rangle$ and the movable mirror is in a coherent state $|\Phi_n\rangle$.

A more rigorous derivation, starting from first principles, of the general coupling between a cavity mode and a movable mirror has been performed by Law [45]. His expression reduces to the above coupling in the limit of adiabatic motion of the mirror. The full Hamiltonian of the cavity mode and movable mirror system is thus

$$H = \hbar\omega_0\, a^\dagger a \;+\; \hbar\omega_m\, b^\dagger b \;-\; \hbar g\, a^\dagger a(b + b^\dagger) \tag{2.5}$$

where

$$g \;=\; \frac{\omega_0}{L}\sqrt{\frac{\hbar}{2m\omega_m}}\,. \tag{2.6}$$

Here, we shall concentrate on the entanglement between the states of the cavity field and the movable mirror arising from this model and on the physical applications of this entanglement. The time evolution operator corresponding to the above Hamiltonian was evaluated by Mancini *et al.* [44] (for completeness we give a proof in Appendix A) and is given by

$$U(t) = \exp\left[-ira^\dagger a\ t\right] \exp\left[ik^2(a^\dagger a)^2(t-\sin t)\right] \exp\left[ka^\dagger a(\eta b^\dagger - \eta^* b)\right] \exp\left[-ib^\dagger bt\right] \ , \quad (2.7)$$

where $\eta = (1 - e^{-it})$, $k = g/\omega_m$ is the scaled coupling parameter, $r = \omega_0/\omega_m$, and $t$ represents a scaled time, being the actual time multiplied by $\omega_m$. We see from the above equation that there is now an explicit Kerr-like term in $U(t)$, so that physically one might expect the cavity field to have an evolution similar to that in a Kerr like nonlinearity in optics. Much quantum [42, 43, 44] and classical [46, 47] work on the system illustrates this similarity. A part of the work to be presented in this chapter (entangling cavity modes which do not interact directly) also depends crucially on the Kerr-like term in Eq.(2.7).

## 2.4 The entanglement between the states of the cavity field and the movable mirror

Let us, for simplicity, assume that initially both the mirror and the cavity field are in coherent states. We will later move over to the more realistic situation in which the macroscopic mirror is taken to be in a thermal state. Thus we write the initial state at time $t = 0$ as

$$|\Psi(0)\rangle = |\alpha\rangle_c \otimes |\beta\rangle_m \quad (2.8)$$

where $|\alpha\rangle_c$ and $|\beta\rangle_m$ are initial coherent states of the field and the mirror respectively. The time evolution of the system in the interaction picture (that is, omitting the free evolution of the field) leads to a state at time $t$ given by

$$|\Psi(t)\rangle \ = \ e^{\frac{-|\alpha|^2}{2}} \sum_{n=0}^{\infty} \frac{\alpha^n}{\sqrt{n!}} e^{ik^2n^2(t-\sin t)} |n\rangle_c \otimes |\phi_n(t)\rangle_m \quad (2.9)$$

where $|n\rangle_c$ denotes a Fock state of the cavity field with eigenvalue $n$, and the $|\phi_n(t)\rangle_m$ are coherent states of the mirror given by

$$|\phi_n(t)\rangle_m = |\ \beta e^{-it} + kn(1 - e^{-it})\ \rangle_m \ . \quad (2.10)$$

During the evolution, the mirror is transformed to a specific coherent state $|\phi_n(t)\rangle_m$, each one corresponding to a specific number state $|n\rangle_c$ of the cavity field. This is shown in

Fig.2.1. From the above equations, it is clear that after a time $t = 2\pi$ the mirror returns to its original state. At all times between $t = 0$ and $t = 2\pi$ the mirror state is *entangled* with the field state in a pure state. To give a quantitative estimate of this entanglement, we evaluate the purity, or the *linear entropy* [48] which is given by $(1 - Tr(\rho_{\rm M}(t)^2))$ [48] of the reduced density matrix $\rho_{\rm M}(t)$ of the mirror. In terms of this linear entropy $S$, the entanglement between the cavity field and the moving mirror as a function of time is given by

$$S(|\Psi(t)\rangle) = 1 - e^{-2|\alpha|^2} \sum_{n,m=0}^{\infty} \frac{|\alpha|^{2(n+m)}}{n!m!} e^{-k^2(n-m)^2(1-e^{-it})^2}. \tag{2.11}$$

This entanglement has been plotted in Fig.2.2 as a function of the scaled time $t$ for three different values of the scaled coupling parameter $k$. As expected, the entanglement between the mirror and the cavity field increases with the increase of the coupling. The range of values used for the coupling constant $k$ is of the order of unity. This can, for example be attained in optical cavity QED with parameters $\omega_0 \sim 10^{16}$ s$^{-1}, \omega_m \sim 1$ KHz, $L \sim 1$ m, $m \sim 10$ mg [44, 46, 47].

In the real case, the macroscopic mirror will start in a thermal state, rather than a coherent state. But even in that case, we would expect some degree of entanglement to be generated between the states of the cavity mode and the movable mirror when they interact. In section 2.5 we will give a sufficiently good reason for believing that this is true. An initial state being a thermal state is, however, not the only characteristic of a macroscopic object such as the mirror. The decoherence of spatially separated states of a macroscopic object is quite large in general. This decoherence, and also the decoherence due to cavity decay, would tend to diminish the entanglement between the cavity mode and the moving mirror with time. Thus we require a parameter domain in which both the above decoherence timescales are lower than the oscillation time period of the movable mirror. Then, at least during the first oscillation, the state of the cavity mode and the moving mirror can be expected to be entangled to a certain degree. We will discuss such a parameter regime in section 2.8.

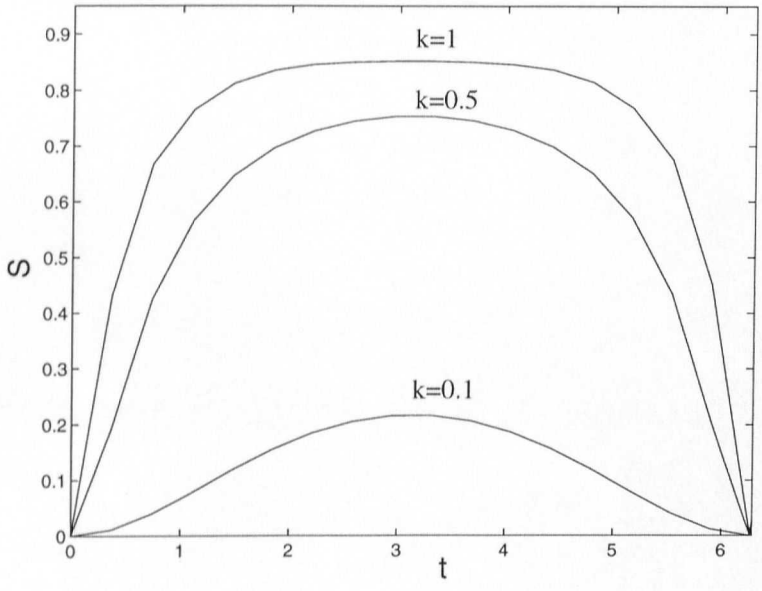



Figure 2.2: The linear entropy, $S$, of the mirror state, in the absence of any damping, is plotted here as a function of time, and for various values of the scaled coupling parameter $k$. We have taken the initial coherent state amplitude of the cavity mode to be $\alpha = 2$, and that of the mirror to be $\beta = 2$. The entanglement of the mirror with cavity field increases from a value of zero to a maximum at $t = \pi$ and subsequently falls back to zero at $t = 2\pi$. Both the scaled time $t$ and the linear entropy $S$ are dimensionless quantities.

## 2.5 Entangling cavity modes that do not interact directly

Two modes of light, each separately interacting with the movable mirror, and with no direct coupling between them, can end up being in an entangled state at time $t = 2\pi$ depending on the value of the parameter $k$. Let there be two different modes of light inside the cavity at $t = 0$. For simplicity we assume them to have the same frequency and hence the same value of the parameter $k$, but with mutually orthogonal polarization directions. We assume them to be initially fully disentangled and prepared in coherent states. Let the initial state

of the composite system of the mirror and the light be

$$|\Psi(0)\rangle = |\alpha_1\rangle_{c1} \otimes |\alpha_2\rangle_{c2} \otimes |\beta\rangle_m \tag{2.12}$$

where $|\alpha_1\rangle_{c1}$ and $|\alpha_2\rangle_{c2}$ are states of the first and second modes respectively, while $|\beta\rangle_m$ is the initial state of the mirror. The state of the two light modes evolves at $t = 2\pi$ to the state (not normalized)

$$|\zeta_E\rangle = e^{-(|\alpha_1|^2+|\alpha_2|^2)/2} \sum_{n,m=0}^{\infty} \frac{\alpha_1^n \alpha_2^m e^{i2\pi k^2(n+m)^2}}{\sqrt{n!}\sqrt{m!}} |n\rangle_{c1} \otimes |m\rangle_{c2}. \tag{2.13}$$

This state is completely disentangled from the mirror's state. The state can be rewritten as

$$|\zeta_E\rangle = e^{-|\alpha_2|^2/2} \sum_{m=0}^{\infty} \frac{\alpha_2^m}{\sqrt{m!}} e^{ik^2 m^2 2\pi} |m\rangle_{c1} \otimes |\xi(m,k)\rangle_{c2} \tag{2.14}$$

where

$$|\xi(m,k)\rangle_{c2} = e^{-|\alpha_1|^2/2} \sum_{n=0}^{\infty} \frac{(\alpha_1 e^{ik^2 4\pi m})^n}{\sqrt{n!}} e^{i2\pi k^2 n^2} |n\rangle_{c2}. \tag{2.15}$$

For the above states we have $\langle \xi(m',k)|\xi(m,k)\rangle_{c2} = e^{\{|\alpha_1|^2(e^{i4\pi k^2(m-m')}-1)\}}$. Thus the state $|\zeta_E\rangle$ is nonfactorizable (an entangled state) for all values of $k^2$ which are not an integer multiple of 0.5. Mathematically, this entanglement originates from the Kerr-like term $e^{i2\pi k^2(n+m)^2}$ in Eq.(2.13) which cannot be factorized into separate functions on $n$ and $m$. The entanglement of the two cavity modes can be expressed in terms of the linear entropy $S_{c1} = (1 - Tr(\rho_{c1}^2))$, where $\rho_{c1}$ is the reduced density matrix of the first cavity mode. This is given by

$$S_{c1}(|\zeta_E\rangle) = 1 - e^{-2(|\alpha_1|^2+|\alpha_2|^2)} \sum_{n,m=0}^{\infty} \frac{|\alpha_2|^{2(n+m)}}{n!m!} |e^{|\alpha_1|^2 e^{i4\pi k^2(m-n)}}|^2. \tag{2.16}$$

In Fig.2.3, we have plotted this entanglement as a function of $k^2$. It is seen that it dips to zero for $k^2$ being integer multiples 0.5 and on average the entanglement increases with increasing amplitudes of the initial coherent states of the two modes inside the cavity. The small oscillations superimposed on this average increase of entanglement also increases with increase of the coherent state amplitudes because the inner product $\langle \xi(m',k)|\xi(m,k)\rangle_{c2}$ oscillates more rapidly for a higher value of $\alpha_1$.

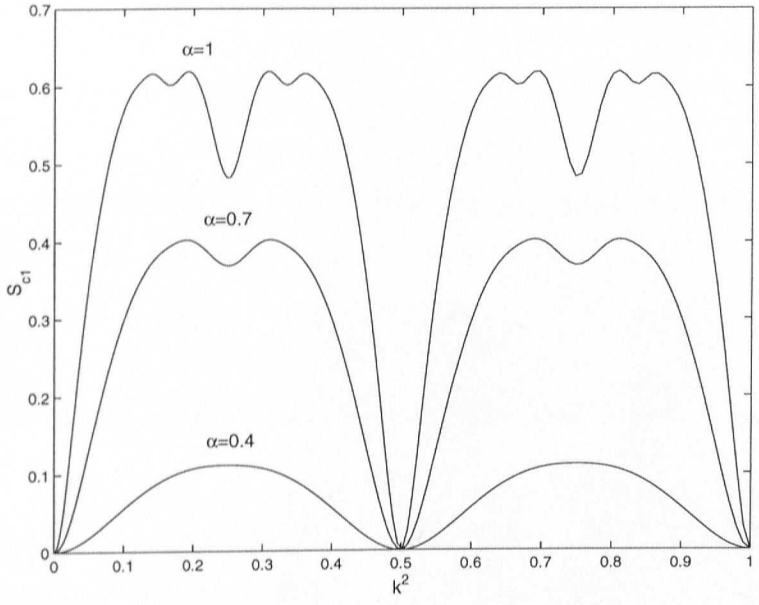



Figure 2.3: The linear entropy, $S_{c1}$, of the state of one of the cavity modes is plotted here as a function of the square of the scaled coupling parameter $k$ for various values of the initial coherent state amplitudes $\alpha_1 = \alpha_2 = \alpha$. Both the scaled coupling $k$ and the linear entropy $S_{c1}$ are dimensionless quantities.

Some simplification of Eq.(14) for k=0.5 results in the entangled state

$$\begin{aligned} |\zeta_E\rangle &= (1+i)|+\alpha_1\rangle_{c1} \otimes |+\alpha_2\rangle_{c2} \\ &+ (1-i)|-\alpha_1\rangle_{c1} \otimes |-\alpha_2\rangle_{c2}. \end{aligned} \tag{2.17}$$

This is an example of a two mode Schrödinger cat state. Note that production of similar entangled states in a Kerr medium, when the two modes of light have a direct interaction between them have been discussed before [49]; however this case is different in the sense that the modes become entangled because they both individually interact with the same movable mirror.

There is no restriction on the number of modes that can be entangled using the above procedure (except that each mode to be entangled has to be resonant with the cavity). It is interesting to demonstrate how eigenstates of the operator $(a_{c1}a_{c2}...a_{cN})^p$ where $a_{c1}, a_{c2}, ..., a_{cN}$

are annihilation operators of $N$ different modes of light and $p$ is an integer can be created in the cavity. As it is possible for resonant modes to have frequencies that are integer multiples of each other, let us consider the case when there are $N$ different modes of light in the cavity, with their frequencies $\omega_{c1}, \omega_{c2}, ...., \omega_{cN}$ being related by $\omega_{cj} = \eta_j \ \omega_{c1}$ where $\eta_j$ are integers. Then from Eq.(2.6) it follows that the value of their $k$ parameters will be related by $k_j = \eta_j \ k_1$. Hence if the initial state of the cavity modes and the mirror is

$$|\Psi(0)\rangle = |\alpha_1\rangle_{c1} \otimes |\alpha_2\rangle_{c2} \otimes .... \otimes |\alpha_1\rangle_{cN} \otimes |\beta\rangle_m \ , \tag{2.18}$$

the final (at time $t = 2\pi$ ) composite state of the cavity modes will be

$$|\zeta_{E_N}\rangle = \sum_{n_1,n_2,...,n_N=0}^{\infty} e^{i2\pi {k_1}^2(\eta_1 \ n_1+\eta_2 \ n_2+...+\eta_N \ n_N)^2} \ \prod_{j=0}^{N} \frac{{\alpha_j}^{n_j}}{\sqrt{n_j!}} \ |n_j\rangle_{cj}. \tag{2.19}$$

As the term $e^{i2\pi {k_1}^2(\eta_1 \ n_1+\eta_2 \ n_2+...+\eta_N \ n_N)^2}$ cannot be split up into a product of the form $f_1(n_1)f_2(n_2)...f_N(n_N)$, for arbitrary values of $k_1$, $|\zeta_{E_N}\rangle$ can, in general, be an entangled state depending on the value of $k_1$. Now consider the case when $2\pi {k_1}^2 = \pi/p$. We have

$$(a_{c1}a_{c2}...a_{cN})^p|\zeta_{E_N}\rangle = \sum_{n_1,n_2,...,n_N=p}^{\infty} e^{i2\pi {k_1}^2(\eta_1 \ n_1+\eta_2 \ n_2+...+\eta_N \ n_N)^2} \ \prod_{j=0}^{N} \frac{{\alpha_j}^{n_j}}{\sqrt{n_j - p!}} \ |n_j - p\rangle_{cj} \ . \tag{2.20}$$

Redefining $n_j$ in the above equation as $n_j + p$ , recasting the equation in terms of the new $n_j$ and using the fact that $\eta_j$ are integers, one gets

$$(a_{c1}a_{c2}...a_{cN})^p|\zeta_{E_N}\rangle = (\alpha_1\alpha_2...\alpha_N)^p e^{i\pi p(\eta_1+\eta_2+...+\eta_N)^2} \ |\zeta_{E_N}\rangle \ . \tag{2.21}$$

Hence $|\zeta_{E_N}\rangle$ are eigenstates of the operator $(a_{c1}a_{c2}...a_{cN})^p$, generalizations of the well known even and odd coherent states which are eigenstates of squares of annihilation operators [50].

Note that the entangled state $|\zeta_E\rangle$ given by Eq.(2.14) is *independent* of the amplitude $\beta$ of the initial coherent state of the mirror. Thus in the realistic case, when the macroscopic mirror starts in a ~~coherent~~ thermal state, this state preparation will not be affected in any way. This is because a thermal state may be expressed as a mixture of different coherent states. At time $t = 2\pi$, when our state preparation is complete, the mirror returns to its original thermal state and its state is completely disentangled from that of the cavity modes.

It is evident that entangling a couple of cavity modes would not have been possible unless each of the cavity modes, when interacting alone with the mirror, became entangled with it. To understand this, we split the continuous interaction of the two light modes with the movable mirror into alternate infinitesimal interaction of the mirror with each mode. Now consider (hypothetically), the two cavity modes $C_1$ and $C_2$ to be spatially separated systems, and the movable mirror $M$ being brought into contact with each of these modes alternately for infinitesimally short intervals of time. If $M$ did not become entangled with either $C_1$ or $C_2$ in any of the instants of interaction, then no entanglement can be established between the spatially separated systems $C_1$ and $C_2$. Otherwise we would end up creating entanglement by local means. Thus entangling cavity modes which do not interact directly, is an application of the entanglement between the movable mirror and each cavity mode. As we have justified in the last paragraph, we can end up with an entangled state of modes $C_1$ and $C_2$ at time $t = 2\pi$ even if the macroscopic mirror started off in a thermal state. This seems to be a pretty good reason for believing that even when the mirror starts in a thermal state, and interacts with any one of the modes, its state gets entangled to a certain degree with the state of that mode.

We now describe how the indirect interaction between two light modes due to their interaction with the mirror can be used to implement quantum logic between the two modes. Consider the case when $k = 0.5$. Then due to one oscillation of the mirror (i.e an interaction of the mirror with the two light modes for a time equal to $t = 2\pi$), initial states $|0\rangle_{c1} \otimes (|0\rangle_{c2} + |1\rangle_{c2})$ and $|1\rangle_{c1} \otimes (|0\rangle_{c2} + |1\rangle_{c2})$ of the cavity modes transform in the following way

$$|0\rangle_{c1} \otimes (|0\rangle_{c2} + |1\rangle_{c2}) \rightarrow |0\rangle_{c1} \otimes (|0\rangle_{c2} - i|1\rangle_{c2}) \tag{2.22}$$

$$|1\rangle_{c1} \otimes (|0\rangle_{c2} + |1\rangle_{c2}) \rightarrow |1\rangle_{c1} \otimes (-i)(|0\rangle_{c2} + i|1\rangle_{c2}). \tag{2.23}$$

The transformation in the above Eqs.(2.22)-(2.23) is an example of conditional quantum logic because the state of the second mode evolves to mutually orthogonal states corresponding to different initial states of the first mode. This will work perfectly even when the macroscopic mirror starts off in a thermal state. However, the decoherence rate of the

macroscopic mirror during it's motion and the decoherence of the cavity fields due to their decay, will have to be kept lower than the oscillation frequency of the mirror. In section 2.8 we will present a potentially achievable parameter domain in which the above controlled logic works. Implementing that would be a curious example of *quantum logic mediated by a "hot" and "macroscopic" object.*

## 2.6 Conditional state preparation of the cavity mode by measurements on the movable mirror

Because of the entanglement of the mirror state with the state of the cavity field during evolution, any measurement on the mirror will project the cavity field to some state which we can determine. We consider here measurements of the mirror's scaled position, $x = b+b^\dagger$ (i.e, scaled position $x$ represents actual position of the mirror multiplied by $(\sqrt{2m\omega_m/\hbar})$, $m$ being the mass of the mirror), at time $t = \pi$, as the entanglement is most pronounced at that time. Such a measurement will project the state of the light to

$$|\eta(x)\rangle_c = N \sum_{n=0}^{\infty} \frac{\alpha^n}{\sqrt{n!}} e^{i\pi k^2 n^2} \langle x|\phi_n(\pi)\rangle |n\rangle_c. \tag{2.24}$$

Thus for different values of the mirror position $x$, different states of the cavity field are produced. Let us choose parameters $k = 1, \alpha = 2$ and $\beta = 2$. Then the peak of the gaussian function $\langle x|\phi_n(\pi)\rangle$ lies at $x_n = 4n - 4$ and its width is $\delta = 1$. Thus the distance between the peaks of $\langle x|\phi_n(\pi)\rangle$ and $\langle x|\phi_{n+1}(\pi)\rangle$, that is, $x_n - x_{n+1} = 4$ , is greater than the width $\delta$. Hence, if the value obtained for $x$ obtained as a result of the measurement is near $x_n$, the most dominant constituent of the state $|\eta(x)\rangle_c$ is $|n\rangle_c$. In this way, we may expect to produce nonclassical states which are very close to number states. For example, if the value obtained for $x$ is near 0 (which is near $x_1$) the cavity field is projected to the state (unnormalized)

$$|\eta(0)\rangle \approx e^{-4}|0\rangle_c - 2|1\rangle_c + 2\sqrt{2}e^{-4}|2\rangle_c + O(10^{-7}) \tag{2.25}$$

which is shown in Fig.2.4(a). Similar methods of Fock state generation (in context of atom-cavity systems) have been discussed by other authors (see for example, Ref.[51]). When

$x$ lies between $x_n$ and $x_{n+1}$ we get essentially a superposition of states $|n\rangle$ and $|n+1\rangle$ as illustrated in Fig.2.4(c) for $n = 2$. Fock state superpositions and their nonclassical properties have been discussed in [52].

It is evident from the above discussion that the generation of the above type of states solely rely on the narrowness of the coherent state width in comparison to the spatial separation between the peaks of the gaussians $\langle x|\phi_n(\pi)\rangle$ and $\langle x|\phi_{n+1}(\pi)\rangle$. As this spatial separation can always be increased by increasing the value of the parameter $k$, the proximity of the states produced to Fock states and their superpositions can always be improved.

In practice, we will not be able to do exact position measurements on the movable mirror, but be able to accomplish only a smeared measurement of position. Such a measurement is a positive operator valued measurement (POVM) [53] and can be described by the operators of the form

$$\Omega(\tilde{x}) = \int_{-\infty}^{+\infty} |x\rangle\Omega(\tilde{x}, x)\langle x|dx, \tag{2.26}$$

where $|x\rangle$ are scaled position eigenkets and $\Omega(\tilde{x})$ needs to satisfy the completeness condition $\int_{-\infty}^{+\infty} |\Omega(\tilde{x}, x)|^2 d\tilde{x} = 1$. The spread of the function $\Omega(\tilde{x}, x)$ describes the degree of smearing of the position measurement. Suppose we are able to measure position only to the accuracy of the *standard quantum limit* [54], which for a harmonic oscillator is $\Delta_x = 1$. Then a set of operators $\Omega(\tilde{x}, x)$ is given by [55]

$$\Omega(\tilde{x}, x) = \frac{1}{\{2\pi\}^{1/4}} \exp\{-\frac{(\tilde{x} - x)^2}{4}\}. \tag{2.27}$$

When an outcome $\tilde{x}$ is registered on the above type of measurement of the mirror's position at time $t = \pi$, the state of the cavity field (not normalized) becomes the mixed state

$$\rho_c(\tilde{x}) = \sum_{n,m=0}^{\infty} \frac{\alpha^n \alpha^{*m}}{\sqrt{n!m!}} e^{i\pi k^2(n^2-m^2)} e^{-\frac{1}{8}\{(\tilde{x}-2\phi_n(\pi))^2+(\tilde{x}-2\phi_m(\pi))^2\}} e^{-\frac{1}{4}(\phi_n(\pi)-\phi_m(\pi))^2} (|n\rangle\langle m|)_c. \tag{2.28}$$

In figures 2.4(b) and 2.4(d), we have shown how the generated cavity field states for $\tilde{x} = x_1$ and $\tilde{x} = x_2 + x_3$ respectively for the above smeared measurement. Comparing the Wigner functions in Figs. 2.4(a) and 2.4(b), we see that the effect of imprecise measurement has

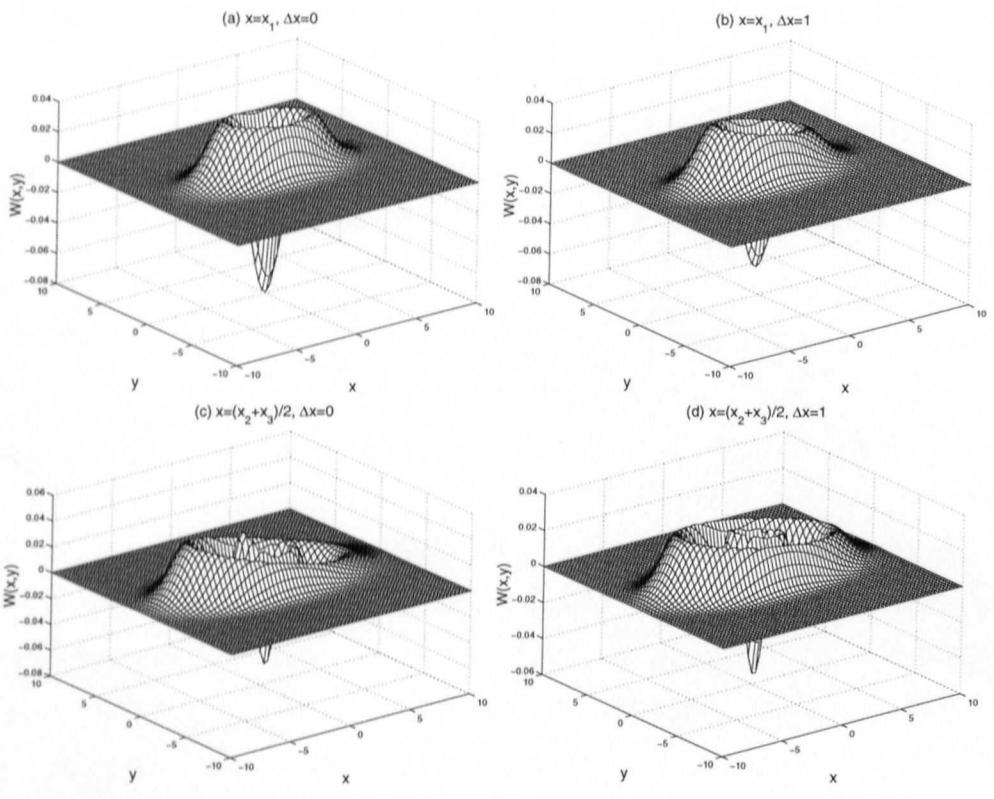



Figure 2.4: The Wigner functions of the state to which the cavity field is projected for various results, $x$, of a measurement of the position of the mirror. We have taken the initial coherent state amplitude of the cavity mode to be $\alpha = 2$, and that of the mirror to be $\beta = 2$. The scaled coupling parameter is $k = 1$, and the measurement is made at time $t = \pi$. The quadratures $x$ and $y$ and the Wigner function $W(x, y)$ are given here in dimensionless form.

been to decrease the negativity of the Wigner function and also a destruction of the circular symmetry of a pure $|1\rangle_c$ due to mixing of other Fock states. On the other hand in going from Fig.2.4(c) to Fig.2.4(d) the circular asymmetry of the coherent superposition of $|2\rangle_c$ and $|3\rangle_c$ is diminished due to decrease of the coherence between them. In practice, if one performs a measurement squeezed in position beyond the SQL [56], the generated Wigner functions will be somewhat intermediate between the left and the right hand sides of Fig.2.4.

Why would we claim that this conditional state preparation is a *genuine application of quantum entanglement*? After all, even if we had the *separable* mixture $\sum_n P_n(|n\rangle\langle n|)_c \otimes (|\phi_n(t)\rangle\langle\phi_n(t)|)_m$, and measured positions (precise or smeared) of the mirror, we would produce near number states of the cavity field. However, we *would not have been able to produce superpositions of adjacent Fock states with the above mixture.* The ability to use the *same state* to produce *both* Fock states and their superpositions stem from the entangled nature of the joint state of the cavity field and the movable mirror. Even if we were only interested in preparing Fock states, the entanglement of the cavity field and the moving mirror offers an advantage. This is because Fock states are unstable *nonclassical* states, and they would not be found naturally. So, from a practical point of view, a classically correlated state of the type $\sum_n P_n(|n\rangle\langle n|)_c \otimes (|\phi_n(t)\rangle\langle\phi_n(t)|)_m$ *cannot* be prepared. The entanglement of the cavity field and the moving mirror over here, offers the advantage of preparing nonclassical states of the field by measurements of an easy to observe observable (the position) of the mirror.

For the physical implementation of the state preparation mentioned above, one will really need to cool down the movable mirror to a pure state or at least a thermal state with a very low temperature. In section 2.8 we will look at the parameter domain required for this. Of course, we would again require the cavity field decoherence rate to be lower than the mirror frequency for the preparation of Fock states to be possible. For the preparation of adjacent Fock state superpositions, we would also require the decoherence rate due to the mirror's motion to be lower than the mirror frequency. A parameter domain which satisfies all the required criteria for the above type of preparation of Fock states and their superpositions, will be described in section 2.8.

## 2.7 Inducing unconventional decoherence of the cavity field

Consider the case when the photon leakage from the cavity is almost absent, but damping of the mirror's motion is significant. As the state of the cavity field is *entangled* with the state of the mirror at times between 0 and $2\pi$, the decoherence of the mirror will *induce* a decoherence of the cavity field. However, its effect on the state of the cavity field is expected to be *unconventional.* During the standard decoherence due to leaking of light from the cavity, the coherent states of light form the relevant pointer basis [57, 58, 59]. This means that the state of an electromagnetic field in a cavity generally evolves into a mixture of coherent states due to its decoherence [60, 61]. However, in the case considered here, coherent states of the mirror are in one to one correspondence with number states of the cavity field. So if decoherence of the mirror forces it towards a coherent state basis, it will induce a decoherence of the cavity field towards the number state basis. Thus the entanglement of the mirror's state with the cavity field *induces* a type of decoherence of the cavity field *which would normally not happen.* This decoherence will leave some imprint on the state produced in the cavity at time $t = 2\pi$. Thus some mixed states of the cavity field which *could not be normally prepared* (with or without the conventional decoherence of the field acting), are now preparable. An example of such a strange state is a *phase diffused Schrödinger cat.* As we will see, such a state is a nonclassical state of the electromagnetic field because of the negativity of its Wigner function.

The equation which governs the decoherence of the mirror depends on the way the mirror is coupled to its environment. Here, for simplicity, we assume that the mirror is amplitude coupled to the environment at zero temperature, which implies the master equation [60]

$$\frac{d\rho(t)}{dt} = -\frac{i}{\hbar}[H, \rho(t)] + \frac{\gamma}{2}(2b\rho(t)b^\dagger - b^\dagger b\rho(t) - \rho(t)b^\dagger b) \tag{2.29}$$

where $H$ is the Hamiltonian of Eq.(2.5). Since we are using a scaled time $t$, $\gamma$ in the above equation is the usual damping constant (that is, the reciprocal of the dissipation timescale) divided by the mirror frequency $\omega_m$. Eq.(2.29) has the feature that it singles out coherent states as the pointer basis [58]. It is expected that natural decoherence of macroscopic objects should force them towards a coherent state basis (to conform with

classical reality), and Eq.(2.29) accomplishes exactly this. So we expect that the solution of Eq.2.29 will at least give the basic features of the effect of mirror decoherence on the cavity states correctly. A similar justification has been given for the use of the above type of decoherence in modelling quantum measurement in Ref.[62]. A more appropriate model for the decoherence of the mirror is quantum Brownian motion [59], but it is also more difficult to solve for our system of interest. We will present the analytic solution for the evolution of our system when decoherence is described according to Eq.(2.29). This solution is expected to have many features (at least the localization of the cavity field towards a number state basis) similar to the solution in the case of quantum Brownian motion because both drive the mirror state to a mixture of coherent states.

The technique we use to solve Eq.(2.29) is to apply the unitary evolution and the nonunitary (decohering) evolution alternately for short instants of time $\Delta t$, and then take the limit as $\Delta t \to 0$. For simplicity, we assume the initial coherent state of the mirror to be the vacuum state. The solution for this initial condition is evaluated in Appendix B, and the result is

$$\rho(t) = e^{-|\alpha|^2} \sum_{n=0,m=0}^{\infty} \frac{\alpha^n \alpha^{*m}}{\sqrt{n!m!}} e^{ik^2(n^2-m^2)(t-\sin t)} e^{-D(n,m,\gamma,t)} |n\rangle\langle m| \otimes |\phi_n(\gamma,t)\rangle\langle\phi_m(\gamma,t)| \tag{2.30}$$

where

$$\phi_n(\gamma,t) = \frac{ikn}{i+\gamma/2}(1 - e^{-(i+\gamma/2)t}), \tag{2.31}$$

are the amplitudes of the coherent states of the mirror and

$$D(n,m,\gamma,t) = \frac{k^2(n-m)^2\gamma}{2(1+\gamma^2/4)}[t + \frac{1-e^{-\gamma t}}{\gamma} - (\frac{(e^{(i-\gamma/2)t}-1)}{i-\gamma/2} - \frac{(e^{-(i+\gamma/2)t}-1)}{i+\gamma/2})]. \tag{2.32}$$

The term $e^{-D(n,m,\gamma,t)}$ in Eq.(2.30) is responsible for decoherence.Note that as $\gamma \to 0$, we have $D(n,m,\gamma,t) \to 0$ and $\phi_n(\gamma,t) \to \phi_n(t)$ where $\phi_n(t)$ is that given by Eq.(3.1), with $\beta$ set equal to zero. In other words, the solution given by Eq.(2.30) reduces to the undamped solution given by Eq.(6.25).

Consider that we initially (at $t = 0$) start with a coherent state $|\alpha\rangle_c$ of the cavity field and a thermal state of the movable mirror. Normally, under such circumstances, at $t = 2\pi$,

and for $k = 0.5$, a Schrödinger cat state of the cavity field would be generated if there was no dissipation [44]. In the presence of *standard decoherence* of the cavity field (due to leakage of light through the mirrors), we would have obtained a Schrödinger cat state decohered towards the coherent state basis. In other words, the negativity of the Wigner function of the generated cat state would have decreased, going to zero in the limit of strong decoherence. It would not have been possible to retain the negativity of the Wigner function, while at the same time loose all phase information about the state. But here we have suppressed the standard decoherence and induced an *unconventional decoherence* of the cavity field due to its entanglement with the movable mirror. The Wigner function for the light field at $t = 2\pi$ for various values of our scaled damping constant $\gamma$ and for $k = 0.5$, is given in Fig.2.5.

From Fig.2.5(a), it is evident that even for a value of scaled $\gamma$ as high as 0.001 (that is, unscaled $\gamma$ of 1), we have almost no decoherence of the Schrödinger cat at all. Thus, unless the mirror is quite heavily damped it has almost no effect on the states produced inside the cavity. A possible cause for this is that the efficiency of decoherence depends on the separation between the coherent states of the mirror corresponding to different number states of the field. This separation is not constant, but oscillates between zero and a maximum value of $2k(n-m)$. The decoherence process, does not, therefore, get the chance to act with as much efficiency as it would have if the mirror was not a harmonic oscillator. Speaking more mathematically, Eq.(2.32) implies that $D(n, m, \gamma, t)$ is proportional to $k^2\gamma$ and not just $\gamma$. As increasing the frequency decreases $k$, it also decreases the rate of decoherence even if $\gamma$ (which relates to the isolation of the system) is held constant. In terms of the absolute time $\tau$ (obtained by dividing the scaled time $t$, which we had been using, by $\omega_m$), the time scale $\tau_d$ of decoherence depends on the frequency as (from Eqs.(2.6), (2.32) and definition of $k$)

$$\tau_d \propto (\omega_m)^3 \tag{2.33}$$

Thus controlling $\omega_m$ offers an alternate way to control the decoherence timescale of our system.

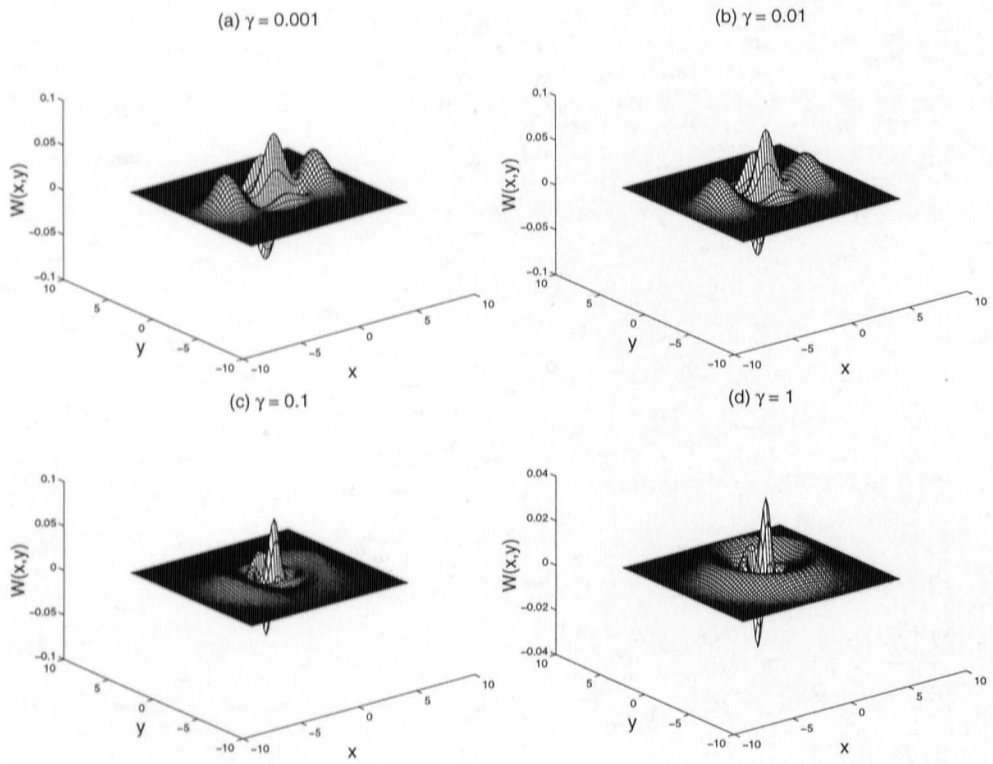



Figure 2.5: The Wigner function $W(x, y)$ of the cavity field at time $t = 2\pi$ for various values of the motional damping constant, $\gamma$, of the mirror. We have taken the initial coherent state amplitude of the cavity mode to be $\alpha = 2$, and that of the mirror to be $\beta = 2$. The scaled coupling parameter is $k = 0.5$. The quadratures $x$ and $y$ and the Wigner function $W(x, y)$ are given here in dimensionless form.

It is worthwhile to mention that an analogous situation has been pointed out in Ref.[63] in the context of the Jaynes Cummings model, where atomic spontaneous emission has a much weaker effect on revivals of atomic inversion than the cavity field damping. In that case, however, the explanation was quite different, namely, that spontaneous emission is independent of the cavity field intensity, while cavity damping is intensity dependent. This logic will also apply to our system when the intensity of the cavity field is large. The term which causes decoherence, $D(n, m, \gamma)$, is completely independent of the intensity of the cavity field. So as this intensity increases, the photon damping begins to dominate over the mirror's motional damping, as far as influencing the final state in the cavity is concerned.

The interference peak of the Schrödinger cat, which is a primary feature of this cat, is not significantly lowered by the decoherence process (See Figs.2.5(b)-2.5(d)), although there is a phase diffusion of the state. The reasoning for this is the simple fact that the decoherence is towards the number state basis, which preserves the photon number distribution. The photon number distribution at $t = 2\pi$ is same for both the decohered state given by Eq.(2.30) and the undecohered state given by Eq.(6.25). This means that one of the primary signatures of the Schrödinger cat, namely, an oscillating photon number distribution (that is, the probability of odd photon numbers being zero for an even coherent state and vice versa) is the same for the final state produced at $t = 2\pi$, irrespective of whether there was decoherence or not. So the decoherence considered here is not acting to eliminate all nonclassical properties of the field that would be produced without decoherence. It does destroy the phase information, but maintains the nonclassicality of the number distribution. This is precisely the reason why the interference peak of the Schrödinger cat does not appear to be destroyed even when scaled $\gamma$ is as high as unity, as depicted in Fig.2.5(d). What we have, in effect been able to produce, is yet another nonclassical state of the electromagnetic field (in this case, a mixed state) called the *phase diffused Schrödinger cat.*

In this section, we have thus shown that entanglement of the cavity field with the movable mirror allows us to decohere the cavity field towards a nonorthodox pointer basis. Moreover, by controlling the frequency of the movable mirror, we can *induce controllable decoherence* of the cavity field.

## 2.8 Relevant parameter domains

There are essentially three types of parameter domains necessary for the successful physical implementation of the applications described in this chapter. For the entangling of different cavity modes (macroscopic object mediated quantum logic) we require the decoherence rate of both the cavity field and the movable mirror to be lower than the oscillation frequency of the mirror. But we do not require the mirror to be in an almost pure state and a thermal state suffices. One good parameter domain emerges when we convert the best finesse optical cavity mirror available (finesse $F \sim 10^6$) [64], to quite a low quality mechanical resonator (say quality factor $Q \sim 1$). This should be rather easy, as much higher quality mechanical resonators (with $Q \sim 10^6$ [65]) have already been fabricated. We choose the other parameters to be $\omega_0 \sim 10^{15}\mathrm{s}^{-1}, L \sim 1cm, m \sim 10\mathrm{m}g$ and $\omega_m \sim 10^5\mathrm{s}^{-1}$ [46, 47, 65]. The mirror is at room temperature $T \sim 100\mathrm{K}$. This leads to a cavity damping rate (which is also the cavity decoherence rate) $\gamma_a \sim 10^4\mathrm{s}^{-1}$ and a mirror damping rate of $\gamma_m \sim 10^4\mathrm{s}^{-1}$ which leads to a mirror decoherence rate of $\Gamma_m \sim 100\mathrm{s}^{-1}$ (the formula for obtaining $\Gamma_m$ from $\gamma_m$ is given in chapter 3). Thus both $\gamma_a$ and $\Gamma_m$ are less than the oscillation frequency of the mirror as required. The value of scaled coupling $k \sim 1$ for the above set of parameters, so we can choose $k = 0.5$ to implement the quantum logic mediated by a hot (100K) macroscopic object and also to generate multi-mode Schrödinger cat states of the cavity field.

One can even envisage coating the high finesse mirrors available on a mechanical resonator such that radiation pressure couples light to internal acoustic modes of the resonator [66]. For such a setup, one gets very low effective values for the mass $m$ of our model and a very high frequency $\omega_m$. We choose $F \sim 10^5$ (as is available [67]), $m \sim 0.1$ mg, $\omega_m \sim 10^6\mathrm{s}^{-1}, \gamma_m \sim 1$ [66], increase $L$ to $10cm$ and keep the other parameters same as before (which means, still working at room temperature). Then it turns out that $\gamma_a \sim 10^4\mathrm{s}^{-1}$ and $\Gamma_m \sim 10^{-6}\mathrm{s}^{-1}$, which are both less than $\omega_m$. This setup will thus also be useful in entangling two noninteracting cavity modes.

For the conditional state preparation, not only must the above low decoherence rates be met, but the movable mirror is also required to be in an almost pure state at the begining.

This moves us to the mesoscopic domain of *nanometer scale cantilevers* [68]. Such mirrors can have a frequency $\omega_m \sim 10^9 \mathrm{s}^{-1}$ and a mass $m \sim 10^{-15}$ Kg. Consequently, they are in an almost pure state (photon number less than unity) at temperatures below 0.01K. Also the value of the scaled coupling $k$ is as high as $10^5$ with a cavity of length 0.01cm. If other parameters are kept the same as in the previous paragraph, we have both $\gamma_a \sim 10^7 \mathrm{s}^{-1}$ and $\Gamma_m \sim 10^{-10} \mathrm{s}^{-1}$ to be less than $\omega_m$. In fact, we can decrease the finesse of the cavity mirror by a couple of orders of magnitude and decrease the quality factor of the mirror's mechanical oscillation by an astounding nineteen orders of magnitude and still remain in our desired domain!

For the entanglement induced unconventional decoherence, we require only the decoherence rate of the cavity field to be lower than the mirror oscillation frequency. This latter type of parameter domain also arises in the next chapter and will be discussed in detail in that chapter.

## 2.9 Conclusions

In this chapter, we have tried to illustrate three practical applications of entanglement in quantum optics with the help of an explicit model. These applications, are however, quite generic in nature. If we want to entangle the states of two objects which do not interact directly, the only way out is to transfer the entanglement via a third object. This is what our first example illustrates. Analogous techniques are always being used in quantum optics such as entangling distant microwave fields via atoms [69] or entangling atoms in a linear trap via their common vibrational mode [70]. The second application, namely the conditional state preparation of one object by measurements on another object, has also had previous applications in quantum optics [71]. This, I believe is a central role of entanglement. I will be discussing more of this aspect in the conclusion of this thesis. The third application: inducing unconventional and controllable decoherence is also an important practical application of entanglement. It would be very impractical (and *rather impossible*) to couple a system in a desired way with an uncountable number of degrees

of freedom to generate a *true* environment which decoheres the system towards a specific pointer basis. It is much cleverer to couple it in a specific way to another single system. The natural decoherence of this other system then induces the desired decoherence of the system of interest. This application of entanglement has also been used previously in quantum optics in designing specific reserviors for the motional states of trapped ions by changing their coupling with the atomic internal degrees of freedom [72]. Despite the common usage of the above techniques, it is not always emphasized that they are really applications of entanglement. In this chapter, I have tried to present these techniques as applications of entanglement.

# Chapter 3

# Entanglement between a microscopic and a macroscopic system II: applications in probing macroscopic decoherence

## 3.1 Introduction

In the last chapter, we were using an opto-mechanical system to highlight some applications of entanglement. In this chapter, we take the same system and look back at the original context in which Schrödinger introduced the term entanglement [13]. Schrödinger wanted to highlight how a poor cat could end up in the absurd situation of being simultaneously dead and alive by virtue of getting entangled with the state of a radioactive atom. We now know *at least* one of the reasons for not seeing such absurd situations. Schrödinger's atom-cat entangled state involves a superposition of states $|no\ decay\rangle \otimes |cat\ alive\rangle$ and $|decay\rangle \otimes |cat\ dead\rangle$, which are macroscopically distinguishable. Such superpositions decay rapidly due to the strong coupling of the macroscopic object with its environment. This process is called environment-induced decoherence (EID) [16].

There are many assumptions involved in modelling the EID of a macroscopic object. For example, the nature of the coupling of a macroscopic object to its environment is generally taken to be a linear [74] or a nonlinear [75] function of the position operator of the object. Assumptions are also made about the environment. Based on these assumptions, various explicit formulae have been derived for the dependence of the decoherence time scale on various parameters of the system, its environment, and the spatial separation between the superposed components [16, 74, 59, 75]. Obviously, the most appropriate model can be selected only through experimentation. Decoherence formulae relevant to the quantum optical domain [60, 76] are now beginning to be tested experimentally [77]. As far as quantum objects bearing mass are concerned, decoherence has been investigated for the motional states of ions in a trap [71]. There have also been other interesting suggestions for testing decoherence experimentally [78, 79, 80]. However, as yet no one has managed to test the the rules of decoherence of a superposition of spatially separated states of a macroscopic object. This is, presumably, because of the implicit assumption that one actually needs to prepare a superposition of distinct states of a macroscopic object in order to probe the rules of its decoherence. Such a superposition is extremely difficult to prepare because of the difficulty of obtaining a macroscopic system in a pure quantum state. In this chapter, we propose a scheme that will allow us to probe the rules of decoherence of a superposition of states of a macroscopic object *without actually creating such a superposition.* We also show that it requires experimental parameters that are close to the potentially realizable domain.

Besides EID, there also exist a set of collapse models [81, 82] developed to resolve the measurement problem of quantum mechanics. Whether such a mechanism is really necessary or whether some reformulation of quantum mechanics such as the Histories,tories approach [83] suffices, is an open question [84]. Some experiments to detect such mechanisms have been suggested [79, 85], and some preexisting experimental data have been analysed [86, 87]. In particular, atomic interferometry experiments provide a great potential to put bounds on such models [86]. However, there is no direct evidence for their existence. We calculate the parameter regime required if our experiment is to probe such models, and

show that this, is a much more difficult task than probing EID.

Our experiment is based on applying the basic set of ideas as used by Schrödinger in his, famous gedanken experiment [13] to the quantum optical system considered in the previous chapter. Obvious differences arise as our set up is meant to be realistic. We begin by recapitulating Schrödinger's technique and describing qualitatively what happens when such a technique is applied to our set up.

## 3.2 Schrödinger's method for creating macroscopic superpositions

The basic idea used by Schrödinger to create macroscopic superpositions was to *entangle the states of a microscopic and a macroscopic system* [13]. It is easy to put the state of a microscopic system (which follows quantum mechanics beyond any controversy, and is fully controllable in the laboratory) into a superposition of distinct states. Subsequently, this system is allowed to interact with a macroscopic system to propel it to macroscopically distinct states corresponding to the different superposed states of the microscopic system. This is why *entanglement is essential for a Schrödinger cat-like experiment.* In Schrödinger's case, the microscopic system was a radioactive atom, while the macroscopic system was a cat. In this chapter, we propose to apply exactly the Schrödinger technique to a cavity field (a microscopic system) coupled to a movable mirror (a macroscopic system). However, there are differences of such a realistic version of Schrödinger's thought experiment from his original version. We will enumerate these problems below and outline why our experiment can still achieve its target (testing the decoherence of a superposition of states of a macroscopic object) despite being quite different from Schrödinger's original experiment.

Firstly, as yet, no technique exists to put a macroscopic oscillator in a pure coherent state (though some progress has been made in cooling of such objects [88]). Thus, unlike the cat in Schrödinger's original experiment, the macroscopic mirror cannot start off in a pure state, and in general, will start off in a thermal state. So only a mixture of Schrödinger's cat states can ever be created through unitary evolutions. So the primary aim of Schrödinger's

experiment (creating macroscopic superpositions) cannot be achieved this, way. However, our aim is to test the decoherence of states of a macroscopic object and not to create a pure Schrödinger's cat state. An important point to realize is that the former *can* be done *without* necessarily doing the latter. We shall show that the state of the cavity field (the system on which we actually perform our measurements) at the end of our experiment is same *irrespective* of whether the macroscopic object (the movable mirror) coupled to it starts off in a thermal state or a coherent state. This is due to the specific nature of the coupling between the field and the mirror. Thus the mixture of Schrödinger's cat states produced has the same observational consequences as a pure Schrödinger's cat as far as our scheme is concerned.

Secondly, it appears that the decoherence of a superposition of states of a macroscopic mirror (which can never be made as isolated as the cat in Schrödinger's thought experiment) will be too fast to detect. To circumvent this, one must note that the decoherence rate of a certain superposition of states of an object increases with the spatial separation between these states [16, 74, 59]. So the amount by which the decoherence rate increases due to the macroscopic nature (large mass) of the object can always be offset by reducing the spatial separation between the superposed states.

Thirdly, in Schrödinger's case, the coupling between radioactivity and the cat involved highly nonlinear biological processes. So even a small trigger of radioactive decay was sufficient (via the breaking of the poison vial) to produce as much of a change in a cat as killing it. Can we get such a nonlinear coupling to produce a drastic change in the state of the macroscopic mirror from small changes in the state of the cavity field? The answer to this, is that it is really not necessary to have a drastic change in the state of the macroscopic mirror. Even a superposition of macroscopically non-discernible states is sufficient to produce a detectable rate of decoherence if the the mirror is sufficiently macroscopic.

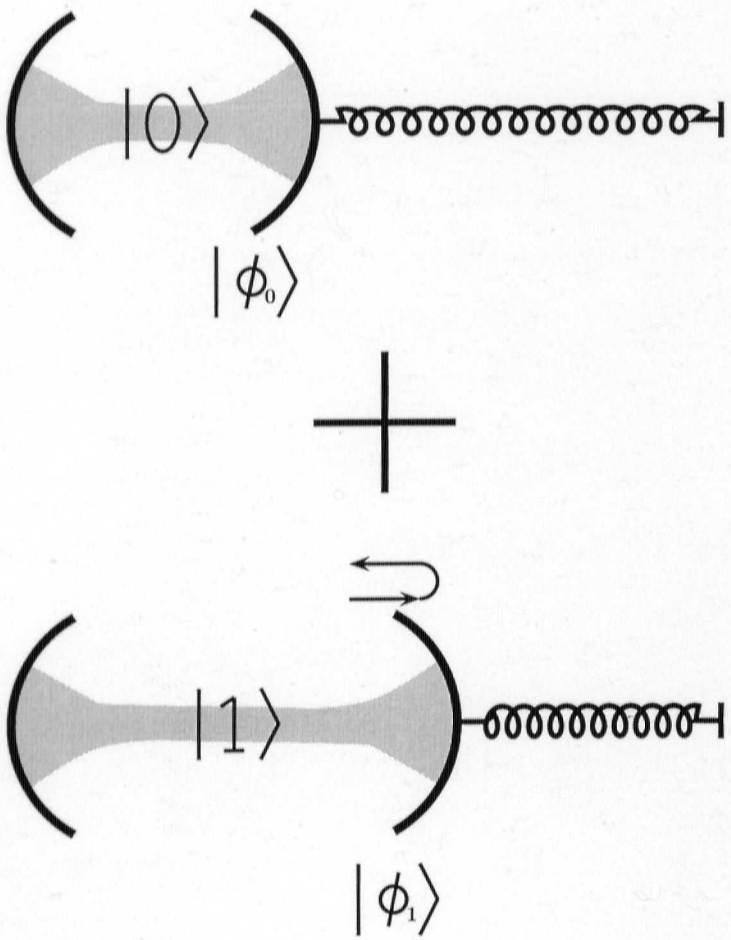



Figure 3.1: The proposed opto-mechanical Schrödinger's cat: the quantized single mode field is modified by the harmonic motion of one of the mirrors. The result is an entangled state of the mirror motion and the cavity field, here labelled by $|0\rangle|\phi_0\rangle$ and $|1\rangle|\phi_1\rangle$. Given that the initial state of the mirror is a thermal state, only a mixture of several such opto-mechanical cats with different mean positions is produced.

## 3.3 The system under consideration

We consider the system introduced in the last chapter. The Hamiltonian is given by Eq.(2.5). We keep the definitions and symbols for all parameters same as the last chapter, but use $t$ to denote the real time over here instead of the scaled time. Thus in all equations of the previous chapter, $t$ is to be simply replaced by $\omega_m t$. We would be using the real time over here because it is easier to compare this with other time-scales (like the decoherence time-scale) of the problem. We will only need to use a simple fact from the study in the last chapter. If the field inside the cavity was initially in a number state $|n\rangle_{\rm c}$ and the mirror was initially in a coherent state $|\beta\rangle_{\rm m}$, then at any later time $t$ the mirror will be in the coherent state

$$|\phi_n(t)\rangle_{\rm m} = |\ \beta e^{-i\omega_m t} + kn(1 - e^{-i\omega_m t})\ \rangle_{\rm m}\ , \tag{3.1}$$

where $k = g/\omega_m$. Thus, in effect the mirror undergoes an oscillation with a frequency $\omega_m$ and an amplitude dependent on the Fock state inside the cavity. This is the only input from the previous chapter which is relevant to the discussion in this chapter. The basic idea of our scheme is as follows: A superposition of two different Fock states is created inside the cavity so that the mirror is driven to an oscillation of different amplitude corresponding to each of these Fock states. As the mirror is a macroscopic object, this situation can be regarded as a version of Schrödinger's cat experiment. Of course, in practice, only a mixture of several Schrödinger's cats is created because the mirror starts off in a thermal state instead of starting in a single coherent state $|\beta\rangle_{\rm m}$. This is, however, good enough for testing the decoherence rules of a macroscopic object.

## 3.4 The proposed scheme

We propose to start with the cavity field prepared in the initial superposition of Fock states

$$|\psi(0)\rangle_{\rm c} = \frac{1}{\sqrt{2}}(|0\rangle_{\rm c} - |n\rangle_{\rm c}). \tag{3.2}$$

Methods of preparing the cavity field in such states has been described in Refs.[89, 90, 91]. When discussing experimental parameters we will choose $n = 1$, which is the simplest to

prepare. The initial state of the movable mirror will be taken to be a thermal state at some temperature $T$, and is given by the density operator

$$\rho_{\rm m} = \frac{1}{\pi\bar{n}} \int (|\beta\rangle\langle\beta|)_{\rm m} \exp(-|\beta|^2/\bar{n})\; d^2\beta, \tag{3.3}$$

where

$$\bar{n} = \frac{1}{e^{\hbar\omega_m/K_{\rm B}T} - 1}, \tag{3.4}$$

and $|\beta\rangle_m$ represents a coherent state of the mirror corresponding to amplitude $\beta$ and $K_{\rm B}$ is the Boltzmann constant. Eq.(3.1) and the initial states given by Eqs.(3.2) and (3.3) imply that at any time $t$, in the absence of any external environment, the joint density operator describing the cavity mode and the mirror is given by

$$\begin{aligned} \rho(t)_{\rm c+m} &= \frac{1}{2\pi\bar{n}} \int (\rho(t)_{00} - \rho(t)_{0n} \\ &- \rho(t)_{n0} + \rho(t)_{nn})_{\rm c+m} \exp(-|\beta|^2/\bar{n})\; d^2\beta, \end{aligned} \tag{3.5}$$

where

$$\rho(t)_{00} = (|0\rangle\langle 0|)_{\rm c} \otimes (|\phi_0(t)\rangle\langle\phi_0(t)|)_{\rm m}, \tag{3.6}$$

$$\begin{aligned} \rho(t)_{0n} &= (|0\rangle\langle n|)_{\rm c} \otimes (|\phi_0(t)\rangle\langle\phi_n(t)|)_{\rm m} \\ &\quad \times e^{-ik^2n^2(\omega_m t - \sin\omega_m t)}, \end{aligned} \tag{3.7}$$

$$\begin{aligned} \rho(t)_{n0} &= (|n\rangle\langle 0|)_{\rm c} \otimes (|\phi_n(t)\rangle\langle\phi_0(t)|)_{\rm m} \\ &\quad \times e^{ik^2n^2(\omega_m t - \sin\omega_m t)}, \end{aligned} \tag{3.8}$$

$$\rho(t)_{nn} = (|n\rangle\langle n|)_{\rm c} \otimes (|\phi_n(t)\rangle\langle\phi_n(t)|)_{\rm m}, \tag{3.9}$$

The phase factors $e^{\pm ik^2n^2(\omega_m t - \sin\omega_m t)}$ in Eqs.(4.1) and (3.8) derive from a Kerr like term in the time evolution operator corresponding to the Hamiltonian $H$. Note that there are absolutely no assumptions involved while writing Eq.(3.5). However, the coherent state basis expansion of the initial thermal state of the mirror (Eq.(3.3)) has been used for a specific purpose. The terms $\rho(t)_{00}$, $\rho(t)_{0n}$, $\rho(t)_{n0}$ and $\rho(t)_{nn}$ appear in Eq.(3.5) only if such an expansion is made. The effect of decoherence on such terms is already well studied [74, 59] and the specific form of Eq.(3.3) allows us to simply utilize these known results.

The situation described by Eq.(3.5) between times $t = 0$ and $t = 2\pi/\omega_m$ is a mixture of several Schrödinger's cat states of the type depicted in Fig. 3.1 (where the value of $n$ has been taken to be equal to 1). Eq.(3.1) implies that at $t = 2\pi/\omega_m$, all states $|\phi_n(t)\rangle_{\rm m}$ will evolve back to $|\beta\rangle_{\rm m}$ irrespective of $n$. Thus the mirror will return to its original thermal state (given by Eq.(3.3)) and the state of the cavity field will be disentangled from the mirror. In the absence of any EID, this, state will be

$$|\psi(2\pi/\omega_m)\rangle_{\rm c} = \frac{1}{\sqrt{2}}(|0\rangle_{\rm c} - e^{ik^2n^2 2\pi}|n\rangle_{\rm c}). \tag{3.10}$$

In reality, two sources of decoherence will be present. The first one is the decoherence due to photons leaking from the cavity and the second one is EID of the motional state of the mirror. The aim of this, paper is to show how the rate of the second type of decoherence can be determined. To simplify our analysis, we shall take $n = 1$ (i.e, the initial state inside the cavity is $\frac{1}{\sqrt{2}}(|0\rangle_{\rm c} - |1\rangle_{\rm c})$). First consider the case when no photon happens to leak out of the cavity up to a time $t$. If the damping constant of the cavity mirror is $\gamma_a$ then the probability for this, to happen is $\frac{1}{2}(1 + e^{-\gamma_a t})$ [92]. In this, case, the amplitude of the state $|1\rangle_{\rm c}|\phi_1(t)\rangle_{\rm m}$ is suppressed with respect to the state $|0\rangle_{\rm c}|\phi_0(t)\rangle_{\rm m}$ by a factor $e^{-\gamma_a t/2}$. In addition to this, form of decoherence, there is EID of the mirror's motional state. This has already been studied quite extensively, the basic result being a rapid decay of those terms in the density matrix that are off-diagonal in the basis of Gaussian coherent states [74, 59]. However, the diagonal terms in the coherent state basis are hardly affected on the same time-scale (in fact, it has been shown that in the case of a harmonic oscillator, coherent states emerge as the most stable states under decoherence [58]). Quite independent of any specific model of decoherence, the satisfactory emergence of classicality would require the off diagonal terms in a coherent state basis to die much faster than the diagonal terms as coherent states are the best candidates for classical points in phase space. Thus, EID of the mirror's motional state decreases the coherence between the states $|0\rangle_{\rm c}|\phi_0(t)\rangle_{\rm m}$ and $|n\rangle_{\rm c}|\phi_n(t)\rangle_{\rm m}$ because $|\phi_0(t)\rangle_{\rm m}$ and $|\phi_n(t)\rangle_{\rm m}$ are spatially separated coherent states of the mirror's motion. Let the average rate of this, decoherence be $\Gamma_m$. Then the state of the system at time $t$ is given by

$$\begin{aligned}\rho(t)_{\mathrm{c+m}} &= \left(\frac{1}{1+e^{-\gamma_a t}}\right)\frac{1}{2\pi\bar{n}}\int[\rho(t)_{00} - e^{-(\frac{\gamma_a}{2}+\Gamma_m)t}\rho(t)_{01} \\ &- e^{-(\frac{\gamma_a}{2}+\Gamma_m)t}\rho(t)_{10} \\ &+ e^{-\gamma_a t}\rho(t)_{11}]_{\mathrm{c+m}}\exp(-|\beta|^2/\bar{n})\, d^2\beta, \end{aligned} \tag{3.11}$$

where the symbols $\rho(t)_{ij}$ denote states as given by Eqs.(3.6)-(3.9). Eq.(3.11) shows that at time $t = 2\pi/\omega_m$ the states of the cavity field and the mirror become dynamically disentangled. Now consider the complementary case (i.e when a photon actually leaks out of the cavity between times 0 and $t$). The total probability for this, to happen is $\frac{1}{2}(1 - e^{-\gamma_a t})$. As soon as the photon leaks out, the state of the cavity field goes to $(|0\rangle\langle 0|)_{\mathrm{c}}$ and its state becomes completely disentangled from the state of the mirror. Moreover, the mirror does not interact with the cavity field any more as the interaction is proportional to the number operator of the cavity field. Thus its state remains disentangled from the state of the cavity field at all times after the photon leakage. Adding both the cases (photon loss and no photon loss) with respective probabilities, one gets the state of the cavity field at time $t = 2\pi/\omega_m$ to be

$$\begin{aligned}\rho(2\pi/\omega_m)_{\mathrm{c}} = \frac{(2 - e^{-2\gamma_a\pi/\omega_m})}{2}|0\rangle\langle 0|_{\mathrm{c}} \; - \\ \frac{e^{-\gamma_a\pi/\omega_m}}{2}e^{-\Gamma_m 2\pi/\omega_m}(e^{ik^2 2\pi}|1\rangle\langle 0|_{\mathrm{c}} \; + \; e^{-ik^2 2\pi}|0\rangle\langle 1|_{\mathrm{c}}) \\ + \frac{e^{-2\gamma_a\pi/\omega_m}}{2}|1\rangle\langle 1|_{\mathrm{c}}. \end{aligned} \tag{3.12}$$

Thus by probing the state of the cavity field at time $t = 2\pi/\omega_m$, it should be possible to determine the value of $\Gamma_m$ and this, gives the rate of decoherence of spatially separated states of the macroscopic mirror.

We should pause here to note that the state of the cavity field at $t = 2\pi/\omega_m$ is completely *independent* of the initial thermal state (given by Eq.(3.3)), in which the mirror starts off. This feature is very important for our proposal. It implies that the effects on the cavity field will be same *irrespective* of whether the mirror started off in a mixture of coherent

states (like a thermal state) or in a single coherent state. This makes the imprint of the demise of a single Schrödinger's cat state on the cavity field identical to the imprint made by the demise of a mixture of several such states.

The simplest method to determine the value of $\Gamma_m$ is to pass a single two level atom (which interacts resonantly with the cavity field) in its ground state $|g\rangle$ through the cavity at time $t = 2\pi/\omega_m$, such that its flight time through the cavity is half a Rabi oscillation period. The state of the cavity will get mapped onto the atom with $|e\rangle$ replacing $|1\rangle_c$ and $|g\rangle$ replacing $|0\rangle_c$ in Eq.(3.12). Then the probability of the atom to be in the state $|+\rangle = \frac{1}{\sqrt{2}}(|g\rangle + |e\rangle)$ after it exits the cavity, is

$$P(|+\rangle\langle+|) = \frac{1}{2}[1 - e^{-\frac{\pi}{\omega_m}(\gamma_a + 2\Gamma_m)} \cos k^2 2\pi]. \tag{3.13}$$

From the above equation it is clear that determining the probability of the exiting atom to be in the state $|+\rangle$ will help us to determine the decoherence rate $\Gamma_m$ if the order of magnitude of $\Gamma_m$ can be made greater than or about the same as that of $\gamma_a$. Another requirement is that $\Gamma_m$ must be of the same order as $\omega_m$ or even lower. Otherwise changes in $P(|+\rangle\langle+|)$ due to changes in $\Gamma_m$ would be too small to observe. Of course, if one initially started with a general state $\frac{1}{\sqrt{2}}(|0\rangle_c - |n\rangle_c)$ of the cavity field, then more general tomography schemes [93] will have to be used.

## 3.5 A heuristic formula for the average decoherence rate

We now proceed to estimate $\Gamma_m$ in terms of the physical parameters of our system to illustrate the importance of this, experiment from the point of view of testing the decoherence of a macroscopic object. According to the models of references [16] and [74], a superposition of coherent states spatially separated by a distance $\Delta x$ decoheres (when $\Delta x$ is greater than the thermal de Broglie wavelength $\lambda_{th} = \hbar/\sqrt{2mK_B\theta}$ ) on a time-scale

$$t_D = \frac{\hbar^2}{2m\gamma_m K_B \theta (\Delta x)^2}, \tag{3.14}$$

where $m$ and $\gamma_m$ stand for the mass and damping constant of the object under consideration and $\theta$ is the temperature of the enclosure where the object is placed. In our case, the spatial separation between the coherent states $|\phi_0(t)\rangle_{\rm m}$ and $|\phi_n(t)\rangle_{\rm m}$ varies with time as

$$\Delta x(t) = \sqrt{\frac{\hbar}{2m\omega_m}} 2kn(1-\cos\omega_m t). \tag{3.15}$$

Assuming, for the time being, that the decoherence process was entirely environment-induced, one can use Eqs.(3.14) and (3.15) to calculate the average value of the decoherence rate $\Gamma_m$ to be

$$\begin{aligned} \Gamma_m &= \frac{1}{(2\pi/\omega_m)} \frac{4\hbar k^2 n^2}{2m\omega_m} \frac{2m\gamma_m K_{\rm B}\theta}{\hbar^2} \int_0^{2\pi/\omega_m} (1-\cos\omega_m t)^2 dt \\ &= \frac{3n^2\omega_0^2}{L^2\omega_m^4 m} K_{\rm B}\theta\gamma_m, \end{aligned} \tag{3.16}$$

where the value of $k$ has been substituted.

## 3.6 Constraints on the parameters

For our scheme to be successful in testing the decoherence of a macroscopic object, and our method of analysis to be valid, certain parameter constraints have to be satisfied. The first constraint comes from Eq.(3.13). The decoherence rate to be measured, $\Gamma_m$, has to be made greater than or about the same order as that of the other decoherence rate $\gamma_a$. An associated requirement is that $\Gamma_m$ must be of the same order as $\omega_m$ or even lower. This is because, in order to be able to measure a finite decoherence rate, we have to have only partial decoherence. If $\Gamma_m$ is much greater than $\omega_m$ then the decoherence will be too fast and essentially complete before even one oscillation period of the mirror and thereby not measurable. Thus we have,

**Constraint 1:**

$$\omega_m \sim \Gamma_m \geq \gamma_a \tag{3.17}$$

The next constraint is required for our heuristic treatment of the decoherence of the mirror to be valid. The use of Eq.(3.14) is valid only when $\Delta x$ is greater than the thermal de Broglie wavelength $\lambda_{th} = \hbar/\sqrt{2mK_{\rm B}\theta}$. Using the expression for $\lambda_{th}$ in Eq.(3.15) we get

**Constraint 2:**

$$\frac{\omega_0^2}{L^2\omega_m^4 m} K_B\theta >> 1 \tag{3.18}$$

A final constraint comes from the fact that the spatial separation $\Delta x$ between the superposed peaks must be greater than or at least of the same order as the width of a single peak. This is a requirement for two reasons: firstly for the validity of our heuristic treatment of decoherence, and secondly for the components of the Schrödinger's cat to be sufficiently separated in space (i.e at least as much separated than the spatial width of each component of the Schrödinger's cat). As the width of each of the components of the cat is simply equal to the width of a coherent state, using Eq.(3.15) and the fact that $n = 1$, we get,

**Constraint 3:**

$$k \geq 1 \tag{3.19}$$

We should stress that while constraint 1 will be a *necessary* constraint in any analysis of our system, constraints 2 and 3 really arise due to our method of analysis. If we could calculate the decoherence rate when the superposed wavepackets almost overlap each other, then neither of the constraints 2 or 3 would be needed. But in that case, the decrease in the decoherence rate may be so much that constraint 1 becomes difficult to achieve. We leave the analysis of this, domain for the future. We now proceed to propose a set of parameters which satisfy the above constraints and which are fairly close to those currently realisable.

## 3.7 Experimental parameter regimes satisfying the constraints

At first, let us briefly state the available ranges of the various parameters involved in our experiment as far as the technology stands today. The frequency of mechanical oscillators ($\omega_m/2\pi$ in our case) is normally in the KHz domain, but can be made to rise up to a GHz [68]. However, in the case of such high frequencies, the mass of the oscillators is very small (about $10^{-17}$ kg [68]). The mass $m$ of the movable mirror has no upper restriction, but is bounded on the lower side by the requirement of having to support the beam waist of an electromagnetic field mode. This means that the masses of mirrors for microwave

cavities should be no smaller than about 0.1g while those for optical cavities can go as low as $10^{-15}$kg. The length $L$ of the cavity can be no lower than 1 cm in the microwave domain but can be as low as 1 $\mu$m in the optical domain. In fact, optical cavities with a length of the order of 10 $\mu$m already exist [67]. While there is essentially no limit to how high the mechanical damping rate, $\gamma_m$, of the moving mirror can be made, there is a lower limit (not necessarily a fundamental limit, but the best achievable in current experiments). Oscillating cavity mirrors with $\omega_m/2\pi \sim 10$ kHz and Q-factor $\sim 10^6$ have been fabricated [65]. We will take the corresponding $\gamma_m \sim 10^{-2}\text{s}^{-1}$ to be a lower limit on the value of the mechanical damping constant. The lowest temperature $\theta$ to which a macroscopic mirror has been cooled as yet, is about 0.5K [94]. As far as the damping constant $\gamma_a$ due to leakage of photons from the cavity is concerned, the lowest values are $10^7$ $\text{s}^{-1}$ for optical cavities of $L \sim 10$ $\mu$m (with stationary mirrors) [67], $10^6$ $\text{s}^{-1}$ for optical cavities of $L \sim 1$ cm (with a moving mirror) [65], and $10\text{s}^{-1}$ for microwave cavities of $L \sim 1$ cm (with a stationary mirror) [94].

Now let us examine a parameter regime in which all our constraints are satisfied. We first look at optical cavities ($\omega_0/2\pi \sim 10^{15}$Hz). For optical cavities we can choose $L \sim 10$ $\mu$m [67]. We choose $m = 1$ mg, $\gamma_m = 10^{-2}$ $\text{s}^{-1}$, $\omega_m/2\pi = 10$ kHz, and $\theta = 0.1$ K. With this, choice of parameters,

$$\frac{\omega_0^2}{L^2\omega_m^4 m} K_B\theta \sim 10^6 \tag{3.20}$$

and

$$k \sim 1. \tag{3.21}$$

So both the constraints 2 and 3 are satisfied. Also we have

$$\Gamma_m \sim \omega_m \sim 10^4\ \text{s}^{-1}. \tag{3.22}$$

Thus, in order to satisfy constraint 3, we require $\gamma_a \leq 10^4$ $\text{s}^{-1}$. While this, value of $\gamma_a$ is only three orders of magnitude removed from the best reflectivity for stationary mirrors and

five orders of magnitude removed from the best reflectivity for moving mirrors in the optical domain at present, all the other parameters assumed here are well within the experimentally accessible domain. We don't see any *fundamental* reason why the reflectivity of the moving mirror cannot be increased by a few orders of magnitude, as the mirror is quite macroscopic (of milligram mass). Note that in the above case the position separation $\Delta x$ between the superposed components is *really* tiny (of the order of $10^{-16}$m !), yet even this, is sufficient to cause an observable rate of decoherence. This is because the macroscopic nature of the moving mirror implies that even this, minute separation is much larger than the thermal de Broglie wavelength. We note that one is allowed to increase the mass of the moving mirror to about 100 mg, if the length of the cavity is decreased to 1 $\mu$m. Our constraints will still have exactly the same values as above when this, change is made. However, it seems that 100 mg is probably the largest mass the mirror in our experiment can possibly have. Note that mirror masses of 1 mg – 100 mg are well within experimentally accessible domains as mirror masses of the order of 10 mg have already been used in optical bistability experiments [46, 47].

The above choice of parameters was entirely motivated by an attempt to keep the parameters as close as possible to an existing optical cavity with a moving mirror experiment [65]. Our constraints require the mirror reflectivity of this, experiment to be improved in order for our proposal to be a success. However, another alternative is to keep the values of mirror reflectivity same as in existing experiments but move on to a mirror oscillating at a much higher frequency. Let us choose $\omega_m \sim \gamma_a \sim 10^7$ s$^{-1}$ (though this, value of $\gamma_a$ is for the best existing static mirror). To make $\Gamma_m \sim 10^7$ and satisfy constraint 1, we are required to choose low $L \sim 10$ $\mu$m, low $m \sim 10^{-15}$kg, temperature $\theta \sim 10$K and high $\gamma_m \sim 100$s$^{-1}$. The frequency of the cavity mode is kept the same ($\omega_0/2\pi \sim 10^{15}$ Hz). This choice also satisfies constraints 2 and 3 as

$$\frac{\omega_0^2}{L^2\omega_m^4 m} K_{\rm B}\theta \sim 10^5 \tag{3.23}$$

and

$$k \sim 1. \tag{3.24}$$

Among the basic changes made here from existing experiments, the temperature and higher $\gamma_m$ will only be too easy to achieve. However, a cavity mirror with a very tiny mass of $10^{-15}$kg should be difficult to fabricate. But mechanical resonators of much lower mass have already been fabricated [68]. Moreover, there is nothing of *principle* which excludes such a mirror for an optical cavity because it can still support an optical beam waist. Besides, small masses are also required for mechanical resonators of very high frequencies [68] as in this case. One might also think that the very small time period of mirror oscillation ($10^{-7}$s) may be a barrier to the tomography of the cavity field using atoms. But cesium atoms with lifetime $\sim$ 10ns should be useful for this purpose.

We should now proceed to examine the prospects of implementing our experiment successfully in the microwave domain. In this domain the lowest possible values of $L$ and $m$ are already fixed to be 1cm and 0.1g. Thus constraint 3 implies that the maximum value $\omega_m/2\pi$ can take is $10^{-2}$ Hz. But this clearly makes constraints 1 and 2 impossible to satisfy unless

$$\theta\gamma_m < 10^{-14}\text{K s}^{-1}. \tag{3.25}$$

This value of the $\theta\gamma_m$ product lies well outside potentially realizable domains. Thus strictly speaking, an experiment of the kind proposed here would not achieve success in the microwave domain. The only way it could, would be to use a much smaller mass for the oscillating mirror. As such a mirror will not be able to support a microwave cavity mode, we would have to introduce it as a small mechanical resonator inside a cavity with fixed mirrors. This should be quite an interesting but different problem to study, because the cavity field–mechanical resonator interaction Hamiltonian in this case may be different.

## 3.8 Parameter regime required to test gravitationally induced collapse theories

We may describe the parameters used in the estimations so far as being potentially realizable. Let us now identify the range of parameters that would be required if one intends to extend the scope of our experiment to test the gravitationally induced objective reduction (OR) models of the type proposed by Penrose and Diosi [82]. According to this model the decoherence rate will be

$$\gamma_{OR} \sim \frac{E}{\hbar} \tag{3.26}$$

where $E$ is the mean field gravitational interaction energy. We will examine only the case in which $\Delta x < R$, where $R$ is the dimension of the object, as this is the easiest to achieve experimentally. In the case of a spherical geometry of the mirror (we use such an assumption just for an estimate) $E \sim Gm^2(\Delta x)^2/R^3$. Using the expression for $\Delta x$ from Eq.(3.15) and substituting $R^3$ by $m/D$, where $D$ is the density of the object, one gets,

$$\gamma_{OR} \sim \frac{n^2\omega_0^2}{L^2\omega_m^4 m} G\hbar D. \tag{3.27}$$

Comparison of Eqs.(6.47) and (3.27) shows that decoherence rates according to EID and OR have exactly the same dependence on parameters $L, m, \omega_m, \omega_0$ and $n$ and therefore one cannot distinguish between these models by varying any of these parameters (Of course this statement is true only for a spherical geometry of the mirror). In order to reduce the effect of EID to such an extent that effects of OR become prominent one needs

$$G\hbar D > K_{\mathrm{B}}\theta\gamma_m. \tag{3.28}$$

Taking the density $D$ of a typical solid to be of the order of $10^3$ kg m$^{-3}$, one gets

$$\theta\gamma_m < 10^{-19}\mathrm{K\ s}^{-1}. \tag{3.29}$$

Currently, temperature of a macroscopic object can be brought down to at most 0.1 K and a fairly optimistic estimate of $\gamma_m$ is $10^{-2}\mathrm{s}^{-1}$ (a mechanical oscillator that dissipates its energy in about 100 s). Thus an improvement of the product $\theta\gamma_m$ by sixteen orders of magnitude would be necessary to test OR using our scheme.

## 3.9 Conclusions

In conclusion, we note that the experiment we have proposed just applies Schrödinger's method to a realistic system of a cavity field and a macroscopic moving mirror. Of course, to achieve Schrödinger's original aim (creating a macroscopic superposition), our scheme will have to be combined with a scheme that prepares the mirror in a pure coherent state. However for testing the rules of decoherence of a macroscopic object, our scheme is sufficient. A special feature of our scheme is that the microscopic system (i.e the cavity field) which creates the mixture of Schrödinger's cats is itself being used later as a kind of meter to read the decoherence that the mirror undergoes while the two systems are entangled. We believe that this is a canonical system for systematic probing of decoherence and offers an extensive scope of further work from both theoretical and experimental points of view. Modelling the EID of our system starting from the very first principles (assuming different types of coupling and environment) is necessary to check the accuracy of formula (6.47). A variant of our set up in which a small mechanical resonator is introduced inside a cavity should be an interesting problem to study. There can be an entire range of masses for such a mechanical oscillator introduced inside a cavity: starting from trapped ions [71], to trapped molecules and nanoparticles [95], to the smallest mechanical resonators that can be fabricated [68]. There can also be other variants of our proposal such as extending schemes in which an atom trapped in a cavity produces Fock states [91] to include the effects of a moving mirror.

The experimental challenge is in either of the two directions: to improve the reflectivity of existing macroscopic mirrors or to decrease the mass of the mirrors without decreasing the existing reflectivity. There is nothing of *principle* which prohibits increasing the reflectivity of a macroscopic mirror, nor any *fundamental* connection between mirror reflectivity and mass (as long as the mirror can support the beam waist). So we don't see any real obstacle in progress directed at the possible realization of our proposal.

Let us briefly clarify the exact relevance of our experiment. It is much more than detecting the presence of a thermal environment around the system. We are really interested

in detecting *how* this environment causes the demise of the coherence between superposed spatially separated states of a macroscopic object. This is interesting, because *irrespective* of any role it plays in the foundations of quantum mechanics, thermal environment induced decoherence is a *real* phenomenon yet to be systematically probed in the macroscopic domain. As far as the relevance of mentioning OR in this chapter is concerned, it is mainly to emphasize the degree of technological improvement necessary in order to bring such effects into the observable domain. This technological feat should be taken up as a challenge unless shown to be impossible by some fundamental principle of physics.

To conclude the chapter, we would like to highlight the role played by entanglement in our proposal. It is because of the existence of entanglement, that one can convert a microscopic coherence to a coherence between states which involve a macroscopic object being in different positions. Next, the entanglement is responsible for the transfer of the motional decoherence of the mirror to a coherence loss between states $|0\rangle_c$ and $|1\rangle_c$ of the cavity field. This enables the use of the cavity field as a meter to study the motional decoherence of the mirror.

# Chapter 4

# Multiparticle entanglement swapping

## 4.1 Introduction

In this chapter we shall describe yet another application of entanglement in state preparation – in this case the preparation of a joint state of several remote objects. For this we require entangled pairs or groups of particles which are spatially separated. Numerous known applications of spatially separated entangled pairs of particles are cryptography based on Bell's theorem [17, 96], teleportation [19], superdense coding [18], cheating bit commitment [97] and, of course, simply testing Bell's inequalities [3, 4, 98, 99]. Three or more spatially separated particles in an entangled state (such as a GHZ state [9, 10, 100]) have varied applications as well. A well known application is in testing nonlocality from new directions [9, 10, 100, 101, 102]. More recently, applications such as reducing communication complexity [103], quantum telecomputation [104] and quantum secret sharing [105] have been suggested. An idea of cryptography with GHZ states [106] has also been suggested earlier. This essentially means that multiparticle entangled states present possibilities of implementing networked cryptographic conferencing [107, 108] in an alternative way and we shall elaborate briefly on this aspect in section 4.5 of this article. In addition,

we shall show (by generalizing superdense coding [18] to the multiparticle case), that the use of multiparticle entangled states can allow one to read messages from more than one source through a single measurement. In short, distributed entangled particles in a multiparticle entangled state may be extremely useful for certain forms of quantum communication. Hence it will become necessary to distribute entangled N-tuplets between nodes of communication networks if any set of users of the network wish to harness the benefits of these forms of quantum communication. The prime focus of this chapter is to present a method of manipulating entanglement in multiparticle systems that can accomplish this task by just a local measurement if each of the users share singlets with a central node prior to that. In a sense, it allows one to construct a Biham-Huttner-Mor (BHM) like telephone exchange [108], with the added capability of setting up multiparticle entanglement between particles belonging to different users of the network.

Our scheme is actually obtained by generalizing an earlier scheme of Zukowski et al [109] known as *entanglement swapping* to the multiparticle case. Building on an earlier proposal by Yurke and Stoler [110] of entangling particles originating from independent sources, they showed that through entanglement swapping one can entangle particles which do not even share any common past. Their aim was to realize 'event ready detectors' for Bell experiments. We will show how our form of multiparticle entanglement manipulation differs from the method proposed recently by Zeilinger et al [111] for the generation of multiparticle entangled states and yet can be used for the same purpose. We begin by briefly recapitulating the original entanglement swapping scheme of Zukowski et al [109] in Section.4.2.

## 4.2 The entanglement swapping scheme of Zukowski et al

In terms of a binary variable $u_i \in \{0, 1\}$ and its complement $u_i^c$ (defined as $1 - u_i$), one can write down any Bell state (not normalized) of two particles $i$ and $j$ as

$$|\Psi(i,j)\rangle_{\pm} = |u_i, u_j\rangle \pm |u_i^c, u_j^c\rangle \ . \tag{4.1}$$

In the above it is understood that $|u_i\rangle$ and $|u_i^c\rangle$ are two orthogonal states of a two state system. Consider the initial state of four particles 1,2,3 and 4 to be

$$\begin{aligned} |\Psi(1,2)\rangle_+ \otimes |\Psi(3,4)\rangle_+ &= |u_1, u_2, u_3, u_4\rangle \\ &+ |u_1^c, u_2^c, u_3, u_4\rangle \\ &+ |u_1, u_2, u_3^c, u_4^c\rangle \\ &+ |u_1^c, u_2^c, u_3^c, u_4^c\rangle \ . \end{aligned} \tag{4.2}$$

That is, particles 1 and 2 are mutually entangled (in a Bell state), and particles 3 and 4 are mutually entangled (also in a Bell state). When we conduct a measurement of the Bell operator (defined in [99]) on particles 2 and 3 (which projects particles 2 and 3 to a Bell state), then the joint state of the four particles become either of the following four :

$$|\Phi_1\rangle = (|u_2, u_3\rangle + |u_2^c, u_3^c\rangle) \otimes (|u_1, u_4\rangle + |u_1^c, u_4^c\rangle) \ , \tag{4.3}$$

$$|\Phi_2\rangle = (|u_2, u_3\rangle - |u_2^c, u_3^c\rangle) \otimes (|u_1, u_4\rangle - |u_1^c, u_4^c\rangle) \ , \tag{4.4}$$

$$|\Phi_3\rangle = (|u_2, u_3^c\rangle + |u_2^c, u_3\rangle) \otimes (|u_1, u_4^c\rangle + |u_1^c, u_4\rangle) \ , \tag{4.5}$$

$$|\Phi_4\rangle = (|u_2, u_3^c\rangle - |u_2^c, u_3\rangle) \otimes (|u_1, u_4^c\rangle - |u_1^c, u_4\rangle) \ . \tag{4.6}$$

To derive the above, only the orthogonality of $|u_i\rangle$ and $|u_i^c\rangle$ is required. In other words, no matter what the outcome is, the particles 1 and 4 are now in one of the Bell states . Whereas prior to the measurement, the Bell pairs were (1,2) and (3,4), after the measurement the Bell pairs are (2,3) and (1,4). It can easily be shown that the same fact would hold true even if (1,2) and (3,4) started in some other Bell states than those in Eq.(4.2). A pictorial way of representing the above process is given in Fig.4.1.

It is clear that the most interesting aspect of this scheme is that particles 1 and 4 which do not share any common past are entangled after the swapping.

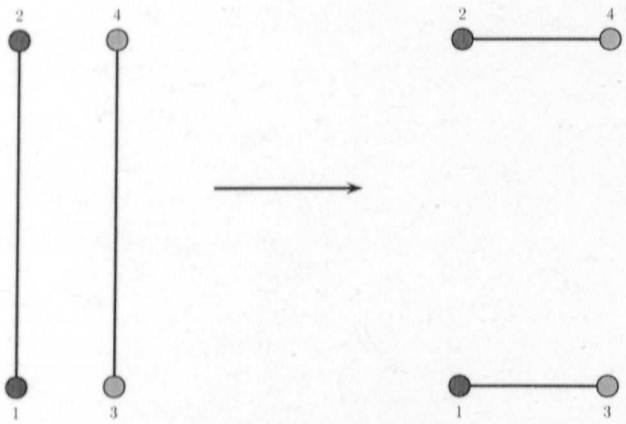



Figure 4.1: The swapping of entanglement between pairs of particles due to a Bell state measurement on two of them is shown. The bold lines connect particles in Bell states and the dashed lines connect particles on which the Bell state measurement is made

## 4.3 A multiparticle generalization of entanglement swapping

The method of entanglement manipulation described in the previous section can readily be generalized to cases where a greater number of particles are involved. An explicit scheme that generalizes entanglement swapping to the case of generating a 3-particle GHZ state from three Bell pairs has already been presented by Zukowski et al [112]. But it should be interesting to demonstrate that their entanglement swapping scheme may actually be significantly generalized. But before that we need to introduce some terminology. In this chapter we shall need to deal extensively with N-particle states of the type

$$|\psi\rangle = \prod_{i=1}^{N} |u_i\rangle \pm \prod_{i=1}^{N} |u_i^c\rangle, \tag{4.7}$$

where $u_i$ stands for a binary variable $\in \{0, 1\}$ and $u_i^c = 1 - u_i$. For the N=2 they reduce to the Bell states and for N = 3 and 4 they represent the GHZ states. For a general N we shall be calling them cat states. We shall show that the entanglement swapping scheme of Zukowski et al can be generalized to the case of starting with cat states involving any number of particles, doing local measurements by selecting any number of particles from

the different cat states and also ending up with cat states involving any number of particles. To see that consider an initial state in which there are $N$ different sets of entangled particles in cat states. Let each of these sets be labelled by $m$ (where $m = 1, 2, .., N$), the $i$th particle of the $m$th set be labelled by $i(m)$ and the total number of particles in the $m$th set be $n_m$. Then the initial state can be represented by

$$|\Psi\rangle = \prod_{m=1}^{N} |\Psi\rangle_m, \tag{4.8}$$

in which each of the cat states $|\Psi\rangle_m$ is given by

$$|\Psi\rangle_m = \prod_{i=1}^{n_m} |u_{i(m)}\rangle \pm \prod_{i=1}^{n_m} |u^c_{i(m)}\rangle \tag{4.9}$$

where the symbols $u_{i(m)}$ stand for binary variables $\in \{0, 1\}$ with $u^c_{i(m)} = 1 - u_{i(m)}$. Now imagine that the first $p_m$ particles from all the entangled sets are brought together (i.e a total of $p = \sum_{m=1}^{N} p_m$ particles) and a joint measurement is performed on all of them. Note that the set of all cat states of $p$ particles forms a complete orthonormal basis. Let the nature of the measurement on the selected particles be such that it projects them to this basis. Such a basis will be composed of states of the type

$$|\Psi(p)\rangle = \prod_{m=1}^{N} \prod_{i=1}^{p_m} |u_{i(m)}\rangle \pm \prod_{m=1}^{N} \prod_{i=1}^{p_m} |u^c_{i(m)}\rangle. \tag{4.10}$$

By simply operating with $|\Psi(p)\rangle\langle\Psi(p)|$ on $|\Psi\rangle$ of Eq.(4.8), we find that the rest of the particles (i.e those not being measured) are projected to states of the type

$$|\Psi(\sum_{m=1}^{N} n_m - p)\rangle = \prod_{m=1}^{N} \prod_{i=p_m+1}^{n_m} |u_{i(m)}\rangle \pm \prod_{m=1}^{N} \prod_{i=p_m+1}^{n_m} |u^c_{i(m)}\rangle, \tag{4.11}$$

which represents a cat state of the rest of the particles. In a schematic way the above process can be represented as

$$\prod_{m=1}^{N} |E(n_m)\rangle \rightarrow |E(p)\rangle \otimes |E(\sum_{m=1}^{N} n_m - p)\rangle \tag{4.12}$$

where $|E(n)\rangle$ denotes a $n$ particle cat state. As a specific example, in Fig.4.2, we have shown the conversion of a collection of two Bell states and a 3 particle GHZ state to a 3

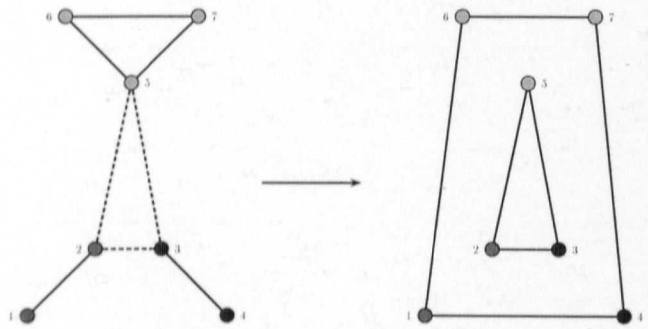


Figure 4.2: The conversion of two Bell states and a 3 particle GHZ state to a 3 particle GHZ state and a 4 particle GHZ state due to a GHZ state projection on three particles (one taken from each of the initially entangled sets) is shown. The bold lines connect mutually entangled particles and the dashed lines connect particles on which the GHZ state projection is made.

particle GHZ state and a 4 particle GHZ state due to a projection of 3 of these particles to a 3 particle GHZ state.

As must be evident from Fig.4.2, there is a general pencil and paper rule for finding out the result when our method of entanglement manipulation is applied to a certain collection of cat states of particles. One just has to connect the particles being measured to frame a polygon and those not being measured to frame a complementary polygon. These two polygons represent the two multiparticle cat states obtained after the manipulation.

## 4.4 Establishing multiparticle entanglement between particles located at different nodes of a communication network

We now describe how our method of multiparticle entanglement manipulation can be used to set up entanglement between particles belonging to N users in a communication network. To begin with, each user of the network needs to share entangled pairs of particles (in a Bell

state) with a central exchange. Consider Fig.4.3: A, B, C and D are users who share the Bell pairs (1,2), (3,4), (5,6) and (7,8) respectively with a central exchange O. Now suppose that A, B and C wish to share a GHZ triplet. Then a measurement which projects particles 2, 3 and 5 to GHZ states will have to be performed at O. Immediately, particles 1, 4 and 6 belonging to A, B and C respectively will be reduced to a GHZ state. In a similar manner one can entangle particles belonging to any N users of the network and create a N particle cat state.

The main advantages of using this technique for establishing entanglement over the simple generation of N particle entangled states at a source and their subsequent distribution are as follows.

(A) Firstly, each user can at first purify [28, 29, 113] a large number of partially decohered Bell pairs shared with the central exchange to obtain a smaller number of pure shared Bell pairs. These can then be used as the starting point for the generation of any types of multiparticle cat states of the particles possessed by the users. The problems of decoherence during propagation of the particles can thus be avoided in principle. Also the necessity of having to purify N-particle cat states can be totally evaded. Purification of singlets followed by our scheme will generate N-particle cats in their purest form.

(B) Secondly, our method allows a certain degree of freedom to entangle particles belonging to any set of users only if the necessity arises. It may not be known in advance exactly which set of users will need to share a N particle cat state. To arrange for all possibilities in an a priori fashion would require selecting all possible combinations of users and distributing particles in multiparticle entangled states among them. That is very uneconomical. On the other hand, generating entangled N-tuplets at the time of need and supplying them to the users who wish to communicate is definitely time consuming.

It is pertinent to compare our scheme with the BHM cryptographic network with exchanges [108]. There are two main differences.

(A) Firstly, they used a time reversed EPR scheme for setting up the connections and had quantum memories to protect their states. They had, of course, compared their scheme with one that uses the original entanglement swapping of two Bell pairs to establish connections.

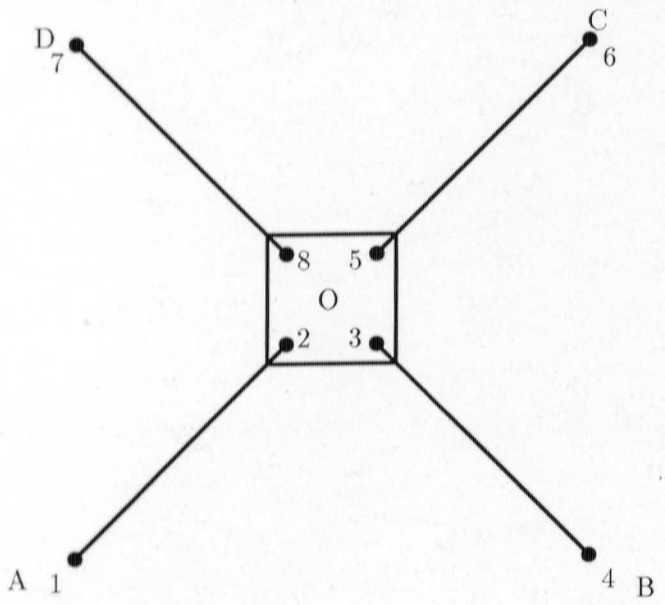



Figure 4.3: The configuration used for the distribution of entanglement. Initially users A,B,C and D share Bell pairs with the central exchange O. Subsequently, a local measurement at O is sufficient to entangle particles belonging to any subset of users chosen from A, B, C and D.

We, use a multiparticle generalization of entanglement swapping for our connections and are thereby unable to take advantage of any type of quantum memories.

(B) Secondly, their prime focus was to connect any pair of users of a N-user network on request, while our main focus is to establish multiparticle entangled states of the particles possessed by the users.

## 4.5 Communication schemes using distributed multiparticle entanglement

So far we have described how particles belonging to several users in a network can be put in a multiparticle entangled state. We now describe how such a situation can be useful. The uses that readily come to mind are tests of nonlocality for many particle entangled states [100, 101, 102]. Reducing the communication complexity of certain functions [103] may also be a field of application of multiparticle entangled states. We describe here two possible applications in communications. These uses would provide motivations for constructing a quantum telephone exchange.

### 4.5.1 Cryptographic conferencing

Consider the following situation. A certain group of users may need to have a secret meeting. Let the meeting be subject to the following two conditions:

(1) All members of the group must be able to decrypt the encrypted public messages broadcasted by any member of the group.

(2) Nobody outside the group must be able to decrypt the encrypted public messages broadcasted by members of this group.

Such requirements may arise when the members of a committee are to take some decision which has to have the consent of everybody within the committee, but must be kept secret from the rest of the world. One can regard this as a special case of networked *cryptographic conferencing* [107, 108].To establish the secret key for this type of meeting, the committee can employ either of two possible options. The first one is to use simple

two-user cryptographic key distributions [17, 96, 114], to set up random keys shared by each pair of users. Whenever a certain user intends to broadcast a secret message for the group, she has to encrypt it using a separate key for each of the other users of the group. However, for the type of conferencing considered here, this is not a good option because of two reasons. Firstly, the broadcaster has to encrypt the same message several times using different keys. Secondly, the broadcaster will have the freedom to send different messages to different members of the group and thereby mislead a subset of the group. A better option is that the users within the group share particles in multiparticle cat states. To generate the random key, all users conduct measurements in two nonorthogonal bases on the particles belonging to them. The results of those measurements in which the bases chosen by all the users coincide, are used to establish the secret key known to all the users within the group. This can then be used to frame encrypted messages that can be decrypted by an user if and only if she is a member of the group. If the users are sure about the fact that they are sharing a perfect N-particle cat state, they can even use a single basis to perform their measurements and thereby reduce the wastage of bits due to the noncoincidence of all their bases. It is known that the 3 particle GHZ states are eigenstates of certain operators of the form $S_x S_x S_y$ [100] and by measuring the eigenvalues of these operators one can verify whether the state is intact or corrupted by some eavesdropper. It should be mentioned here that the idea of using GHZ states for cryptography is not entirely new but has been presented earlier [106].

### 4.5.2 A multiparticle generalization of superdense coding

Consider the following scenario. There are $N+1$ users (all spatially separated) in a network and one of them (the receiver) is recieving messages from all the rest (the senders). It is known, that at a given instant of time, *only one* out of these $N$ senders would need to send 2 bits of information to the receiver and the rest would be content with sending only a single bit. But apriori, it is *not known exactly which sender requires to send the two bits of information.* If we want to *minimize the total number of qubits stored and transmitted* in the above process, what is the most efficient way of doing this? The receiver could

share a separate Bell pair with each of the senders and the sender who needs to send 2 bits actually uses this to do superdense coding. The rest just use their telephones (classical channel). This would entail storing $2(N-1)$ qubits unnecessarily (without being used in any communication). Thus a better strategy (storing less number of unnecessary qubits) is needed. This can be done using multiparticle entanglement. Suppose the $N+1$ users are sharing a $N+1$ particle maximally entangled state, possessing one particle each. Just before the instant of communication, they come to know which of the $N$ senders needs to send two bits (they can make each other aware of this knowledge by calling each other by telephones). The sender transmitting 2 bits of information is then allowed 4 possible unitary operations at his/her disposal, while each of the others will have any of 2 possible unitary operations at their disposal. They will be encoding bits onto the particles possessed by them through these unitary operations. In that way, one of the senders will be encoding 2 bits on his/her particle, while each of the others will be encoding 1 bit each. Now, the unitary transformations must be so chosen that for each possible combination of unitary transformations performed by the senders, the state of the $N+1$ particles go to a different member of the set of cat states of $N+1$ particles. This is certainly possible because the $N$ senders are allowed to perform $4 \times 2 \times 2 \times ... \times 2 = 2^{N+1}$ different combinations of unitary operations on the initial $N+1$ particle cat state and there are exactly $2^{N+1}$ states in the set of cat states of $N+1$ particles. After performing their unitary operations, each of the $N$ senders send their particles to the receiver. The receiver then performs a measurement on the $N+1$ particles possessed by him/her, which identifies the particular cat state in which these particles are. Since each of these cat states correspond to a different combination of unitary transformations performed by the senders, he/she can learn about the messages sent by each of the senders from the outcome of his measurement. All the $N+1$ qubits stored are thus used, and this prevents the unnecessary storage of extra qubits for not knowing which sender will need to send two bits of information.

Another motivation for a multiparticle version of superdense coding can be the fact that the receiver can get to know the messages from all the senders through a single measurement. Can this speed up the rate at which the receiver can read messages and thereby the rate

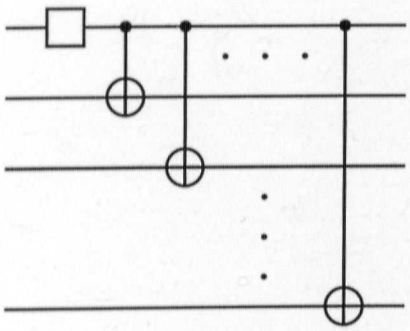


Figure 4.4: The general circuit to generate a $N$ particle cat state from disentangled inputs is shown. One can generate any desired state chosen from the basis of cat states of $N$ particles by inputting an appropriate combination of zeros and ones at the input port on the left hand side. When we input any specific $N$ particle cat state from the right hand side, then by measuring the bits obtained on the left hand side, one can conclude which cat state was put in. In other words, when run in the reverse direction, the circuit represents a measuring device for $N$ particle cat states. The box in the figure stands for a Hadamard transformation.

at which he/she gains information? Let us compare the rate of information recieved by the receiver in the above scheme (with a $N+1$ particle entangled state), with the case when the receiver performs a superdense coded communication [18] with each of the $N$ senders separately. For that we have to refer to the quantum circuits needed to perform measurements of multiparticle cat states. The circuit shown in Fig.4.4 does exactly this when run in the reverse direction (i.e inputs from the right and output from the left). The vertical lines are Controlled Nots [115] and the box is a unitary transformation equivalent to a rotation on the Bloch sphere known as the Hadamard transformation [115] (For optical implementations of elementary gates, see e.g. [116]). Thus, if the receiver was using our scheme then he/she would need to measure a $N+1$ particle cat state and therefore require $N$ Controlled Nots and one Hadamard transformation gate. He/she learns $N+1$ bits of information from this measurement. Thus if a Hadamard transformation takes time $t_h$ and a Controlled Not takes time $t_c$, then the rate of information gain is

$$r_1 = \frac{N+1}{t_h + Nt_c} \tag{4.13}$$

bits per unit time. On the other hand, if the receiver was separately doing superdense coded communication with each of the $N$ senders, he/she would need to do $N$ Bell state measurements which require one Controlled Not and one Hadamard transformation each. He/she gains $2N$ bits of information from this. Thus the rate of information gain in this case is

$$r_2 = \frac{2N}{N(t_h + t_c)}. \tag{4.14}$$

If one assumes that the time-scale of operation of all quantum gates can be brought to the same order of magnitude (i.e $t_h = t_c$), then $r_2 = r_1$. However if one defines efficiency as rate divided by the number of qubits used (considering qubits as an important resource), then our method is definitely more efficient because it requires only $N+1$ qubits as opposed to superdense coded communication with each sender, which requires $2N$ qubits in total.

Of course, the rate of information transfer could be made far more faster than ours if only one of the senders did superdense coding with the receiver and the rest of the senders simply communicated with the receiver via classical channels. Then there would only be one

Hadamard gate and one Controlled Not gate involved. However, this increase of the rate of information gain comes at the expense of having to know before hand, which sender needs to send two bits of message. The use of multiparticle entanglement (as in our scheme), gives the flexibility of knowing which sender needs to send two bits much after the distribution of entangled qubits have taken place.

## 4.6 Entangled states of higher number of particles from entangled states of lower number of particles

Entangled states involving higher number of particles can be generated from entangled states involving lower number of particles by employing our scheme. The basic ingredients which we need are GHZ (three particle maximally entangled) states and a Bell state measuring device. Let us describe how to proceed from a $N$ particle cat state to a $N+1$ particle cat state. One has to take one particle from the $N$ particle cat state and another particle from a GHZ state and perform a Bell state measurement on these two particles. The result will be to put these two particles in a Bell state and the remaining $N+1$ particles in a cat state . Symbolically, the way of proceeding from a $N$ particle cat state to a $N+1$ particle maximally entangled state is given by

$$|E(N)\rangle \otimes |E(3)\rangle \overset{\text{Bell State Meas.}}{\longrightarrow} |E(N+1)\rangle \otimes |E(2)\rangle.$$

An example of proceeding from a 4 particle cat state to a 5 particle maximally entangled state by the above procedure is shown in Fig.4.5 .

As far as the question of generating the GHZ state, which is a basic ingredient, is concerned, one can perhaps use the method suggested by Zeilinger et al. [111] which is described in the next section. Alternatively, one can generate GHZ states using our

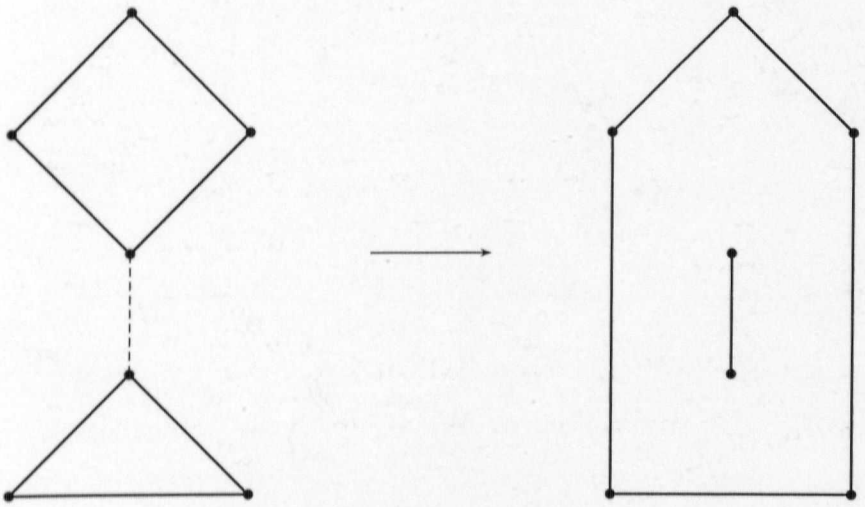


Figure 4.5: Building of a 5 particle entangled state from a 4 particle entangled state using a GHZ state and a Bell state measurement

method by starting from three Bell pairs and performing a GHZ state measurement taking one particle from each pair. An explicit scheme to produce 3-particle GHZ states from 3 entangled pairs have been suggested by Zukowski et al. [112] earlier.

## 4.7 Comparison with the method of Zeilinger et al.

We would now like to compare our method of generating multiparticle entangled states to that of Zeilinger et al [111]. We describe how the Zeilinger group's scheme works in the spirit of the former sections, i.e. using projections onto the Bell states. We then use simple quantum computational networks, consisting of Controlled Not and Not operations [115], to present measurements in the Bell and generalized Bell basis. This quantum computational approach, as we will see shortly, immediately reveals a basic similarity between the two schemes of generating multiparticle entangled states and shows precisely how they differ.

Assume that we start with two entangled pairs $(1,2)$ and $(3,4)$ of two-level systems in a state

$$
\begin{aligned}
|\Psi(1,2)\rangle \otimes |\Psi(3,4)\rangle &= (|0,0\rangle + |1,1\rangle) \otimes (|0,0\rangle + |1,1\rangle) \\
&= |0,0,0,0\rangle + |0,0,1,1\rangle \\
&+ |1,1,0,0\rangle + |1,1,1,1\rangle \ . \qquad (4.15)
\end{aligned}
$$

As before we omit the normalization. The fact that we use this particular, "computational" basis $(0,1)$ does not limit the generality of our method, but is more convenient in describing the action of quantum gates. Suppose now that we affect a Controlled Not gate between qubits 2 (control) and 3 (target), i.e. qubit 3 changes its value only if qubit 2 is in the state $|1\rangle$. The above state then becomes:

$$
|0,0,0,0\rangle + |0,0,1,1\rangle + |1,1,1,0\rangle + |1,1,0,1\rangle \qquad (4.16)
$$

Now we measure the value of the third qubit. We have two possibilities depending on whether the outcome of this measurement is 0 or 1:

$$
|0,0,0\rangle + |1,1,1\rangle \qquad \text{outcome} \quad 0 \qquad (4.17)
$$

$$
|0,0,1\rangle + |1,1,0\rangle \qquad \text{outcome} \quad 1 \qquad (4.18)
$$

So, by the action of a single Controlled not gate and a measurement , we can create a GHZ state out of two pairs initially in a Bell state. A network for this operation is given in Fig.4.6.

Now this directly generalizes to more entangled particles. Suppose that we have a group of $N$ entangled particles and $M$ entangled particles, each one in a cat state. It is then enough to perform a Controlled Not operation between a particle from the first and a particle from the second group, and then a measurement of the target particle. The end product will clearly be a maximally entangled state of $N + M - 1$ particles and a single particle disentangled from the rest. This completes our description of Zeilinger et al's scheme.

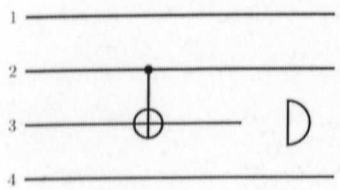



Figure 4.6: Implementation of Zeilinger's scheme using quantum gates. The production of a GHZ state with the use of a controlled not, and a measurement is shown.

Let us now compare this to our scheme of generating multiparticle entanglement. The basic ingredient in our protocol is a projection onto a cat state of $N$ particles. The network for a measurement in this basis is an inverse of the network which generates cat state from a disentangled input in the computational basis. It is simply the circuit of Fig.4.4 run in the reverse direction. In order to generate a $N+1$ particle cat state , we have to do a Bell state measurement selecting one particle from the GHZ state and another particle from a $N$ particle cat state. A Bell state measurement will require a Controlled Not gate and a Hadamard transformation gate, as is evident from Fig.4.4 , specializing to the case of two inputs. Meanwhile, to generate a $N+1$ particle cat state using Zeilinger group's scheme one may require to start with a $N$ particle cat state and a Bell state and will have to perform a Controlled Not choosing one particle from each set followed by a measurement on one of the particles. Hence as far a comparing our scheme with Zeilinger group's scheme is concerned, in the case of generating $N+1$ particle cat state from a $N$ particle cat state, our scheme has just one extra Hadamard transformation. However, our method necessarily requires a GHZ state for proceeding from $N$ to $N+1$ particle cat state, while for the scheme of Zeilinger et al, Bell states are sufficient. In that sense the latter method is simpler. However as far as setting up entanglement between particles belonging to distant

users is concerned, our method is necessary. For example, if the operator at O in Fig.4.3 performed the manipulation described by the Zeilinger group manipulation on particles 2 and 3, then 1, 2 and 4 will go into a GHZ state and essentially the subsystem of particles 1 and 4 will be in a disentangled state. This method will thus not be applicable to setting up entanglement between particles belonging to distant users.

## 4.8 Conclusion

In this chapter we have described a scheme for manipulation of multiparticle entangled states and have demonstrated its potential applications. Our analysis remains at a very schematic and theoretical level, and practical implementations have not been considered. The direction from which practical implementations of our scheme and similar schemes may be approached is uncertain at present. There is, however, a number of possible practical implementations involving entangled photons [111, 116], entangled ions in a linear trap [117] and entangled nuclear spins in NMR [118]. In general, any medium that proves to be useful for quantum computation will immediately support implementation of the multiparticle entanglement manipulations described here. In chapter 7 we will describe a physical implementation of quantum teleportation [19] and that same setup would be useful in constructing a quantum telephone exchange. We leave out a more rigorous analysis of the utility of a quantum telephone exchange with considerations of the costs of qubit storage and distribution and the decoherence in the channels during distribution, for the future. In the next chapter, we show how entanglement swapping can be helpful in the physical implementation of another interesting manipulation of entanglement, namely, entanglement concentration.

# Chapter 5

# Entanglement concentration via entanglement swapping and conserved entanglement

## 5.1 Introduction

In the last chapter, we described entanglement swapping [109] and generalized it to the multiparticle case. This is an entanglement manipulation finding use in the distribution of entanglement between distant parties. There exists another manipulation of entanglement which upgrades the quality of entanglement shared between distant parties. In this type of entanglement manipulation, local actions and classical communication are used by two distant parties to distill a certain number of shared Bell states from a larger number of shared but less entangled states. When the initial shared but less entangled states are pure, this manipulation is termed as entanglement concentration [28, 113], while for the more general case of the initial shared states being mixed, the process is termed as entanglement purification or distillation [29, 30]. The importance of such a scheme in the distribution of entanglement is obvious as Bell pairs are essential for the implementation of quantum

communication schemes with perfect fidelity. Curiously, such an important procedure remains to be realized in an experiment. This stands in contrast with so many applications of the resource of entanglement [119] being tested by an active body of experimentalists. For example, polarization entangled photons have been used to demonstrate both dense coding [120] and teleportation [121]. Teleportation has also been realized using path-entangled photons [122] and entangled electromagnetic field modes [123]. More recently, entanglement swapping has been demonstrated experimentally with polarization entangled photons [124]. In this chapter, we will show that a simple variant of the entanglement swapping scheme can be viewed as a type of entanglement concentration procedure and has a physical realization with polarization entangled photons. Moreover, we show that there exists a certain measure of entanglement which remains conserved on average in this type of entanglement concentration. Note that, in this chapter, we will often use the terms entanglement concentration and entanglement purification in an interchangeable manner, though what we demonstrate is, in the strict sense, only the concentration of pure shared entanglement.

## 5.2 The scheme of entanglement concentration via entanglement swapping

Let pairs of photons $(1,2)$ and $(3,4)$ be in the following polarization entangled states

$$|\Phi(\theta)\rangle_{12} = \cos\theta|H_1, H_2\rangle + \sin\theta|V_1, V_2\rangle, \tag{5.1}$$

$$|\Phi(\theta)\rangle_{34} = \cos\theta|H_3, H_4\rangle + \sin\theta|V_3, V_4\rangle, \tag{5.2}$$

where the *phase angle* $\theta$ satisfies $0 < \theta < \pi/2$. There are a number of ways to prepare photons in such polarization entangled states. For example, one may first use type-II down conversion followed by suitable birefringent crystals to prepare two photons in the Bell state state $|\Phi\rangle^+ = |HH\rangle + |VV\rangle$ [125] (the other Bell states being $|\Phi\rangle^- = |HH\rangle - |VV\rangle$ and $|\Psi\rangle^\pm = |HV\rangle \pm |VH\rangle$). This may be followed by placing a dichroic element (such as the local filters described in Ref.[126]) which selectively absorbs any one of the polarization components (say $H$) along the path of one of the photons. In cases when this photon

exits the element unabsorbed, the pair of photons are in the state $e^{-\gamma L}|HH\rangle \pm |VV\rangle$ (not normalized), where $L$ is the length of the crystal and $\gamma$ is the absorption per unit length. Thereby states of the type given by Eqs.(5.1) and (5.2) with $\sin\theta = \sqrt{1/(1+e^{-2\gamma L})}$ is generated. This procedure may seem inefficient because of the possibility of the photon being absorbed by the dichroic element. However, due to the absence of two qubit logic gates for polarization entangled photons, there is no way to proceed unitarily from $|HH\rangle \pm |VV\rangle$ to the states given by Eqs.(5.1) and (5.2) and dissipative processes are necessary. Alternatively, one can use the recently suggested tunable ultrabright source of polarization entangled photons [127] to directly produce the states given in Eqs.(5.1)-(5.2). Photons 2 and 3 are brought together, while photons 1 and 4 are allowed to travel to separate distant locations as shown in Fig.5.1. If one now performs a Bell state measurement on photons 2 and 3, then immediately the states of the photons 1 and 4 become entangled. This effect, called entanglement swapping, has been tested for maximally entangled photons (when $\theta = \pi/4$) [124]. We shall refer to this tested case (i.e when maximally entangled photons are used) as standard entanglement swapping. For the more general case of an arbitrary $\theta$, the combined state of the photons 1 and 4 is projected to either of the following four states, depending on the outcome of the Bell state measurement on photons 2 and 3:

$$|\Phi'(\theta)\rangle_{14}^{+} = \frac{1}{N}(\cos^2\theta|H_1,H_4\rangle + \sin^2\theta|V_1,V_4\rangle), \tag{5.3}$$

$$|\Phi'(\theta)\rangle_{14}^{-} = \frac{1}{N}(\cos^2\theta|H_1,H_4\rangle - \sin^2\theta|V_1,V_4\rangle), \tag{5.4}$$

$$|\Psi\rangle_{14}^{+} = \frac{1}{\sqrt{2}}(|H_1,V_4\rangle + |V_1,H_4\rangle), \tag{5.5}$$

$$|\Psi\rangle_{14}^{-} = \frac{1}{\sqrt{2}}(|H_1,V_4\rangle - |V_1,H_4\rangle), \tag{5.6}$$

where, $N = \sqrt{\cos^4\theta + \sin^4\theta}$. The probabilities to obtain the four states are

$$P(|\Phi'(\theta)\rangle_{14}^{+}) = P(|\Phi'(\theta)\rangle_{14}^{-}) = \frac{\cos^4\theta + \sin^4\theta}{2}, \tag{5.7}$$

$$P(|\Psi\rangle_{14}^{+}) = P(|\Psi\rangle_{14}^{-}) = \cos^2\theta\sin^2\theta, \tag{5.8}$$

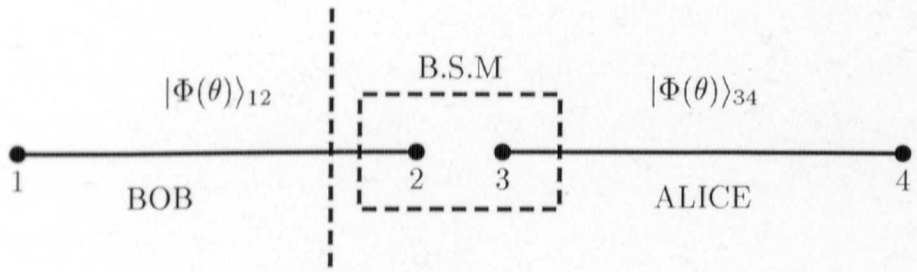



Figure 5.1: The figure illustrates the procedure of purification via entanglement swapping. The solid lines connect initially entangled photon pairs. The dashed line divides the set of photons to those held by Alice and those held by Bob. B.S.M denotes the local Bell state measurement done by Alice.

where the symbol $P(|\psi\rangle)$ is used to denote the probability of the state $|\psi\rangle$. We now proceed to explain the sense in which the above variant of standard entanglement swapping is a purification procedure. Say photons 2,3 and 4 are held by one party (Alice) and photon 1 is possessed by the other party (Bob) as shown in Fig.5.1. Now, Alice can change the magnitude of the entanglement she shares with Bob by doing a Bell state measurement on photons 2 and 3 and thereby projecting photons 1 and 4 to one of the states given by Eq.(5.3)-(5.6). In the cases when she projects photons 1 and 4 to either $|\Psi\rangle_{14}^{+}$ or $|\Psi\rangle_{14}^{-}$ (which are Bell states), she actually increases the magnitude of entanglement she shares with Bob. In the other cases she reduces the magnitude of entanglement she shares with Bob even further. If she initially shared a large enough ensemble of photons in the state $|\Phi(\theta)\rangle_{12}$ with Bob and applied the procedure described above on each shared pair separately, then she would be able to change the states of a certain fraction of the shared pairs to Bell states at the expense of degrading the entanglement of the other shared pairs even further. This qualifies as a type of purification procedure because local actions (by Alice) are used to concentrate the entanglement of a fraction of the shared states while the entanglement of the remaining fraction is being diluted, just as in other purification procedures [28, 29].

We should pause here briefly to mention a fact relevant from the experimental viewpoint. It is known that a complete Bell state measurement is not possible with only linear elements

[128]. However, a complete Bell state measurement is *not* really *necessary* to implement the above purification protocol. One only needs to be able to discriminate the states $|\Psi\rangle_{23}^{+}$ and $|\Psi\rangle_{23}^{-}$ from each other and from the rest of the Bell states, which can be done in existing experiments [120, 121, 109, 124]. The reason for this is that the photons 1 and 4 are projected to Bell states ($|\Psi\rangle_{14}^{+}$ or $|\Psi\rangle_{14}^{-}$) only when the outcome of the Bell state measurement on photons 2 and 3 is either $|\Psi\rangle_{23}^{+}$ or $|\Psi\rangle_{23}^{-}$. To verify whether the purification has indeed taken place, one simply has to pass the resultant Bell states of photons 1 and 4 through a Bell state analyser [120, 121, 109, 124].

## 5.3 A conserved measure of entanglement in concentration via swapping

An interesting feature of the original collective entanglement concentration procedure (called the "Schmidt projection method") described in Ref.[28] was that the average of the entropy of entanglement (the von Neumann entropy of the partial density matrix seen by either party) of all the shared pairs remained constant under purification (an asymptotic result). In the scheme described here, the average von Neumann entropy of entanglement of the shared pairs is, in fact, decreased. However, we shall show that there is a different measure of entanglement whose average remains conserved in this procedure of purification via entanglement swapping. This measure of entanglement is defined as the maximum probability with which two parties sharing a pure entangled state can convert it to a Bell state by classically communicating and performing local actions on their respective sides. As this is already the maximum probability, it can only remain constant or decrease under any set of local general measurements and classical communications (This is the basic criterion to be satisfied by any measure of entanglement [30, 31, 32, 33]). Thereby, it qualifies as a measure of entanglement which can be termed as *entanglement of single pair purification* (This measure, is however, not an additive measure). We shall denote this measure by $E_S$ and refer to it henceforth simply as entanglement.

We now proceed to show that $E_S$ is conserved in the purification process described

above. From the results of Lo and Popescu [97], it follows that the maximum probability with which a Bell state can be obtained by purifying a single entangled pair (in a pure state) is twice the modulus square of the Schmidt coefficient of smaller magnitude. In the case of the states given by Eqs.(5.1) and (5.2), this is simply $2\cos^2\theta$ if $\cos\theta$ is the smaller of the two Schmidt coefficients. Therefore, before the entanglement swapping, the average value of the entanglement shared between Alice (A) and Bob (B) is

$$\langle E_S \rangle_{AB} = 2\cos^2\theta. \tag{5.9}$$

After the entanglement swapping, when the shared states are those given by Eqs.(5.3)-(5.6) with probabilities given by Eqs.(5.7)-(5.8),

$$\begin{aligned}
\langle E_S \rangle_{AB} &= P(|\Phi'(\theta)\rangle_{14}^{+}) E_S(|\Phi'(\theta)\rangle_{14}^{+}) \\
&+ P(|\Phi'(\theta)\rangle_{14}^{-}) E_S(|\Phi'(\theta)\rangle_{14}^{-}) \\
&+ P(|\Psi\rangle^{+}) E_S(|\Psi\rangle^{+}) + P(|\Psi\rangle^{-}) E_S(|\Psi\rangle^{-}) \\
&= 2\cos^2\theta,
\end{aligned} \tag{5.10}$$

where $E_S(|\psi\rangle)$ denotes the entanglement of the state $|\psi\rangle$. Therefore, the ensemble average of the entanglement of single pair purification is a conserved quantity in the process of purification by entanglement swapping. This result also indicates that the purification via entanglement swapping is an optimal protocol for single pair entanglement purification, as the average entanglement of the purified pairs is equal to the original entanglement. Here, by optimality we mean the best combination of entangled states that can be finally obtained by the purification. A positive implication of this optimality is that the purification process can be separately repeated on the final subensembles, which turn out to be less entangled, without destroying any entanglement on average (though for that, one needs to be able to do complete Bell state measurements, for which schemes have been suggested [129]). If one continues this process indefinitely, in the limit of an infinite sequence, the final ensemble generated will comprise of a certain fraction of Bell pairs and a certain fraction of completely disentangled pairs. This fraction of Bell pairs should be equal to $2\cos^2\theta$ as the average of the

entanglement has been conserved in each step. Thus in the limit of an infinite sequence, the process of purification via entanglement swapping allows us to convert all the entanglement that can possibly be extracted by single pair purifications from the ensemble into Bell pairs.

Here, it is worthwhile to mention that a procedure for single pair purification called the "Procrustean method" had also been suggested in the original entanglement concentration chapter [28]. The Procrustean method also conserves $E_S$ and its fractional yield of Bell states is optimal (i.e equal to $E_S$). From the point of view of efficiency, our method lies somewhere between the Schmidt projection method (when it is implemented with two entangled pairs, but one pair totally belonging to Alice) and the procrustean method. Our method has a fractional yield of Bell states equal to the Schmidt projection method (with two entangled pairs), but the non-Bell state outcomes are also entangled. It is because of the extra entanglement of the non-Bell state outcomes that $E_S$ is conserved on average in our method of purification. Hence the improvement over the Schmidt projection method, brought in by entanglement swapping is *to make the non-Bell state outcomes entangled as well.*

## 5.4 The scheme viewed as a generalization of entanglement swapping

Next, we proceed to consider the case when photon pairs $(1,2)$ and $(3,4)$ are not in the same type of entangled state. Suppose, photons 1 and 2 start in the entangled state $|\Phi(\theta_1)\rangle_{12}$ and photons 3 and 4 start in the entangled state $|\Phi(\theta_2)\rangle_{34}$ (defined as in Eqs.(5.1) and (5.2)). Let the entanglement of the first photon pair be $E_S = \alpha$ and the entanglement of the second photon pair be $E_S = \beta$. Then a simple calculation shows that projecting photons 2 and 3 onto a Bell state basis projects the photons 1 and 4 to states $(\cos\theta_1 \cos\theta_2|H_1, H_4\rangle \pm \sin\theta_1 \sin\theta_2|V_1, V_4\rangle)$ and $(\cos\theta_1 \sin\theta_2|H_1, V_4\rangle \pm \sin\theta_1 \cos\theta_2|V_1, H_4\rangle)$ (not normalized) with specific probabilities. The average of the entanglement between the photons 1 and 4 after the projection turn out to be $\langle E_S\rangle = \min\{\alpha, \beta\}$. The manipulation

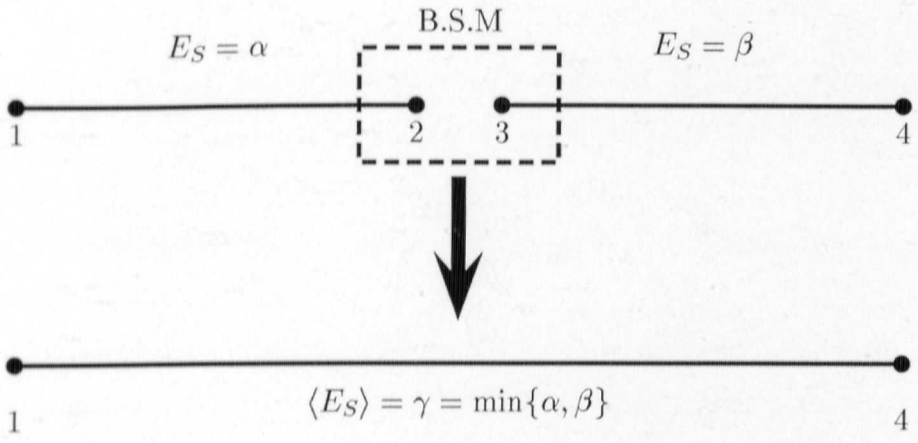



Figure 5.2: The figure shows the generalization of entanglement swapping to pure states with arbitrary entanglement.

of entanglement described above can be visualized as a step towards the complete generalization of entanglement swapping. The original scheme involved the use of two Bell states and Bell state measurements [109, 124]. In the last chapter we generalized it to cases when many particle Greenberger-Horne-Zeilinger (GHZ) states are used and many particle GHZ measurements are conducted. The procedure presented here is a generalization of the original scheme to the case when two particle pure states which are less entangled than Bell states are used, but measurements conducted are still Bell state measurements. This result is illustrated in Fig.5.2. One can get an intuitive feel of this result from the golden rule that entanglement, on average, cannot be increased under local actions and classical communications [31, 32, 33]. In the situation depicted in Fig.5.2, we have the freedom to choose which photons belong to Alice and which to Bob. For $\alpha < \beta$, we choose to allot the photon 1 to Bob and the rest to Alice, while for $\alpha > \beta$ we allot the photon 4 to Bob and the rest to Alice. Then a Bell state measurement on Alice's side cannot increase the entanglement she shares with Bob on average. As this initial entanglement is the smaller of the numbers $\alpha$ and $\beta$, the final average entanglement has to be smaller than or equal to $\min\{\alpha, \beta\}$. However, the fact that it is actually equal, is a peculiar feature of the entanglement swapping process.

One may envisage a situation in which Alice tries to purify the state $|\Phi(\theta_1)\rangle_{12}$ shared with Bob with the help of the state $|\Phi(\theta_2)\rangle_{34}$ (which we can call the purifier) in her possession. As long as $\beta < \alpha$, she degrades the entanglement shared with Bob on average, while when $\beta \geq \alpha$, she conserves the entanglement shared with Bob on average. Thus in order not to loose any entanglement the purifier state should have at least as much entanglement as the state to be purified. Moreover, the degree to which the entanglement is concentrated (i.e inhomogeneously redistributed among the four measurement outcomes) gets better as $\beta$ approaches $\alpha$. Bell pairs are produced *only* when $\beta$ *exactly equals* $\alpha$. Thus, as Alice increases the entanglement of her purifier, the degree of entanglement concentration increases yielding Bell pairs when $\beta$ reaches $\alpha$ (a criterion which can be called *entanglement matching*). On increasing $\beta$ further, the degree of concentration starts going down. When $\beta$ reaches unity (maximal entanglement), there is no concentration of entanglement (all the four outcomes have an entanglement equal to that of the original state: a situation equivalent to the perfect fidelity teleportation of an entangled state).

## 5.5 Conclusions

In this chapter we have shown that entanglement swapping can be used to purify single pairs of polarization entangled photons. Such a scheme may be achieved by an extension of an existing experiment [124]. In contrast, physical implementation of the entanglement purification schemes involving collective measurements (like the Schmidt projection method of Ref.[28]) will be difficult, as they would involve measurements on many photons at once. The absence of two qubit logic gates for polarization entangled photons also make purification procedures described in Ref.[29] difficult to realize. From this point of view, the method described here should be a positive first step in the direction of implementation of purification procedures. In the chapter we have also introduced a measure of entanglement for single pure pairs and demonstrated that this quantity is conserved in the above process. This makes purification via entanglement swapping interesting from a purely theoretical angle. The non-additive nature of the introduced measure implies that additivity is not an

essential requirement for an entanglement measure to have a physical interpretation. As a natural generalization of our measure one may use the maximum possible fractional yield of Bell states from various *finite* collections of shared pairs as physically relevant measures of entanglement. The physical relevance stems from the fact that in a real implementation of entanglement concentration one would always have access to only a finite number of systems. All the results presented in this chapter hold only for pure states. An extension to mixed states will not be trivial, as single pairs in such states cannot, in general, be purified [130]. However, it would still be interesting to investigate whether one can generalize the measure of entanglement presented here to some quantity which is conserved in entanglement swapping with mixed states.

# Chapter 6

# Mixed state dense coding and entanglement measures

## 6.1 Introduction

One of the many surprising applications of shared entanglement [119] is superdense coding introduced by Bennett and Wiesner [18]. In the simplest example of this protocol, two people (Alice and Bob) share a pair of entangled qubits (spin half particles or any other two state systems) in a Bell state. Alice can then perform any of the four unitary operations given by the identity $\mathbf{I}$ or the Pauli matrices $\sigma_1(\sigma_x), \sigma_2(\sigma_y)$ and $\sigma_3(\sigma_z)$ on her qubit. Each of these four unitary operations map the initial state of the two qubits to a different member of the Bell state basis. Clearly, these four orthogonal and therefore fully distinguishable states can be used to encode two bits of information. After encoding her qubit, Alice sends it off to Bob who can extract these two bits of information by performing a joint measurement on this qubit and his original qubit. This apparent doubling of the information conveying capacity of Alice's qubit because of prior entanglement with Bob's qubit is referred to as superdense coding (which we shall henceforth refer to as just dense coding). Dense coding has been implemented experimentally with polarization entangled photons [120]. Some generalizations of the scheme to pairs of entangled N-level systems

in non-maximally entangled states (as opposed to qubits in Bell states) [131, 132] and to distributed multiparticle entanglement (as described in chapter 4) have also been studied.

In the simplest example, the power of the method stems from the accessibility of all the four possible Bell states through local operations done by Alice alone on her qubit [18, 120]. Obviously this accessibility is related to the fact that the qubits shared by Alice and Bob are in an *entangled* state. So an important question to ask is: *In what way does the capacity of conveying information through dense coding depend upon the degree of entanglement of the initial shared pair of qubits?* Barenco and Ekert [131] and Hausladen *et al.* [132] have investigated this question when the initial shared entangled state is a pure state. Their analysis shows that the amount of information conveyed by the dense coding procedure decreases monotonically from its maximum value (two bits per qubit) with the decrease of the magnitude of the shared entanglement. It becomes one bit per qubit when the entanglement becomes zero.

Recently, there has been a lot of work in quantifying the entanglement of systems in mixed states [30, 31, 32, 33]. These measures of entanglement have their physical interpretation in the process of entanglement purification [28, 30, 29]. A natural question to ask is: *in what way does the capacity to do dense coding depend on the degree of entanglement as specified by these measures?* Answering such a question, in effect, would mean *linking up the apparently disconnected concepts of purification and channel capacity.* In this chapter we take a step in this direction by obtaining bounds on the number of bits of information conveyed per qubit (let us call this **C** after capacity) during dense coding in terms of the various measures of entanglement. It should be noted that **C** is a classical capacity as it quantifies number of bits of information, but the carriers of the information are quantum (qubits).

We also invert our results so that the value of **C** gives us information about the range within which the initial shared entanglement lies. In other words, bounds on entanglement measures (and hence on purification procedures) can be expressed in terms of the classical capacity **C**. This might be helpful, because, as we shall show, the classical capacity for dense quantum coding is readily calculable for certain special classes of dense coding protocols.

## 6.2 The Holevo function as a measure of C

Suppose, Alice has a set of mixed quantum states $W_i$ at her disposal to convey some classical information (sequences of ones and zeros) to Bob. Each state $W_i$ can be regarded as a separate letter. Also suppose that Alice sends the state $W_i$ to Bob with an *a priori* probability $p_i$. The ensemble that Alice uses to communicate with Bob is therefore given by

$$W = \sum p_i W_i. \tag{6.1}$$

In the above case, the average number of bits of information that Alice can convey to Bob per transmission of a letter state is bounded from above by the Holevo function [133]

$$H = S(W) - \sum p_i S(W_i), \tag{6.2}$$

where $S(\rho) = -\mathrm{Tr}\ \rho \log \rho$ denotes the von Neumann entropy of the state $\rho$ (Here, and throughout the rest of the chapter, log stands for $\log_2$). Using a different notation, the Holevo function can be rewritten as

$$H = \sum p_i S(W_i||W), \tag{6.3}$$

where $S(\sigma||\rho)$ stands for $\mathrm{Tr}\{\sigma \log \sigma - \sigma \log \rho\}$ and is known as the quantum relative entropy between the states $\sigma$ and $\rho$ [134]. It was recently shown that this bound can be achieved in the limit of an infinite ensemble by appropriate Block coding (grouping together and pruning long strings of letter states to represent messages) at Alice's end and appropriate measurements at Bob's end [135].

Now consider the case of dense coding. Alice and Bob initially share an entangled pair of qubits in some state $W_0$, which may be mixed. Alice then performs local unitary operations on her qubit to put this shared pair of qubits in either of the states $W_0, W_1, W_2$ or $W_3$. In general, Alice may use a completely arbitrary set of unitary operations to generate these states:

$$W_i = \mathbf{U_i} \otimes \mathbf{I}\ W_0\ \mathbf{U_i} \otimes \mathbf{I}. \tag{6.4}$$

In the above equation, $\mathbf{U_i}$ acts on Alice's qubit and $\mathbf{I}$ acts on Bob's qubit. By sending her encoded qubit to Bob, Alice is essentially communicating with Bob using the states

$W_0, W_1, W_2$ and $W_3$ as separate letters. The number of bits she can communicate to Bob using this procedure is thus bounded by the holevo function $H$ given in Eq.(6.3). Moreover, if some block coding is done on a large enough collection of qubits in addition to the dense coding, then the number of bits of information communicated is equal to the Holevo function. We will thus take

$$\mathbf{C} = H, \tag{6.5}$$

assuming that any additional necessary block coding will automatically be done to supplement the dense coding. Exactly the same assumption has been used in Ref.[132] to calculate the capacity for dense coding in the case of pure letter states. Eqs.(6.4) and (6.5) define the most general version of dense coding and we shall refer to this as completely general dense coding (CGCD).

A simpler example of dense coding is the case when the letter states are generated from the initial shared state $W_0$ by

$$W_0 = \mathbf{I} \otimes \mathbf{I}\ W_0\ \mathbf{I} \otimes \mathbf{I}, \tag{6.6}$$

$$W_1 = \sigma_1 \otimes \mathbf{I}\ W_0\ \sigma_1 \otimes \mathbf{I}, \tag{6.7}$$

$$W_2 = \sigma_2 \otimes \mathbf{I}\ W_0\ \sigma_2 \otimes \mathbf{I}, \tag{6.8}$$

$$W_3 = \sigma_3 \otimes \mathbf{I}\ W_0\ \sigma_3 \otimes \mathbf{I}. \tag{6.9}$$

In the above set of equations, the first operator of the combination $\sigma_i \otimes \mathbf{I}$ acts on Alice's qubit and the second operator acts on Bob's qubit. We shall refer to this case (i.e when the letter states are generated by Eqs.(6.6)-(6.9)) as simply general dense coding (GDC). The generality present in GDC is that Alice is allowed to prepare the different letter states with unequal probabilities. In other words, one has to use Eqs.(6.1),(6.2) and (6.5)-(6.9) to estimate the capacity $\mathbf{C}$.

In the more special case when Alice not only generates the four letter states according to Eqs.(6.6)-(6.9) but also with equal probability, the ensemble is given by

$$W = \frac{1}{4}\sum_{i=0}^{3} W_i. \tag{6.10}$$

and the capacity becomes

$$\mathbf{C} = \frac{1}{4}\sum_{i=0}^{3} S(W_i||W). \tag{6.11}$$

We shall call this simplest case special dense coding (SDC). Among all the possible ways of doing GDC, SDC is the optimal way to communicate when $W_0$ is a pure state (as we shall show in the next section) or a Bell diagonal state. However, we do not know the optimal way to communicate when $W_0$ is a completely general state and CGCD is allowed. For most of our chapter, we shall obtain bounds on the classical capacity $\mathbf{C}$ for SDC only. But we shall point out those results which are valid for GDC and CGDC as well. Though the main aim of this chapter is to establish bounds on the capacity $\mathbf{C}$ when the letters are mixed states, we shall begin with a calculation of $\mathbf{C}$ for pure letter states.

## 6.3 Capacity of SDC with pure letter states

Consider the initial shared pure state $W_0$ to be,

$$|\psi_0\rangle = (a|00\rangle + b|11\rangle). \tag{6.12}$$

Then, according to Eqs.(6.6)-(6.9), the other letter states are given by

$$|\psi_1\rangle = (a|10\rangle + b|01\rangle), \tag{6.13}$$

$$|\psi_2\rangle = -i(a|10\rangle - b|01\rangle), \tag{6.14}$$

$$|\psi_3\rangle = (a|00\rangle - b|11\rangle), \tag{6.15}$$

from which we obtain $W_i = |\psi_i\rangle\langle\psi_i|$. As all $W_i$ are pure states we have

$$S(W_i) = 0. \tag{6.16}$$

Thus from Eqs.(6.2) and (6.5) we have

$$\mathbf{C} = S(W). \tag{6.17}$$

We will consider only the case of SDC. Thus the ensemble used is obtained from Eq.(6.10) to be

$$\begin{aligned} W &= \frac{|a|^2}{2}|00\rangle\langle 00| + \frac{|b|^2}{2}|01\rangle\langle 01| \\ &+ \frac{|a|^2}{2}|10\rangle\langle 10| + \frac{|b|^2}{2}|11\rangle\langle 11|. \end{aligned} \tag{6.18}$$

Thus from Eq.(6.17) for the capacity $\mathbf{C}$, we get

$$\mathbf{C} = -(|a|^2 \log \frac{|a|^2}{2} + |b|^2 \log \frac{|b|^2}{2}) \tag{6.19}$$

$$= 1 - (|a|^2 \log |a|^2 + |b|^2 \log |b|^2). \tag{6.20}$$

Now we should recall that a good measure of entanglement for a pure state of a system composed of two subsystems A and B is given by the von Neumann entropy of the state of either of the subsystems [28, 136]. Let us call this measure the von Neumann entropy of entanglement and label it by $E_v$. Thus

$$E_v(|\psi\rangle\langle\psi|_{A+B}) = S(\mathrm{Tr}_A(|\psi\rangle\langle\psi|_{A+B})), \tag{6.21}$$

where $\mathrm{Tr}_A$ stands for partial trace over states of system A. Therefore, for all the states $W_i$,

$$E_v(W_i) = -(|a|^2 \log |a|^2 + |b|^2 \log |b|^2). \tag{6.22}$$

Thus,

$$\mathbf{C} = 1 + E_v(W_i). \tag{6.23}$$

We now prove that for pure states, SDC (using all alphabet states with equal *a priori* probability) is the optimal way to communicate among all possible ways of doing GDC (i.e when the letter states are generated by Eqs.(6.6)-(6.9)). Consider the general case when the states $W_i$ are sent with probabilities $p_i$. Then from Eq.(6.1) we have

$$W = \rho_1 + \rho_2, \tag{6.24}$$

where

$$\begin{aligned} \rho_1 &= (p_0 + p_3)|a|^2|00\rangle\langle 00| + (p_0 + p_3)|b|^2|11\rangle\langle 11| \\ &+ (p_0 - p_3)a^*b|11\rangle\langle 00| + (p_0 - p_3)ab^*|00\rangle\langle 11|, \end{aligned} \tag{6.25}$$

and

$$\begin{aligned}\rho_2 &= (p_1+p_2)|a|^2|10\rangle\langle 10| + (p_1+p_2)|b|^2|01\rangle\langle 01| \\ &+ (p_1-p_2)a^*b|01\rangle\langle 10| + (p_1-p_2)ab^*|10\rangle\langle 01|. \end{aligned} \tag{6.26}$$

Therefore, $\rho_1$ and $\rho_2$ form separate blocks inside the matrix $W$ and

$$S(W) = S(\rho_1) + S(\rho_2). \tag{6.27}$$

Eq.(6.17) indicates that we need to choose the probabilities $p_i$ in such a way that $S(W)$ is maximized. Density matrices with same diagonal elements have the highest von Neumann entropy when the nondiagonal elements are zero. Applying this fact to Eqs.(6.25) and (6.26) we get

$$p_0 = p_3, \tag{6.28}$$

$$p_1 = p_2. \tag{6.29}$$

Using Eqs.(6.28) and (6.29) in the expressions for $\rho_1$ and $\rho_2$ and calculating the entropy $S(W)$ gives

$$\begin{aligned} S(W) &= -\sum_{i=0}^{1} 2p_i(|a|^2 \log 2p_i|a|^2 + |b|^2 \log 2p_i|b|^2) \\ &= -\sum_{i=0}^{1} 2p_i \log 2p_i - (|a|^2 \log |a|^2 + |b|^2 \log |b|^2), \end{aligned} \tag{6.30}$$

where the normalizations of the state amplitudes and the probabilities $p_i$ have been used. From analysis of von Neumann entropies it is well known that the expression $-\sum_{i=0}^{1} 2p_i \log 2p_i$ has a maximum value when both $p_0$ and $p_1$ are equal. Thus $S(W)$, and hence the classical capacity $\mathbf{C}$ is maximized when

$$p_0 = p_1 = p_2 = p_3 = \frac{1}{4}. \tag{6.31}$$

Thus, among all the possible ways of performing GDC, SDC is the optimal way to communicate when pure states are being used as letters. From the above result and Eq.(6.23) we

can conclude that in the case of GDC with pure letter states we have

$$\mathbf{C} \leq 1 + E_v(W_i). \tag{6.32}$$

This result (Eq.(6.32)) had also been obtained in Ref.[132] from logical arguments. Following a procedure analogous to the above proof it can be shown that for Bell diagonal letter states SDC is again the optimal way to communicate among all the possible ways of doing GDC.

## 6.4 Nature of the ensemble used in SDC

In order to derive a lower bound on the classical capacity $\mathbf{C}$ for SDC we need to prove a crucial lemma concerning the nature of the ensemble used in SDC:

*For states $W_i$ defined in accordance to Eqs.(6.6)-(6.9), the ensemble $W$ for SDC as defined in Eq.(6.10) is a disentangled state irrespective of the nature of $W_0$.*

To prove this, we have to start by assuming $W_0$ to be a most general state of two qubits. This is given by [137]

$$\begin{aligned} W_0 &= \frac{1}{4}[I \otimes I + \sum_m r_m \sigma_m \otimes I \\ &+ I \otimes \sum_m s_m \sigma_m + \sum_{m,n} t_{mn} \sigma_m \otimes \sigma_n], \end{aligned} \tag{6.33}$$

where the indices $m$ and $n$ take on values from 1 to 3. Substituting $W_0$ from Eq.(6.33) into Eqs.(6.6)-(6.9) we get

$$\begin{aligned} W_1 &= \frac{1}{4}[I \otimes I + r_1 \sigma_1 \otimes I - \sum_{m \neq 1} r_m \sigma_m \otimes I + I \otimes \sum_m s_m \sigma_m \\ &+ \sum_n t_{1n} \sigma_1 \otimes \sigma_n - \sum_{m \neq 1, n} t_{mn} \sigma_m \otimes \sigma_n], \end{aligned} \tag{6.34}$$

$$\begin{aligned} W_2 &= \frac{1}{4}[I \otimes I + r_2 \sigma_2 \otimes I - \sum_{m \neq 2} r_m \sigma_m \otimes I + I \otimes \sum_m s_m \sigma_m \\ &+ \sum_n t_{2n} \sigma_2 \otimes \sigma_n - \sum_{m \neq 2, n} t_{mn} \sigma_m \otimes \sigma_n], \end{aligned} \tag{6.35}$$

$$W_3 = \frac{1}{4}[I \otimes I + r_3 \sigma_3 \otimes I - \sum_{m \neq 3} r_m \sigma_m \otimes I + I \otimes \sum_m s_m \sigma_m$$

$$+ \sum_n t_{3n}\sigma_3 \otimes \sigma_n - \sum_{m\neq 3,n} t_{mn}\sigma_m \otimes \sigma_n]. \tag{6.36}$$

Using expressions for $W_i$ from Eqs.(6.33)-(6.36) in Eq.(6.10) we get

$$W = I \otimes \frac{1}{4}[I + \sum_m s_m \sigma_m]. \tag{6.37}$$

This is very clearly a disentangled state. This result is, of course, valid only for SDC, where the equal probabilities of the letter states result in the careful cancellation of all the entanglement carrying terms. It allows us to easily derive a lower bound on **C** for SDC in terms of one of the measures of entanglement.

## 6.5 The relative entropy of entanglement as a lower bound on C

To investigate quantitatively the relationship between entanglement and **C** for arbitrary mixed letter states, it is necessary to use some measure of entanglement for mixed states. One such measure of entanglement, the relative entropy of entanglement, has been introduced in Ref.[31]. It has been shown to have a statistical interpretation [32] as well as a physical interpretation [33, 138] in forming bounds on the process of entanglement purification [30, 28, 29]. We will use the symbol $E_R$ to represent this measure of entanglement. For an arbitrary mixed state $\sigma$ it is given by

$$E_R(\sigma) = \min_{\rho\in\mathcal{D}} S(\sigma||\rho), \tag{6.38}$$

where $\mathcal{D}$ is the set of disentangled states. A property which has to be satisfied by any legitimate entanglement measure is its invariance under local unitary operations [33]. $E_R(\sigma)$ is thus invariant under local unitary operations of the state $\sigma$.

As the state $W$ of the ensemble used for SDC has been shown to be a disentangled state (*i.e.* $W \in \mathcal{D}$) in the previous section, we have

$$S(W_i||W) \geq \min_{\rho\in\mathcal{D}} S(W_i||\rho) = E_R(W_i). \tag{6.39}$$

Using the above inequality in Eq.(6.11) for $\mathbf{C}$ of SDC we get

$$\mathbf{C} = \frac{1}{4}\sum_{i=0}^{3} S(W_i||W) \geq \frac{1}{4}\sum_{i=0}^{3} E_R(W_i). \tag{6.40}$$

As each of the states $W_i$ are derived from $W_0$ via local unitary operations only, we have

$$E_R(W_i) = E_R(W_0) \tag{6.41}$$

for all values of $i$. Combining Eqs.(6.41) and (6.40) we get

$$\mathbf{C} \geq E_R(W_0). \tag{6.42}$$

This means that the classical capacity $\mathbf{C}$ for SDC is bounded from below by the relative entropy of entanglement of the initial shared mixed state. This result is however, not generalizable to GDC as it relies crucially on $W$ for SDC being a disentangled state.

## 6.6 Average distinguishability as an upper bound on C

In this section, we are going to divert a little bit from the main theme linking $\mathbf{C}$ to entanglement measures and point out another interesting bound on $\mathbf{C}$ stemming from the mutual distinguishability of the letter states $W_i$. It is known that the relative entropy $S(W_i||W_j)$ is a kind of statistical measure of the distinguishability between the quantum states $W_i$ and $W_j$ [32]. Thus for GDC one can define an average mutual distinguishability function as

$$\delta(p_i, W_i) = \sum_i \sum_j p_i p_j S(W_i||W_j). \tag{6.43}$$

We show below that this average mutual distinguishability function forms an upper bound on $\mathbf{C}$. Putting $W$ from Eq.(6.1) into Eq.(6.5) we obtain

$$\begin{aligned} \mathbf{C} &= \sum_{i=0}^{3} p_i \; S(W_i||\sum_{j=0}^{3} p_j \; W_j) \\ &= \sum_{i=0}^{3} p_i \; S(\sum_{j=0}^{3} p_j \; W_i||\sum_{j=0}^{3} p_j \; W_j), \end{aligned} \tag{6.44}$$

where the factor $\sum_{j=0}^{3} p_j$ has been inserted before $W_i$ in the second step as its value equals unity. We now use the joint convexity property of the relative entropy

$$S(\sum \lambda_i \sigma_i || \sum \lambda_i \rho_i) \leq \sum \lambda_i S(\sigma_i || \rho_i) \tag{6.45}$$

to expand the right hand side of Eq.(6.44) and obtain

$$\mathbf{C} \leq \sum_{i,j=0}^{3} p_i p_j \; S(W_i || W_j) = \delta(p_i, W_i). \tag{6.46}$$

Note that the above result is completely general because neither does it require the special class of local unitary operations given by Eqs.(6.6)-(6.9), nor does it require the probabilities to be uniform. Thus the classical capacity for CGDC is bounded from above by the average mutual distinguishability function. Note that we are pointing this out just as an interesting bound and it is not linked to the main theme of the chapter (relating entanglement measures stemming from purification procedures to dense coding capacities).

## 6.7 An upper bound on C in terms of the entanglement of formation

In this section we find an upper bound on **C** in terms of yet another measure of entanglement, namely, the entanglement of formation $E_F$. Consider a decomposition of an arbitrary mixed state $\sigma$ in terms of pure states $\sigma_i$ :

$$\sigma = \sum_i \lambda_i \sigma_i. \tag{6.47}$$

Then the entanglement of formation of this state is defined as [30, 139]

$$E_F(\sigma) = \min \sum_i \lambda_i E_v(\sigma_i), \tag{6.48}$$

where the minimum is taken over all decompositions of $\sigma$ of the type given by Eq.(6.47).

The initial shared state $W_0$ used in dense coding, will, in general, have several decompositions in terms of pure states. Let the particular decomposition from which its entanglement of formation $E_F(W_0)$ is calculated (referred to as the entanglement minimizing

decomposition [139]) be

$$W_0 = \sum_m q_m W_{0m}, \tag{6.49}$$

where $W_{0m}$ are pure states and $q_m$ are probabilities. As Eq.(6.49) gives the entanglement minimizing decomposition, we have

$$E_F(W_0) = \sum_m q_m E_v(W_{0m}), \tag{6.50}$$

while the normalization of the probabilities imply

$$\sum_m q_m = 1. \tag{6.51}$$

As each of the signal states $W_i$ are derived from $W_0$ by local unitary operations, they can be decomposed as

$$W_i = \sum_m q_m W_{im}, \tag{6.52}$$

where each pure state $W_{im}$ is connected to the pure state $W_{0m}$ by exactly the same local unitary operation as that which connects $W_i$ to $W_0$. As any legitimate measure of entanglement has to remain invariant under local unitary operations, we have

$$E_v(W_{im}) = E_v(W_{0m}), \tag{6.53}$$

and

$$E_F(W_i) = E_F(W_0). \tag{6.54}$$

From Eqs.(6.53) and (6.54) we have

$$\begin{aligned} \sum_m q_m E_v(W_{im}) &= \sum_m q_m E_v(W_{0m}) \\ &= E_F(W_0) = E_F(W_i). \end{aligned} \tag{6.55}$$

Now, in the case of SDC, the capacity (from Eq.(6.11)) is

$$\begin{aligned} \mathbf{C} &= \frac{1}{4}\sum_i S(W_i || \frac{1}{4}\sum_j W_j) \\ &= \frac{1}{4}\sum_i S(\sum_m q_m W_{im} || \frac{1}{4}\sum_j \sum_m q_m W_{jm}) \qquad (6.56) \\ &= \frac{1}{4}\sum_i S(\sum_m q_m W_{im} || \sum_m q_m W_m) \qquad (6.57) \end{aligned}$$

where we have put

$$W_m = \frac{1}{4}\sum_j W_{jm}. \tag{6.58}$$

Using joint convexity (Eq.(6.45)) to expand the right hand side of Eq.(6.57), we get

$$\begin{aligned} \mathbf{C} &\leq \frac{1}{4}\sum_i \sum_m q_m S(W_{im}||W_m) \\ &= \sum_m q_m (\frac{1}{4}\sum_i S(W_{im}||W_m)). \end{aligned} \tag{6.59}$$

Now, for each value of $m$, the expression $\frac{1}{4}\sum_i S(W_{im}||W_m)$ can be regarded as the classical capacity $\mathbf{C}$ for SDC with the states $W_{im}$ as the four letter states. As each of the states $W_{im}$, are pure, Eq.(6.23) implies

$$\frac{1}{4}\sum_i S(W_{im}||W_m) = 1 + E_v(W_{im}). \tag{6.60}$$

Putting Eq.(6.60) into Eq.(6.59) we get

$$\mathbf{C} \leq \sum_m q_m (1 + E_v(W_{im})). \tag{6.61}$$

Using Eqs.(6.51) and (6.55) to simplify the right hand side of Eq.(6.61) we get

$$\mathbf{C} \leq 1 + E_F(W_i). \tag{6.62}$$

The above bound is valid for GDC as well. To see this one just has to repeat the above proof starting with

$$\mathbf{C} = \sum_i p_i \; S(W_i||\sum_j p_j W_j) \tag{6.63}$$

and replace Eq.(6.58) with

$$W_m = \sum_j p_j \; W_{jm}. \tag{6.64}$$

Eq.(6.59) then gets replaced by

$$\mathbf{C} \leq \sum_m q_m (\sum_i p_i \; S(W_{im}||W_m)). \tag{6.65}$$

Now note the fact that $\sum_i p_i \; S(W_{im}||W_m)$ is the expression for the classical capacity $\mathbf{C}$ for CGDC with $W_{im}$ being the letter states. When the states $W_{im}$ are generated from $W_{i0}$

according to Eqs.(6.6)-(6.9) (i.e. when GDC protocol is being followed), then the purity of the states $W_{im}$ guarantees that $\mathbf{C}$ is less than $1 + E_v(W_{im})$ (as shown in section 6.3). Using this fact in Eq.(6.65) we again end up with Eq.(6.62). Thus even in the case of GDC, the capacity $\mathbf{C}$ is bounded by $1 + E_F(W_i)$.

## 6.8 An upper bound on C in terms of the relative entropy of entanglement

Having analytically proven that $1 + E_F(W_i)$ is an upper bound on $\mathbf{C}$ for GDC, we now proceed to check whether the even smaller (as proved in Ref.[33]) quantity $1+E_R(W_i)$ is also an upper bound. However, we do not attempt to prove this analytically for a completely general initial shared state $W_0$. Instead we calculate the capacity $\mathbf{C}$ (for SDC only) for those specific classes of the initial shared state $W_0$ whose relative entropy of entanglement $E_R(W_0)$ is already known. We then plot this capacity $\mathbf{C}$ as a function of the relative entropy of entanglement $E_R$ for each of these classes of states and check whether the curve $\mathbf{C}(E_R)$ lies below the plot of $1 + E_R$.

At first we have a look at mixed states of the type [33]

$$\Lambda_A = \lambda|\Phi^+\rangle\langle\Phi^+| + (1-\lambda)|01\rangle\langle 01|, \tag{6.66}$$

where $|\Phi^+\rangle$ is one of the four Bell states which are defined by

$$|\Phi^\pm\rangle = \frac{1}{\sqrt{2}}(|00\rangle \pm |11\rangle) \tag{6.67}$$

$$|\Psi^\pm\rangle = \frac{1}{\sqrt{2}}(|01\rangle \pm |10\rangle) \tag{6.68}$$

We shall refer to the states described by Eq.(6.66) as lambda states of the type A. For them, the relative entropy of entanglement is [33]

$$E_R(\Lambda_A) = (\lambda - 2)\log(1 - \frac{\lambda}{2}) + (1-\lambda)\log(1-\lambda), \tag{6.69}$$

while the $\mathbf{C}$ for SDC is

$$\begin{aligned} \mathbf{C} &= (1-\lambda)\log(1-\lambda) + \frac{1}{2}(\lambda-2)\log(1-\frac{\lambda}{2}) && (6.70)\\ &+ \frac{1}{2}\lambda\log\lambda + (1+\frac{\lambda}{2}). && (6.71)\end{aligned}$$

The plot of the classical capacity $\mathbf{C}$ for these states as a function of $E_R$ of the state has been shown in Fig.6.1 and it is indeed found that

$$\mathbf{C} \leq 1 + E_R. \tag{6.72}$$

The equality holds true only at the two ends of the graph, namely at maximal entanglement $E_R = 1$ (when $\sigma_1$ approaches a Bell state) and zero entanglement $E_R = 0$ (when $\sigma_1$ approaches $|01\rangle\langle 01|$).

Next we look at states of the type [33]

$$\Lambda_B = \lambda|\Phi^+\rangle\langle\Phi^+| + (1-\lambda)|00\rangle\langle 00| \tag{6.73}$$

which we call lambda states of the type B. For these [33]

$$\begin{aligned} E_R(\Lambda_B) &= s_+\log s_+ + s_-\log s_- \\ &- (1-\frac{\lambda}{2})\log(1-\frac{\lambda}{2}) - \frac{\lambda}{2}\log\frac{\lambda}{2}\ , \end{aligned} \tag{6.74}$$

where

$$s_\pm = \frac{1 \pm \sqrt{1-2\lambda(1-\lambda)}}{2} \tag{6.75}$$

are the eigenvalues of $\Lambda_B$. The $\mathbf{C}$ for SDC in this case is given by

$$\begin{aligned} \mathbf{C} &= s_+\log s_+ + s_-\log s_- \\ &- (1-\frac{\lambda}{2})\log\frac{1}{2}(1-\frac{\lambda}{2}) - \frac{\lambda}{2}\log\frac{\lambda}{4}. \end{aligned} \tag{6.76}$$

As is clear from a simple comparison of Eqs.(6.74) and (6.76), for lambda states of the type B,

$$\mathbf{C} = 1 + E_R. \tag{6.77}$$

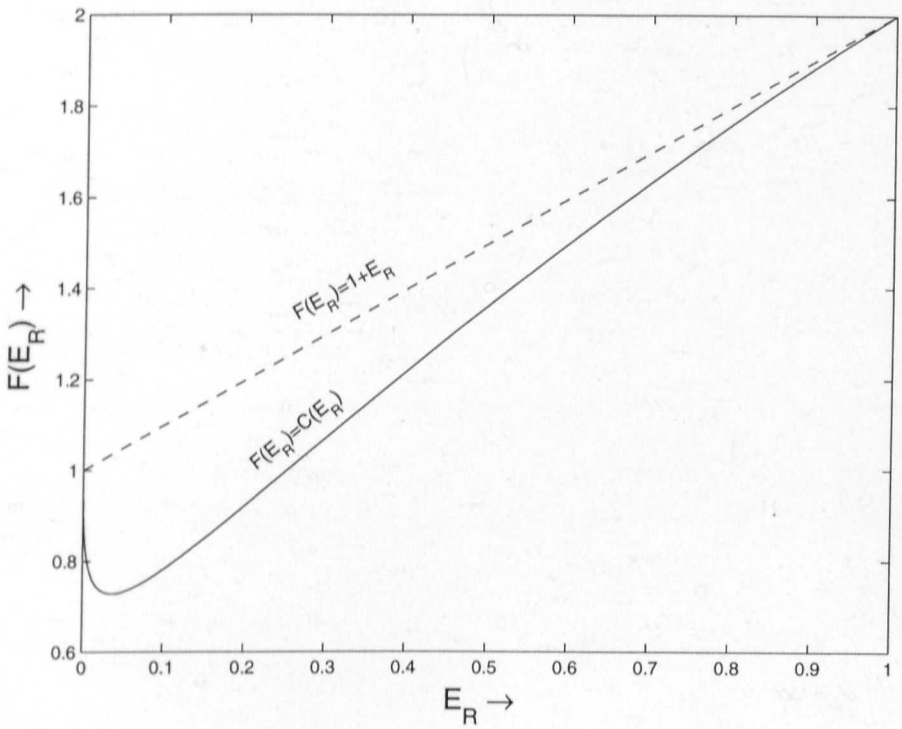



Figure 6.1: Two different functions $F(E_R)$ of the relative entropy of entanglement $E_R$ are plotted. The continuous line shows the capacity $\mathbf{C}$ for SDC as a function of the relative entropy of entanglement $E_R$ if the initial shared state is a lambda state of the type A. The dashed line shows the function $1 + E_R$. The figure illustrates that the capacity $\mathbf{C}$ for SDC is bounded from above by $1 + E_R$

Thus, a curious feature of lambda states of type B is that the capacity for SDC is actually always *equal* to $1 + E_R$. We will discuss a bit more about this curious aspect later in the section.

Now we consider another special class of states called the Werner states [30, 23] parameterized by a number F called the fidelity [30] and given by

$$\begin{aligned} W_F &= F|\Psi^-\rangle\langle\Psi^-| + \frac{1-F}{3}(|\Psi^+\rangle\langle\Psi^+| \\ &+ |\Phi^+\rangle\langle\Phi^+| + |\Phi^-\rangle\langle\Phi^-|). \end{aligned} \tag{6.78}$$

The relative entropy of entanglement of these states is given by [33]

$$E_R(W_F) = F\log F + (1-F)\log(1-F) + 1, \tag{6.79}$$

and the **C** for SDC is calculated to be

$$\mathbf{C} = 2 + F\log F + (1-F)\log\frac{(1-F)}{3}. \tag{6.80}$$

The plot **C** versus $E_R$ has been drawn in Fig.6.2 and it is found that even in this case,

$$\mathbf{C} \leq 1 + E_R. \tag{6.81}$$

Now consider the case of a general Bell diagonal state

$$\begin{aligned} B_D &= \lambda_1|\Psi^-\rangle\langle\Psi^-| + \lambda_2|\Psi^+\rangle\langle\Psi^+| \\ &+ \lambda_3|\Phi^+\rangle\langle\Phi^+| + \lambda_4|\Phi^-\rangle\langle\Phi^-|. \end{aligned} \tag{6.82}$$

It has been proved in Ref.[31] that when all $\lambda_i \in [0, \frac{1}{2}]$ then

$$E_R(B_D) = 0, \tag{6.83}$$

while when any of the $\lambda_i$ (say $\lambda_1$) $\geq \frac{1}{2}$, then

$$E_R(B_D) = \lambda_1\log\lambda_1 + (1-\lambda_1)\log(1-\lambda_1) + 1. \tag{6.84}$$

The **C** for SDC always turns out to be

$$\mathbf{C} = 2 + \sum_i \lambda_i \log\lambda_i. \tag{6.85}$$

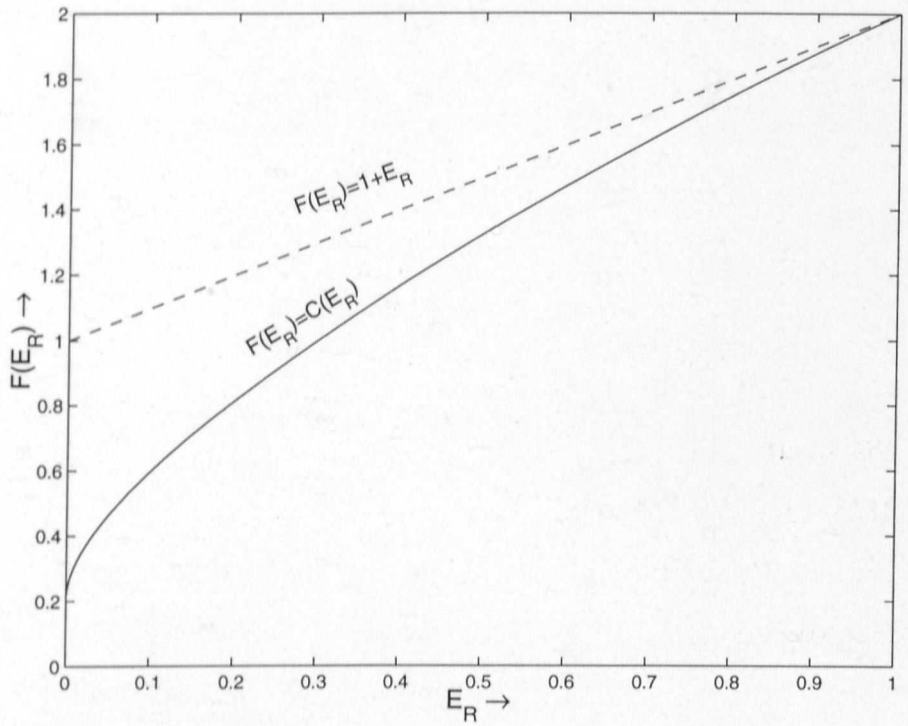



Figure 6.2: The continuous line shows how the capacity **C** for SDC varies with the relative entropy of entanglement $E_R$ of the initial shared Werner state. The dashed line shows that it is bounded from above by $1 + E_R$

First consider the case when all $\lambda_i \in [0, \frac{1}{2}]$. From Eqs.(6.83) and (6.85) we find that

$$\begin{aligned} 1 + E_R(B_D) - \mathbf{C} &= -\sum_i \lambda_i \log \lambda_i - 1 \\ &= -\sum_i \lambda_i (\log \lambda_i + 1) \\ &\geq 0, \end{aligned} \tag{6.86}$$

where $\sum_i \lambda_i = 1$ has been used to proceed from the first to the second step and $\log \lambda_i \leq -1$ (because $\lambda_i \in [0, \frac{1}{2}]$) has been used to proceed from the second to the third step.

Now consider the complementary case ($\lambda_1 \geq \frac{1}{2}$). From Eqs.(6.84) and (6.85) we find that

$$\begin{aligned} 1 + E_R(B_D) - \mathbf{C} &= (1 - \lambda_1) \log(1 - \lambda_1) - \sum_{i \neq 1} \lambda_i \log \lambda_i \\ &= (\sum_{i \neq 1} \lambda_i) \log(\sum_{j \neq 1} \lambda_j) - \sum_{i \neq 1} \lambda_i \log \lambda_i \\ &= \sum_{i \neq 1} \lambda_i (\log(\sum_{j \neq 1} \lambda_j) - \log \lambda_i) \\ &\geq 0, \end{aligned} \tag{6.87}$$

where in order to proceed from the third to the fourth step we have used the simple fact that $\log(\lambda_2 + \lambda_3 + \lambda_4)$ is greater than either of the terms $\log \lambda_2$,$\log \lambda_3$ or $\log \lambda_4$. Thus for all Bell diagonal states we have

$$\mathbf{C} \leq 1 + E_R. \tag{6.88}$$

Now we will point out a curious fact about the situation when any two of the eigenvalues of a Bell diagonal state (say $\lambda_3$ and $\lambda_4$) are zero. When $\lambda_1 = \lambda_2 = \frac{1}{2}$ (which means $E_R = 0$), we have $\mathbf{C} = 1$ (using Eq.(6.85)). In all the other cases (for which we use Eqs.(6.84) and (6.85)) we have

$$\begin{aligned} 1 + E_R(B_D) - \mathbf{C} &= (1 - \lambda_1) \log(1 - \lambda_1) - \lambda_2 \log \lambda_2 \\ &= 0, \end{aligned} \tag{6.89}$$

where we have used the simple fact that $\lambda_1 + \lambda_2 = 1$. Thus for all Bell diagonal states with only two nonzero eigenvalues we have

$$\mathbf{C} = 1 + E_R. \tag{6.90}$$

On the basis of the results obtained in this section let us conjecture:

**Conjecture** : *The* $\mathbf{C}$ *for SDC with completely general (possibly mixed) states is bounded from above by* $1 + E_R$.

A great deal of empirical evidence has been presented in this section in support of the conjecture. In the next section we proceed to give a heuristic justification in support of our conjecture. In fact, we will try to justify an even stronger upper bound on $\mathbf{C}$.

## 6.9 SDC and purification

To justify the conjecture of the previous section, we will have to examine the following interesting question: How does the capacity $\mathbf{C}$ change if Alice and Bob first locally purify their ensemble and distill Bell states (following the optimal purification procedure) and follow this up by SDC? Various purification procedures have been described in Refs.[30, 28, 29]. Here we assume that Alice and Bob follow the optimal purification process: One which helps them to distill the maximum fraction of Bell states from the initial ensemble. They will, after optimal purification, have a fraction $E_D$ (where $E_D$ is called the *entanglement of distillation*) shared pairs in Bell states and a fraction $(1 - E_D)$ pairs in a disentangled state. They now complete their 'purification' process by converting the final subensemble of disentangled pairs to pure states by projective measurements. We refer to such a protocol as *complete purification.* After a complete purification, Alice can use the fraction $E_D$ of Bell pairs to send Bob information at the rate of 2 bits/pair and the fraction $(1 - E_D)$ of pure disentangled pairs to send information at the rate of 1 bit/pair (see Fig.6.3). Thus if Alice and Bob initially shared $n$ pairs, the classical capacity after a complete and optimal purification procedure is

$$\mathbf{C} = \frac{1}{n}\{2nE_D + n(1 - E_D)\}$$

$$= 1 + E_D. \tag{6.91}$$

Note that the above result is only asymptotically true ($n \to \infty$). Naively, one might expect this $\mathbf{C}$ to be lower than the $\mathbf{C}$ before purification.

This is because, as mentioned in Ref.[28], entanglement concentration is a more destructive process than quantum data compression. Some amount of shared entanglement is destroyed in the process of purification. So it might be expected that the final ensemble after a purification will be able to convey less classical information than the original ensemble. On the contrary, as we will justify, the capacity for SDC with the purified ensemble is greater than that with the unpurified ensemble when an optimal and complete purification protocol is used. The gain comes from the fact that *now there are two separate sub-ensembles instead of a single ensemble.* In this section, we will try to justify, albeit heuristically, the following statement (as a more fundamental conjecture than the one presented in the previous section):

**Conjecture**: *The capacity for SDC is more when it is preceded by a complete and optimal purification procedure.*

We will first consider the special case of Bell diagonal mixed states, for which the proof of the increase in the SDC capacity on a complete and optimal purification (our conjecture) can be rigorously proved. For Bell diagonal states with entropy $S(\rho) \leq 1$, there is a purification protocol called hashing (with the distillable fraction being $E_{DH} = 1 - S(\rho)$) [30]. From Eq.(6.85) we see that for these Bell diagonal states, the $\mathbf{C}$ for SDC is equal to $1 + E_{DH}$. As hashing may not necessarily be the optimal protocol, we have $E_{DH} \leq E_D$. This immediately implies $\mathbf{C} \leq 1 + E_D$. For the complementary case of Bell diagonal states with $S(\rho) > 1$, we have (from Eq.(6.85) for SDC), $\mathbf{C} < 1$. This is obviously less than $1 + E_D$ for any finite value of the entanglement of distillation (i.e for all inseparable states [140]). Thus for all Bell diagonal states the $\mathbf{C}$ for SDC can be improved by a prior optimal and complete purification of the ensemble of shared states.

For the more general case of arbitrary mixed entangled states, the proof will, essentially, be heuristic. Our approach will be to split the change in the classical information capacity

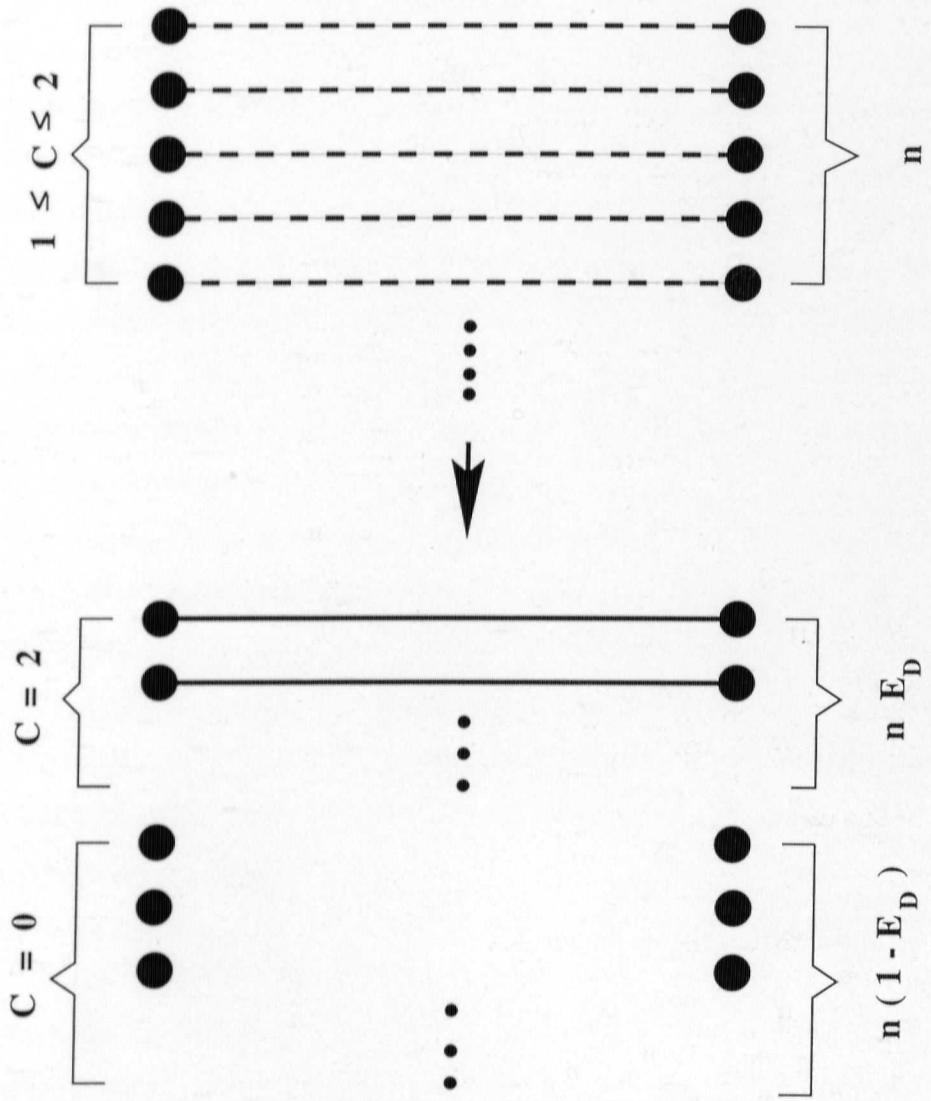



Figure 6.3: This figure illustrates how the capacity of SDC changes if Alice and Bob perform a complete and optimal purification procedure on their shared ensemble prior to performing SDC.

due to complete and optimal purification into two parts. The first part is positive (an increase in capacity) and due to the addition of classical side channels during the purification procedure. These side channels are used by Alice (A) to communicate the results of her measurements to Bob (B), or vice versa. As this communication during purification is already conveying information from A to B (or vice versa), the channel capacity of the classical side channels should be directly added to the classical capacity (of course, for this, we have to implicitly assume the additivity of classical capacities). The information conveyed from A to B (or vice versa) during purification is actually used by the two parties to precisely identify their entangled and disentangled subensembles. There is also a negative contribution (decrease in capacity) during the purification as a fraction $1 - E_D$ of shared pairs loose all their entanglement. Of course a part of this entanglement is pumped into the entangled subensemble, but the remaining is lost. Our job will be to argue that the positive contribution in channel capacity due to addition of classical side channels outweighs the negative contribution due to loss of entanglement in an optimal and complete purification procedure.

Consider the process of purification as a process of information gain by A and B. Before the purification, both A and B have an equal amount of knowledge about their shared system (they both know the full density matrix). Finally, each of their shared states are pure (because of the completeness of the purification procedure) and both of them have equal knowledge (i.e each know which of the pairs form the disentangled subensemble and which of the pairs form the maximally entangled subensemble). Thus they have both gained an equal amount of information I/pair about their shared pairs during the process of purification. Now, acquiring a part of this information may not cause any destruction of shared entanglement (lets call it $I_1$/pair), while the remaining part (lets call it $I_2$/pair) does cause a lowering of shared entanglement. We now contend, that this part, $I_2$/pair has to be equal to the number of classical communication channels used in the optimal purification procedure. The logic follows from the fact that the optimal strategy would be for A and B to collaborate in such a way that both of them gain the entire information $I_2$/pair with the least destruction of entanglement. They must then each acquire only a

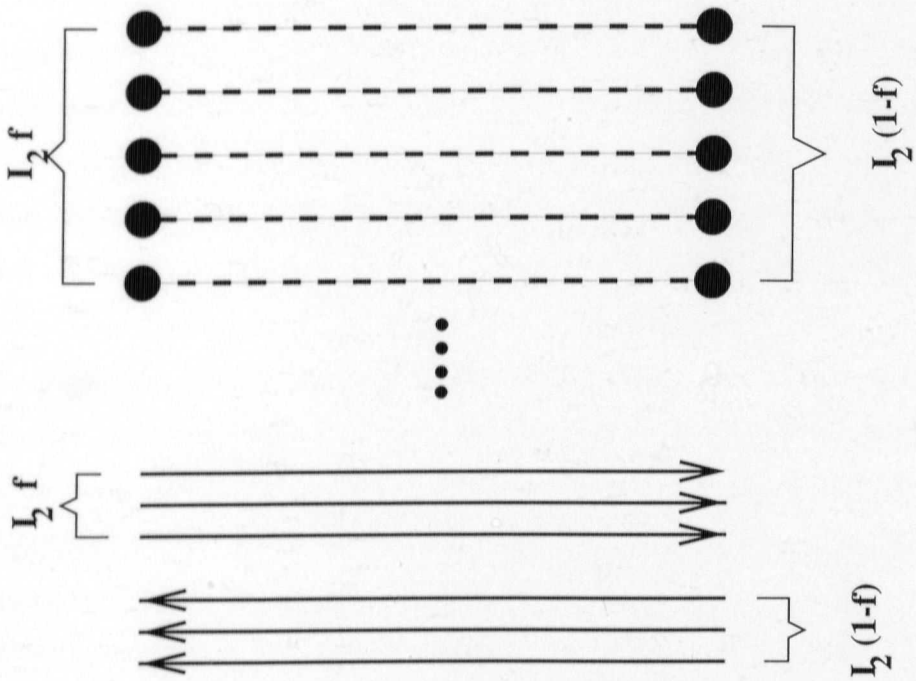



Figure 6.4: The figure illustrates the wisest way for A and B to gain the entanglement destroying information $I_2$/pair. They should each only gain complementary fractions $f$ and $1-f$ of this information and pass this on to the other party by classical side channels. In this way they destroy the least amount of entanglement.

fraction $f$ of the information complementary to the fraction acquired by the other. In this way, the total information acquired by A and B from the shared pairs through direct entanglement degrading measurements is $I_2$/pair. They can then use a minimum of $I_2$ classical side channels per pair to communicate their fraction of the acquired information to the other party (Fig. 6.4 illustrates this procedure). On the other hand, if each wanted to acquire a fraction of the total information by direct measurements which was not entirely complementary to the part acquired by the other, they would destroy more entanglement than is really necessary. Thus we would expect that the classical side channels contribute to boosting the capacity up by at least an amount $I_2$/pair in the optimal purification procedure.

Now consider how much the capacity decreases due to the degradation of shared entanglement during the purification procedure. The classical capacity of a fraction $1 - E_D$ of the pairs drops from *at most* 2 bits/pair to 1 bit/pair (due to the *completeness* of the purification procedure, the final capacity cannot be lower than 1 bit/pair). Thus the drop in classical capacity of each of the finally disentangled pairs is not more than 1 bit. This implies that the net decrease in classical capacity of the entire ensemble due to loss of entanglement hasn't been more than $1 - E_D$ bits/pair.

When the information $I_2$ is greater than 1 bit/pair, the proof of our statement is straightforward. The increase in capacity due to classical side channels (i.e $I_2$/pair) is more than 1 bit/pair, while the decrease in capacity due to loss of entanglement is less than $1 - E_D$ bits/pair. As $1 - E_D$ is a fraction (i.e $1 - E_D < 1$), the increase in capacity on purification overrides the inevitable decrease in capacity due to degradation of shared entanglement. Clearly, thus the capacity to do SDC increases on prior purification when $I_2 \geq 1$ bit.

Now, we have to show that no matter what the value of $I_2$ is, it is *possible* to find a purification protocol for which $I_2$ is greater than $1 - E_D$ bits. In other words, if initially there are $n$ shared pairs (with $n$ being large), then the number of shared pairs which loose all their entanglement on gaining an information of $I_2$/pair can be made less than $nI_2$ by an appropriate choice of the purification protocol. From such a statement it directly follows that the increase in capacity on purification overrides the inevitable decrease in capacity due to degradation of shared entanglement. A simple way in which one may try to justify the above proposition is from the fact that one pair generally allows the extraction of upto two bits of information (one bit from each of A's and B's qubit). So, it should be possible, in general, to extract $nI_2$ amount of information from measurements on less than $nI_2$ shared pairs (whose entanglement is degraded). This intuitive understanding leaves open the question as to whether the information $I_2$/pair *relevant* to purification can be acquired in this way. For that we resort to explicit exemplification. Consider the class of mixed states $\rho$ (having nonzero entropy $S(\rho)$) and a diagonal decomposition $\sum \lambda_i |\psi_i\rangle\langle\psi_i|$ in terms of the pure states $|\psi_i\rangle$. Also suppose that this diagonal decomposition does not coincide with the entanglement minimizing decomposition [139] of $\rho$. For such states, acquiring the

information about the entropy ($S(\rho)$/pair) is essential during purification, as the final ensemble is pure. We now contend that acquiring this $S(\rho)$ /pair of information *necessarily* destroys some amount of shared entanglement. We will justify this by the method of contradiction. Suppose, it was really possible to acquire the information about the entropy $S(\rho)$ without destroying any entanglement. On acquiring an information of the amount equal to $S(\rho)$/pair, A and B will be able to divide their initial ensemble to four separate pure subensembles, each being comprised of one of the states $|\psi_i\rangle$. The weight of each of these subensembles will be equal to the eigenvalues $\lambda_i$. The average entanglement shared by A and B after extracting the information $S(\rho)$/pair is thus $\sum \lambda_i E_v(|\psi_i\rangle)$. However, for the class of states $\rho$ that we are considering, $\sum \lambda_i E_v(|\psi_i\rangle)$ is necessarily greater than the initial shared entanglement (as quantified by the entanglement of formation $E_F$). Thus by purely local actions and classical communications, A and B have been able to increase the shared entanglement for these classes of mixed states. This contradicts the definition of entanglement as a quantity that cannot be increased by local actions and classical communications. Thus, *mixed states with the diagonal decomposition not coincident with the entanglement minimizing decomposition cannot be locally purified without necessarily destroying some shared entanglement.* Thus the information about the entropy of these states is of the type $\mathrm{I}_2$ (i.e acquiring the information necessarily causes degradation of entanglement). A corollary which immediately follows (though not directly relevant to the main point of the chapter), is: *the optimal purification of mixed states with the diagonal decomposition not coincident with the entanglement minimizing decomposition necessarily has a nonzero $I_2$ and thus necessarily requires the use of classical side channels.* Now consider such states when their entropy, and thereby $\mathrm{I}_2$, exceeds 1 bit. Thus the total information $n\mathrm{I}_2$ needed to be acquired is greater than $n$ bits. However, purifiability (nonzero $E_D$) implies that the total entanglement loss can be entirely concentrated to the entanglement loss of $n(1 - E_D)$ pairs which is less than $n\mathrm{I}_2$ pairs. Therefore, it is *possible* to gain the relevant $n\mathrm{I}_2$ bits of information by destroying the entanglement of less than $n\mathrm{I}_2$ pairs. Now we really need an unproven extension of the above statement: *even when* $\mathrm{I}_2 \leq 1$ bit and *irrespective of the nature of the decomposition of* $\rho$, it is *possible* to gain the relevant $n\mathrm{I}_2$ amount of

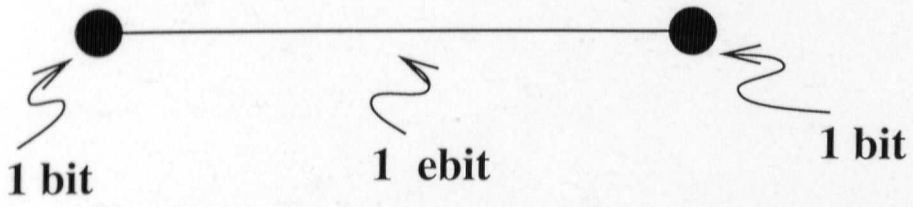



Figure 6.5: The figure shows that an entangled pair of qubits allow the extraction of up to two bits of information, and allow at most one ebit of entanglement (their maximum possible initial entanglement) to be destroyed in the process.

information by destroying the entanglement of less than $nI_2$ pairs. Though this may seem a large extrapolation, it seems highly *plausible* because one shared pair allows the extraction of upto two bits of information and gives at most one ebit of entanglement to destroy (see Fig.6.5). Thus we would expect that, no matter what the value of $I_2$ is, the increase in capacity on purification overrides the inevitable decrease in capacity due to degradation of shared entanglement.

Thus the capacity to do SDC with the two pure subensembles (maximally entangled and fully disentangled) after a complete and optimal purification, is expected to be greater than the initial mixed (and uniformly entangled) ensemble. We thus conjecture, with the help of Eq.(6.91), the following bound on the capacity of doing SDC with any mixed entangled state

$$\mathbf{C} \leq 1 + E_D. \tag{6.92}$$

This is an even stronger upper bound on the classical capacity than the bound conjectured in the previous section as the relative entropy of entanglement $E_R$ is necessarily greater than $E_D$ [33]. From Eq.(6.92), it directly follows that $\mathbf{C} \leq 1 + E_R$ (our previous conjecture). Note that in this section, this conjecture has been rigorously proved for all Bell diagonal states, heuristically proved for all states with entropy $S(\rho) \geq 1$ bit whose diagonal decomposition is not coincident with the entanglement minimizing decomposition

and shown to be highly plausible for other types of states.

## 6.10 Conclusion

In this chapter we have obtained bounds on the capacity of doing dense coding in terms of the different measures of entanglement stemming from purification procedures. The rigorously proved part of the results of this chapter is that for SDC one always has

$$E_R \leq \mathbf{C} \leq 1 + E_F. \tag{6.93}$$

On the other hand if we allow for a conjecture (well supported by examples and heuristically justified in Section.6.9), we have the stronger result

$$E_R \leq \mathbf{C} \leq 1 + E_R. \tag{6.94}$$

What is the significance of bounds on the $\mathbf{C}$ for SDC when it can be readily calculated? The importance can be realized when we invert the above equation and write

$$\mathbf{C} - 1 \leq E_R \leq \mathbf{C}. \tag{6.95}$$

Thus by calculating (or measuring) the channel capacity for SDC, we can draw an inference about the range in which the entanglement of the shared states (as quantified by $E_R$) lies. Also one of the bounds, namely, $\mathbf{C} \leq 1 + E_F$ continues to hold even when we are allowed to vary the a priori probability of the various signal states (GDC). Thus, our inequality allows one to impose a readily calculable (from the expression for $E_F$ in Ref.[139]) limit on the capacity for GDC, without having to optimize GDC over all possible a priori signal probabilities.

The physical interpretation of the upper bounds become clear from the considerations given in Section.6.9. During optimal and complete entanglement purification procedures one generally enhances the classical capacity much more due to added classical side channels than the inevitable decrease in capacity brought by the loss of entanglement. The information transferred through these classical side channels during purification helps to

identify the entangled and disentangled subensembles. It is through this identification that they directly play the role of boosting the capacity. As after an optimal and complete entanglement purification procedure, the capacity is $1 + E_D$, this post-purification capacity is an upper bound on the pre-purification capacity. As both the entanglement measures $E_F$ and $E_R$ are upper bounds on $E_D$, all our upper bounds follow immediately. It is interesting to note that the upper and the lower bounds are trivial in complementary regimes. When $\mathbf{C} \leq 1$, the upper bounds are trivial, but the lower bound ($E_R \leq \mathbf{C}$) is non trivial. On the other hand when $\mathbf{C} \geq 1$, the upper bounds are non trivial while the lower bound is trivial.

We believe that this chapter imparts physical significance to the various measures of entanglement from the viewpoint of forming bounds on certain kinds of dense coding procedures. This direction of physical interpretation of the entanglement measures is very different from the standard interpretations which stem from entanglement dilution and distillation processes. In a sense, this chapter *links up the apparently disconnected notions of entanglement purification and dense coding.* The considerations of the previous section imply the following lower bound on the distillable entanglement: $E_D \geq \mathbf{C} - 1$. This is important because, as yet, there is no explicit formula for $E_D$ for a general mixed entangled state. Thus the readily calculable quantity $\mathbf{C} - 1$ (in the case of SDC) may offer a convenient lower bound on the distillable entanglement of a given mixed state.

The interesting question to examine is what apart from entanglement is involved in determining the dense coding capacity. This may be some measure of distinguishability between the letter states (hinted by the fact that the average mutual distinguishability function forms an upper bound on the classical capacity $\mathbf{C}$). An aim of further research should be to work towards a complete formula for the capacity of dense coding. Moreover, working with a similar motivation as this chapter, one can also try to relate entanglement measures stemming from purification procedures to the other uses of shared entanglement such as teleportation [19] and secret key distribution [17].

# Chapter 7

# Teleportation of an atomic state via cavity decay

## 7.1 Introduction

Perhaps the most popular application of entanglement is teleportation [19]. In this chapter we will present a rather unorthodox physical implementation of teleportation; an implementation that relies on decays.

A spontaneous decay is popularly regarded as a mechanism of coherence loss in a quantum system. As such, it is hardly expected that such a process can come to any aid in the processing of quantum information [141]. Two recent papers [142, 143] tend to dispel this myth by showing how the detection (or the non detection) of decays can be used to entangle the states of distinct atoms. In this chapter, we show that the above approach is not limited to the setting up of entanglement, but can actually be used for as *genuine* a quantum information processing as teleportation. In our proposal, the states to be teleported (the "stationary qubits") are atomic states which are ideal for the storage of quantum information. On the other hand, quantum information is being physically transferred from place to place via photonic states (the "flying qubits" [144]), which are the best long distance carriers of quantum information. In all experimental implementations of teleportation to

date [121, 122, 123], and in some related proposals [145], the stationary qubits have been of the "difficult to hold" optical origin. On the other hand, in some earlier proposals for atomic state teleportation [69, 146], the flying qubits have been atomic states and thereby non-ideal for long distance teleportation. The scheme to be described here differs from these earlier experiments and proposals in using both the ideal stationary and the ideal flying qubit. It also differs crucially from the much studied quantum communication setup in which a photon *directly* transfers quantum information from an atom trapped in a cavity to another atom in a distant cavity [144, 147, 148, 149, 150]. Our scheme does not require any direct carrier of quantum information between distant atoms. A joint detection of photons *leaking out* of distinct cavities enables a *disembodied* transfer of quantum information from an atom in one of the cavities to an atom in the other. We thus provide a quantum state transfer scheme that completely avoids the difficult task of feeding a photon into a cavity from outside by sophisticated experimental techniques [147, 148].

## 7.2 The basic idea

The basic setup consists of two optical cavities, each containing a single trapped $\Lambda$ three level atom, as shown in Fig.7.1. Atoms 1 and 2 are trapped in cavities A and B (supporting cavity modes A and B) respectively.The photons leaking out from both the cavities impinge on the $50-50$ beam splitter $S$ and gets detected at the detectors $D_+$ and $D_-$. Initially we will assume that these detectors have unit efficiency and will include a finite detector efficiency analysis at a later point. The cavity A, atom 1, beam splitter $S$ and the detectors $D_+$ and $D_-$ belong to Alice. The cavity B with atom 2 belongs to Bob. By following our teleportation protocol, Alice can teleport an unknown state of her atom 1 to the atom 2 held by Bob. The protocol takes place in three stages.

In the preparation stage, Alice maps her atomic state to her cavity state [151]. At the same time Bob creates a maximally entangled state of his atom and his cavity mode. In the next stage (the detection stage) Alice waits for a *finite* time for either or both of her detectors to click. If any one of the detectors register a single click during this time period,

then the protocol is successful. Otherwise Alice informs Bob about her failure.

A correspondence of this protocol with the standard teleportation protocol [19] can be made by noting that the beam splitter and the detectors constitute a device for measurement of the joint state of the two cavities in the basis $\{|0\rangle_A|0\rangle_B, |1\rangle_A|1\rangle_B, \frac{1}{\sqrt{2}}(|0\rangle_A|1\rangle_B + |1\rangle_A|0\rangle_B), \frac{1}{\sqrt{2}}(|0\rangle_A|1\rangle_B - |1\rangle_A|0\rangle_B)\}$. Here $\{|0\rangle_A, |1\rangle_A\}$ and $\{|0\rangle_B, |1\rangle_B\}$ are photon number states in cavities A and B respectively. The teleportation is probabilistic, because it is successful only for the pair of Bell state outcomes of the above measurement (later we will describe how to convert such a probabilistic teleportation to a *reliable* quantum state transfer protocol). At the end of the detection period, if the protocol has been successful, Alice lets Bob know whether $D_+$ or $D_-$ had clicked. This corresponds to the classical communication part of the standard teleportation protocol [19]. Dependent on this information Bob applies a local unitary operation to his atom to obtain the teleported state. We call this the post-detection stage.

## 7.3 The scheme in detail

Let us now describe and analyse the scheme in detail. As the cavities are leaky, and we wish to look at single realizations conditioned on detection (or not) of decays, the ideal unravelling of the system's evolution is through the quantum jump approach [152]. Let us assume that the photon decay rate from both the cavities is $\kappa$. While Alice/Bob is applying a Hamiltonian $H$ to her/his atom-cavity system, its evolution subject to no detector click, is governed by the effective Hamiltonian (with $\hbar = 1$) $H_{\text{eff}} = H - i\kappa c^\dagger c$ (where $c^\dagger$ and $c$ are the creation and the destruction operators for the cavity mode under consideration). The coherent evolution due to $H_{\text{eff}}$ is interrupted by quantum jumps when there is a click in either the detector $D_+$ (corresponds to an action of the operator $(c_{\text{A}} + c_{\text{B}})/\sqrt{2}$ on the joint state vector of the pair of atom-cavity systems, $c_{\text{A}}$ and $c_{\text{B}}$ being the lowering operators for modes A and B respectively) or the detector $D_-$ (corresponds to an action of the operator $(c_{\text{A}} - c_{\text{B}})/\sqrt{2}$ in the same way).

The three level atoms have two ground states $|g\rangle$ and $|e\rangle$ (e.g. Zeeman sub-levels) and an

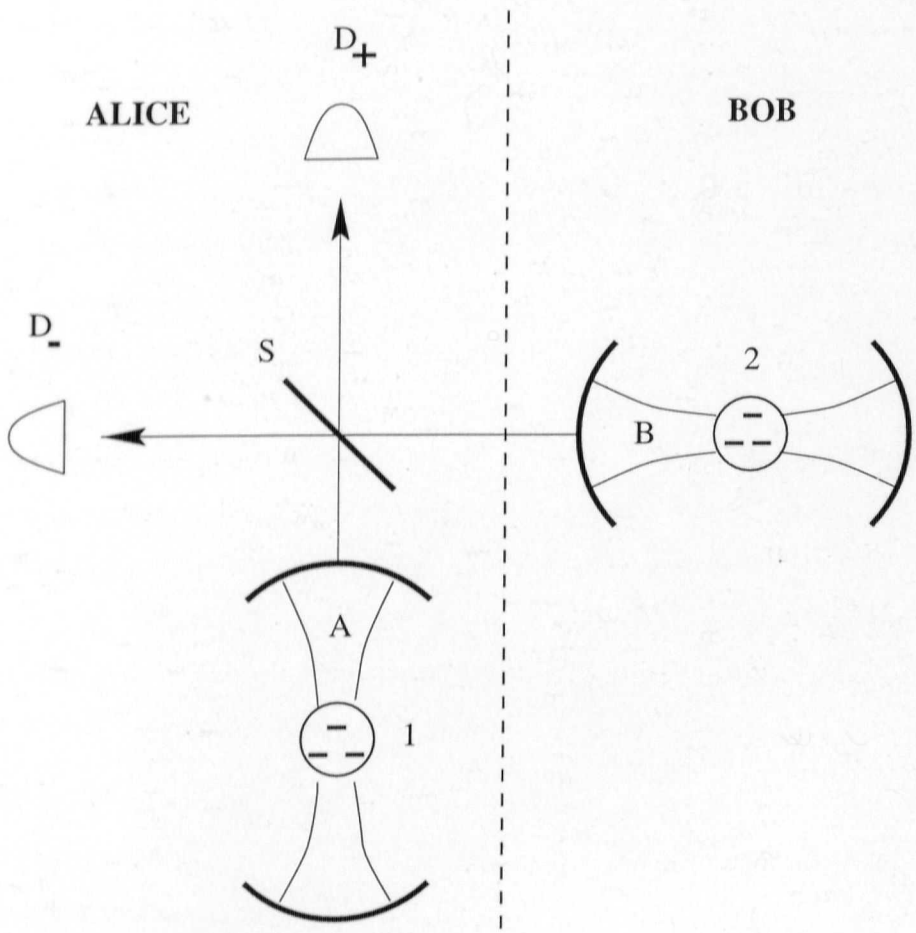



Figure 7.1: The atomic state teleportation setup. The cavity A, atom 1, beam splitter $S$ and the detectors $D_+$ and $D_-$ belong to Alice, while the cavity B and atom 2 belong to Bob.

excited state $|r\rangle$ (with a spontaneous decay rate $\gamma$) as shown in Fig.7.2. Alice and Bob use two types of time evolutions of the atom-cavity system as their basic local operations. The first type is called the adiabatic evolution (shown in Fig.7.2) which is initiated by switching on a classical laser field which drives the $|e\rangle \rightarrow |r\rangle$ transition with a coupling constant $\Omega$. The $|r\rangle \rightarrow |g\rangle$ transition is driven by the quantized cavity mode of coupling $g$. Both the classical laser field and the cavity modes are assumed to be detuned from their respective transitions by the same amount $\Delta$. As the atom is trapped in a specific position in the cavity, we can assume that the couplings $\Omega$ and $g$ remain constant during the interaction. We choose parameters such that $g\Omega/\Delta^2 \ll 1$ (the upper level $|r\rangle$ can be decoupled from the evolution) and $\Delta \gg \gamma$ (the spontaneous decay rate from $|r\rangle$ can be neglected). The Hamiltonian for the evolution of the system in such conditions (and $g = \Omega$ for simplicity), is given by $H^{(1)} = E|e\rangle\langle e| + E|g\rangle\langle g| + E(c|e\rangle\langle g| + c^\dagger|g\rangle\langle e|)$ where $E = g\Omega/\Delta$ [148]. The other local operation accessible to Alice and Bob is the Zeeman evolution which is used to give an arbitrary phase shift of the level $|e\rangle$ relative to the level $|g\rangle$. The Hamiltonian for this evolution by $H^{(2)} = \delta E|e\rangle\langle e|$, where $\delta E$ is an energy difference.

Let the unknown state of the atom 1 which Alice wants to teleport be

$$|\Psi\rangle_1^I = a|e\rangle_1 + b|g\rangle_1, \tag{7.1}$$

where the superscript $I$ in $|\Psi\rangle_1^I$ stands for input and $a$ and $b$ are complex amplitudes. We will assume that the initial state of Alice's cavity is $|0\rangle_A$ and the initial state of Bob's atom-cavity system is $|e\rangle_2|0\rangle_B$. At first, Alice maps the state of atom 1 onto the cavity mode A by switching the Hamiltonian $H^{(1)}$ on for a period of time $t_I$ given by $\tan\frac{\Omega_\kappa t_I}{2} = -\frac{\Omega_\kappa}{\kappa}$ where $\Omega_\kappa = \sqrt{4E^2 - \kappa^2}$. Subject to no decay being recorded in the detectors, the cavity state is given by

$$|\Psi\rangle_A^I = \frac{1}{\sqrt{|a|^2\alpha^2 + |b|^2}}(a\alpha|1\rangle_A + b|0\rangle_A), \tag{7.2}$$

where $\alpha = (\frac{e^{-\frac{\kappa}{2}t_I}}{\Omega_\kappa} 2E \sin\frac{\Omega_\kappa t_I}{2})$. The probability that no photon decay takes place during this evolution is given by $P_{ND}(A) = (|a|^2\alpha + |b|^2)$. Meanwhile, Bob also switches on the Hamiltonian $H^{(1)}$ in his cavity for a shorter length of time $t_E$ given by $\tan\frac{\Omega_\kappa t_E}{2} = -\frac{\Omega_\kappa}{2E-\kappa}$.

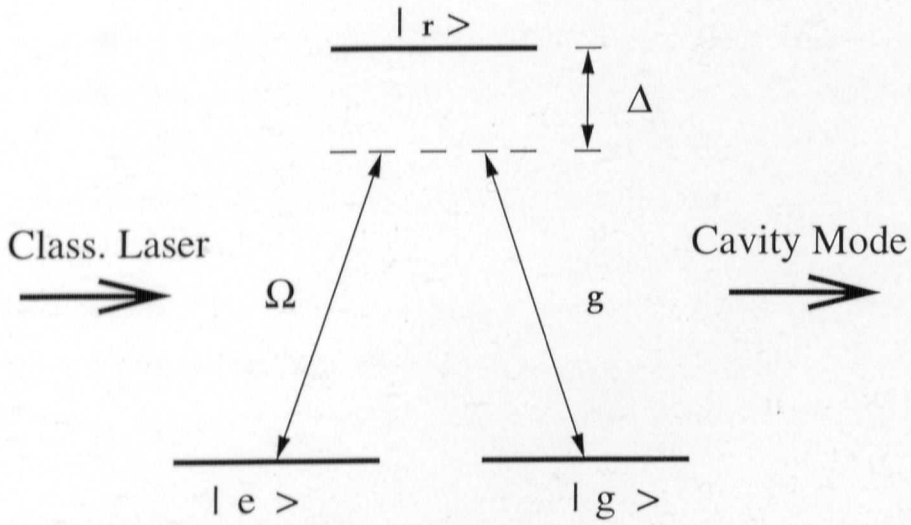



Figure 7.2: The level configuration of the trapped atom showing the fields responsible for the adiabatic evolution. The $|e\rangle \rightarrow |r\rangle$ transition being driven by a classical laser field of coupling $\Omega$ and the $|r\rangle \rightarrow |g\rangle$ transition being driven by the quantized cavity mode of coupling $g$. $\Delta$ is the detuning of both the classical laser field and the quantized field mode from their respective transitions.

His atom-cavity system thus evolves to the entangled state

$$|\Psi\rangle_{2,B}^{E} = \frac{1}{\sqrt{2}}(|e\rangle_2|0\rangle_B + i|g\rangle_2|1\rangle_B). \tag{7.3}$$

The probability that no photon decay takes place during this evolution is given by $P_{ND}(B) = |\beta|^2$ where $\beta = \frac{e^{-\frac{\kappa}{2}t_E}}{\Omega_\kappa} 2\sqrt{2}E \sin\frac{\Omega_\kappa t_E}{2}$. For keeping our calculations simple, we shall assume that Alice and Bob synchronize their actions in such a way that the preparation of the states $|\Psi\rangle_A^I$ and $|\Psi\rangle_{2,B}^E$ terminate at the same instant of time. This concludes the preparation stage of the protocol. The probability that this stage is a success is the probability that no photon decays from either cavity during the preparation. This is given by $P_{\text{suc}}(\text{prep}) = P_{ND}(A)P_{ND}(B)$. We will choose $\Omega_\kappa \gg \kappa$ which makes $P_{\text{suc}}(\text{prep}) \sim 1$.

Now comes the detection stage, in which Alice simply waits for any one of the detectors $D_+$ or $D_-$ to click. She waits for a finite detection time denoted by $t_D$. Alice and Bob reject the cases in which Alice does not register any click or registers two clicks. The joint state of Alice's and Bob's system at the beginning of the detection stage is

$$|\Phi(0)\rangle = |\Psi\rangle_A^I \otimes |\Psi\rangle_{2,B}^E. \tag{7.4}$$

Assume Alice registers a single click at a time $t_j \leq t_D$. The joint state of Alice's and Bob's system evolves as $|\Phi(t)\rangle_{A,2,B} = |\Psi(t)\rangle_A^I \otimes |\Psi(t)\rangle_{2,B}^E$ [152], where

$$|\Psi(t)\rangle_A^I = \frac{1}{\sqrt{|a\alpha|^2 e^{-2\kappa t} + |b|^2}}(a\alpha e^{-\kappa t}|1\rangle_A + b|0\rangle_A) \tag{7.5}$$

and

$$|\Psi(t)\rangle_{2,B}^E = \frac{1}{\sqrt{1 + e^{-2\kappa t}}}(|e\rangle_2|0\rangle_B + ie^{-\kappa t}|g\rangle_2|1\rangle_B). \tag{7.6}$$

The registering of a click at one of the detectors corresponds to an action of the jump operators $(c_A \pm c_B)/\sqrt{2}$ on the state $|\Phi(t_j)\rangle_{A,2,B}$. Then the resultant joint state of Alice's and Bob's system becomes

$$\begin{aligned} |\Phi(t_j)\rangle_{A,2,B}^{J\pm} &= \frac{1}{\sqrt{P_{ND}(A) + 2|a|^2\alpha^2 e^{-2\kappa t_j}}}\{(a\alpha|e\rangle_2 \\ &\pm\ ib|g\rangle_2) \otimes |0\rangle_A|0\rangle_B \\ &+\ e^{-\kappa t_j} a\alpha|g\rangle_2 \otimes (|1\rangle_A|0\rangle_B \pm |0\rangle_A|1\rangle_B)\}. \end{aligned} \tag{7.7}$$

$|\Phi(t_j)\rangle^{J\pm}_{A,2,B}$ corresponds to the click being registered in $D_\pm$ and the superscript $J$ stands for jump. At the end of a successful detection stage the joint state of the cavities A, B and atom 2 will be $|\Phi(t_D)\rangle^{J\pm}_{A,2,B}$. In the post detection stage, Bob uses $H^{(2)}$ to give $|g\rangle_2$ an extra phase shift with respect to $|e\rangle_2$. This phase shift is $-i$ if $D_+$ had clicked and $i$ if $D_-$ had clicked. This concludes the entire protocol.

## 7.4 Estimates of efficiency and success

We now proceed to estimate the fidelity of the teleported state generated at Bob's end with respect to Alice's input state $|\Psi\rangle^I_1$. First we must note that though the field *continues to decay* even after the protocol is over (i.e Alice has ceased to keep track of detector clicks), the reduced density matrix of atom 2 remains unchanged as this atom is not interacting with the cavity field any more. Thus the average density matrix generated at Bob's end due to our teleportation procedure is given by

$$\rho_2^{Tel} = \frac{P_{ND}(A)|\Psi\rangle_2\langle\Psi|_2 + 2|a|^2\alpha^2 e^{-2\kappa t_D}|g\rangle_2\langle g|_2}{P_{ND}(A) + 2|a|^2\alpha^2 e^{-2\kappa t_D}}, \tag{7.8}$$

where $|\Psi\rangle_2 = (a\alpha|e\rangle_2 + b|g\rangle_2)/\sqrt{|a|^2\alpha^2 + |b|^2}$. The fidelity of this state with respect to the input state is $F(t_D, a, b) = \{P_{ND}(A)(|a|^2\alpha + |b|^2) + 2|a|^2\alpha^2 e^{-2\kappa t_D}|b|^2\}/\{P_{ND}(A) + 2|a|^2\alpha^2 e^{-2\kappa t_D}\}$. We thus see that apart from the system parameters $\kappa$ and $\Omega_\kappa$, the fidelity of the generated state also depends on the detection time $t_D$ and the modulus of the amplitudes $a$ and $b$ of the initial state. It is thus a teleportation protocol with a *state dependent fidelity.*

We have plotted the variation of the average fidelity of teleportation over all possible input states as a function of the detection time $t_D$ in Fig.7.3. We see that the fidelity increases with an increase of the detection time. This happens because the measurement done by the beam splitter and the detectors is completed only in an infinite time. Increasing the detection time makes the measurement more complete and thereby increases the fidelity. The parameter regime used for this plot $\{(g : \Omega : \kappa : \gamma : \Delta)/2\pi = (10 : 10 : 0.01 : 1 : 100)$ MHz$\}$, is carefully chosen to satisfy all our constraints $(g\Omega/\Delta^2 \ll 1, \Delta \gg \gamma, \Omega_\kappa \gg \kappa)$. One can, for example, try to approach this regime by increasing the cavity finesse of Ref.[67]

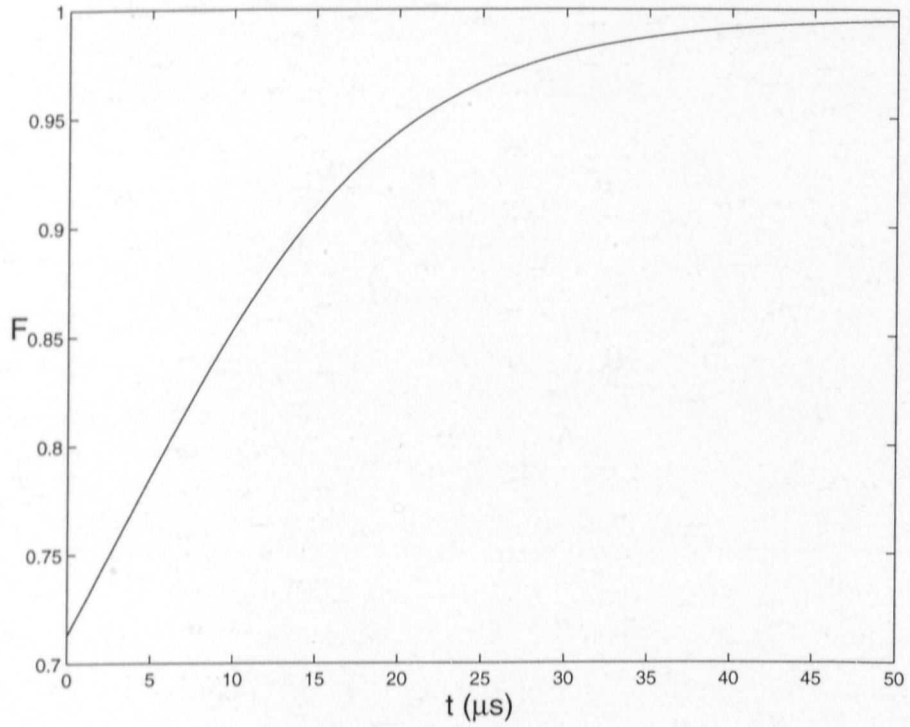



Figure 7.3: The improvement of average teleportation fidelity with the length of the detection stage. The parameter regime is $(g : \Omega : \kappa : \gamma : \Delta)/2\pi = (10 : 10 : 0.01 : 1 : 100)$ MHz

by an order of magnitude and increasing the length of that cavity to about a millimetre while keeping the beam waist and other parameters constant. As evident from the plot, the average fidelity approaches optimum value of 99.5 percent for a detection time of about half the cavity life time.

The total probability of success of the protocol is also state dependent and given by

$$\begin{aligned} P_{\text{suc}} &= P_{\text{suc}}(\text{prep}) \times P_{1D}(0, t_D) \\ &= \frac{P_{ND}(A) + 2|a|^2\alpha^2 e^{-2\kappa t_D}}{2} P_{ND}(B)(1 - e^{-2\kappa t_D}), \end{aligned} \tag{7.9}$$

where $P_{1D}(0, t_D)$ is the probability of a single decay during the detection period. In the parameter domain under consideration, for $t_D = 50\mu$s, we find that the average of the

probability of success over all input states is about 48.7 percent. This is a little lower than the ideal success probability of 50 percent (for Alice registering any of the pair of Bell state outcomes) because the preparation stage has an extremely small, but finite, chance of failure.

Let, in a real experiment, the total efficiency of photon detection (including all detector and other unwanted losses) be $\eta$. In the detection stage, Alice will be able to detect only a fraction $\eta$ of all her successful protocols. On the other hand, during this stage, she will erroneously regard a fraction $2\eta(1-\eta)$ of the cases with two decays as successful cases. Then the probability of a successful protocol changes to $P_{\rm suc}(\eta) = \eta P_{1D}(0,t_D) + 2\eta(1-\eta)(1 - P_{ND}(0,t_D) - P_{1D}(0,t_D))$, and the fidelity of the corresponding state generated at Bob's end would be $\{\eta P_{1D}(0,t_D)F(t_D,a,b)+2\eta(1-\eta)(1-P_{ND}(0,t_D)-P_{1D}(0,t_D))|b|^2\}/P_{\rm suc}(\eta)$, where $P_{ND}(0,t_D)$ is the probability of no decay during the detection period. In the parameter domain under consideration, and for $\eta$ not lower than 10 percent, we can neglect the effect of undetected photon losses during the preparation stage on the fidelity. For a $\eta$ of 60 percent and detection times large compared to the cavity decay time, the fidelity of the state generated at Bob's end is about 81 percent.

The main practical role of teleportation is as a device for linking up distant quantum processors with entanglement. To set up entanglement between their atoms, Alice and Bob must both prepare their respective atom-cavity systems in the state $(|e\rangle|0\rangle + i|g\rangle|1\rangle)/\sqrt{2}$ during the preparation stage. Entanglement is established if there is a single click during the detection period. The resultant entangled state is $|\Psi_{12}\rangle = \{\eta(1-e^{-4\kappa t})/4\}|\psi^{\pm}\rangle\langle\psi^{\pm}| + \{\eta(1-\eta)(1+e^{-4\kappa t}-2e^{-2\kappa t})/2\}|g\rangle_1|g\rangle_2\langle g|_1\langle g|_2$, where $|\psi^{+}\rangle = |e\rangle_1|g\rangle_2+|g\rangle_1|e\rangle_2$. The relative entropy of entanglement of this state can be calculated [33] and for $t_D$ large compared to the cavity decay time and a reasonable $\eta$ of 60 percent it is about 0.16, while for a high $\eta$ of 90 percent it is about 0.48 (note that $|\Psi_{12}\rangle$ is entangled for arbitrary $\eta$). From the viewpoint of setting up of entanglement, our scheme is related to the scheme described by Cabrillo *et al.* [142]. But the efficiency of success can be much higher (nearing 50 percent).

## 7.5 A reliable state transfer protocol

It is interesting to note that the above probabilistic teleportation protocol can be modified to a *teleportation with insurance*. This means that in the cases when the protocol is unsuccessful, the original state of Alice's atom 1 is not destroyed, but mapped onto another reserve atom $r$ trapped in Alice's cavity. To accomplish this, Alice has to follow the *local redundant encoding* of Ref.[149] and code her initial state $|\Psi\rangle_1^I$ as $a(|e\rangle_1|g\rangle_r + |g\rangle_1|e\rangle_r) + b(|g\rangle_1|g\rangle_r + |e\rangle_1|e\rangle_r)$. After this, she just follows the same protocol as before. But in cases when the protocol is unsuccessful, she is left with either the state $a|g\rangle_r + b|e\rangle_r$ or a state that can be converted to $a|g\rangle_r + b|e\rangle_r$ by a known unitary transformation. She can now exchange the roles of atom 1 and atom $r$ and try to teleport the state $|\Psi\rangle_1^I$ again. She can repeat this procedure until teleportation is successful (Of course, this holds true perfectly only when $\eta = 1$).

## 7.6 Conclusions

To conclude, we would like to mention that we have presented a simple scheme for atomic state teleportation, which could be implemented as soon as one could trap single three level atoms in a cavity. Moreover, by adding one more atom to Alice's cavity, it can be converted to a *reliable* state transfer protocol. This state transfer protocol can be viewed as an *alternative* to designer laser pulses and adiabatic transfers (Refs.[147, 148]) for getting quantum information into a cavity from outside. This state transfer should work for distances of the order of the absorption length scales of a fibre. All the model independent portions of the analysis of communication through a noisy quantum channel [149, 150, 153] should carry over to this decay induced scenario of state transfer. The scheme described here is also a rare example of a quantum decay playing a constructive role in quantum information processing.

# Chapter 8

# Conclusions

In this thesis we have described some applications and manipulations of entanglement and some physical implementations of these processes. Most of the applications and manipulations described are connected in one way or other to the common theme of state preparation of one system by actions performed on another system. For example, in the second chapter, we deal with preparation of nonclasical states of a cavity field by conditional measurements on a macroscopic mirror. In the third chapter, we use the fact that decoherence of a macroscopic mirror (which is equivalent to measurements done on the macroscopic mirror by an external environment) induces decoherence of the state of a cavity field entangled with it. Multiparticle entanglement swapping is also state preparation of several distant systems by measurements on some systems brought together. Entanglement concentration by swapping projects a pair of systems to a maximally entangled state corresponding to certain measurement outcomes on another pair of systems. Dense coding (which we generalize to mixed states in chapter 6) is an example to preparation of a joint state of two systems by unitary rotations on one system alone. In chapter 7, we give a physical implementation of teleportation. Teleportation is, beyond doubt, the most striking example of state preparation at a distance. Can this common theme point to a direction for quantifying entanglement? For example, could the total number of states of one system (as quantified by some kind of volume) accessible by measurements on another system entangled with it be a meausure of

entanglement? We leave such questions for the future.

Each of the aspects described in the thesis would have further extensions to consider for the future. For example, one could analyse the state preparation methods described in the second chapter from a more practical perspective. This would involve full consideration of decoherences of the cavity fields and the mirrors and finite time and accuracy of measurements done on the mirror. The heuristic considerations of decoherence in our third chapter need to be backed up by more detailed calculations. Especially interesting would be the prospects of preparing nonclassical states of phononic vibrations when the movable mirror is replaced by a deformable mirror coated on the face of a crystal. All analysis in the chapter on multiparticle entanglement swapping has been very schematic. There is still an enormous scope of further study of the efficacy of entanglement swapping for different types of entanglement distribution channels used prior to swapping. Whether a quantum telephone exchange really provides advantage while setting up multiparticle entanglement would depend on the cost of distribution of bipartite entanglement and the decoherence in the channels used for the distribution. Such an analysis, identifying the cases in which a quantum telephone exchange is an useful concept, deserves further study. In entanglement concentration via swapping, questions of extensions to higher dimensional bipartite entanglement and to mixed entangled states remain open. In chapter 6 we have described how the capacity of dense coding with mixed states is related to the measures of entanglement stemming from purification procedures. A physical meaning of this relationship has also been presented. It would be of interest to be able to rigorously justify the conjectures used while presenting the physical meaning. It would also be of interest to relate the fidelity of teleportation and the security of entanglement based cryptography to the measures of entanglement in the same way. In the previous chapter we have described a method of teleportation through the detection of cavity decays. Similar techniques can also be used for dense coding and the concentration of shared entanglement. These remain to be analysed in a future work.

# Appendix A

# The time evolution operator for a cavity mode interacting with a movable mirror

The time evolution operator is given by

$$U(t) = e^{-ira^\dagger a} e^{-itb^\dagger b + ikta^\dagger a(b+b^\dagger)} \tag{A.1}$$

where $t$ is the time multiplied by $\omega_m$, $k = g/\omega_m$ and $r = \omega_0/\omega_m$. We now consider a unitary transformation using the operator

$$T = e^{-ka^\dagger a(b^\dagger - b)}. \tag{A.2}$$

Note that this is a displacement operator for the mirror in which the displacement amplitude has been replaced by the number operator for the cavity mode. Using the Baker-Campbell-Hausdorff expansion [73], the effect of this transformation is readily shown to be

$$TbT^\dagger = b + ka^\dagger a, \tag{A.3}$$

$$Tb^\dagger T^\dagger = b^\dagger + ka^\dagger a, \tag{A.4}$$

$$Ta^\dagger a T^\dagger = a^\dagger a. \tag{A.5}$$

Using the fact that

$$Uf(\{X_i\})U^\dagger = f(\{UX_iU^\dagger\}), \tag{A.6}$$

for any function $f$, unitary operator $U$, and arbitrary set of operators $\{X_i\}$, the effect of the transformation on the time evolution operator is easily calculated to be

$$TU(t)T^\dagger = e^{-ira^\dagger at}e^{-ib^\dagger bt - ik^2(a^\dagger a)^2}. \tag{A.7}$$

Multiplying on the left by $T^\dagger$, and on the right by $T$, we obtain the following expression for the time evolution operator:

$$U(t) = e^{-ira^\dagger at}e^{ik^2(a^\dagger a)^2 t}e^{ka^\dagger a(b^\dagger - b)}e^{-ib^\dagger bt}e^{-ka^\dagger a(b^\dagger - b)}. \tag{A.8}$$

(Note that to obtain this expression we have swapped various exponentials which contain commuting arguments.) To obtain the final form of $U(t)$, we need to swap the last two exponential factors in this expression. To achieve this we note first that the BCH expansion gives

$$e^{-ib^\dagger b}[a^\dagger a(b^\dagger - b)]e^{ib^\dagger b} = a^\dagger a(b^\dagger e^{-it} - be^{it}), \tag{A.9}$$

and again using Eq.(A.6) we obtain

$$e^{-ib^\dagger b}e^{-ka^\dagger a(b^\dagger - b)}e^{ib^\dagger b} = e^{-ka^\dagger a(b^\dagger e^{-it} - be^{it})}. \tag{A.10}$$

Multiplying both sides on the right by $e^{-ib^\dagger b}$ we arrive at the relation required to swap the exponentials, namely

$$e^{-ib^\dagger b}e^{-ka^\dagger a(b^\dagger - b)} = e^{-ka^\dagger a(b^\dagger e^{-it} - be^{it})}e^{-ib^\dagger b}. \tag{A.11}$$

We may now write the expression for $U(t)$ as

$$\begin{aligned} U(t) &= e^{-ira^\dagger at}e^{ik^2(a^\dagger a)^2 t}e^{ka^\dagger a(b^\dagger - b)} \\ &\times\ e^{-ka^\dagger a(b^\dagger e^{-it} - be^{it})}e^{-ib^\dagger b}, \end{aligned} \tag{A.12}$$

and to obtain the final expression given in Eq.(2.7), we need only combine the arguments of the $3^{rd}$ and $4^{th}$ exponentials, which is readily achieved with the BCH relation [73].

# Appendix B

# Solution to the master equation for the system when the mirror's motion is damped

We need to solve Eq.(2.29), which contains two parts. The solution of the first part

$$\frac{d\rho(t)}{dt} = -\frac{i}{\hbar}[H, \rho(t)] \,, \tag{B.1}$$

is known to be

$$\rho(t) = U(t)\rho(0)U^{\dagger}(t) \tag{B.2}$$

where, $U(t)$ is given by Eq.(2.7). On the other hand, the second part,

$$\frac{d\rho(t)}{dt} = \frac{\gamma}{2}(2b\rho(t)b^{\dagger} - b^{\dagger}b\rho(t) - \rho(t)b^{\dagger}b) \tag{B.3}$$

is known to transform $|\lambda_i\rangle\langle\lambda_j|$ as [60]

$$P_{ij}|\lambda_i\rangle\langle\lambda_j| \rightarrow P_{ij}\langle\lambda_i|\lambda_j\rangle^{(1-e^{-\gamma t})}|\lambda_i e^{-\gamma t/2}\rangle\langle\lambda_j e^{-\gamma t/2}| \tag{B.4}$$

where, $|\lambda_i\rangle$ and $|\lambda_j\rangle$ are coherent states.

Let the initial state of our system be

$$\rho(0) = |\alpha\rangle\langle\alpha|_{\rm c} \otimes |0\rangle\langle 0|_{\rm m}, \tag{B.5}$$

that is, we assume the mirror to be in a vacuum state initially (for simplicity). As the damping localizes the mirror state to a coherent state basis, and corresponding to each number state of the field, the mirror is driven to a separate coherent state, at any time $t$ the general form of the density matrix will be

$$\rho(t) = \sum_{n=0,m=0} \rho_{nm}(t)|n\rangle\langle m|_{\rm c} \otimes |\phi_n(\gamma,t)\rangle\langle\phi_m(\gamma,t)|_{\rm m}. \tag{B.6}$$

Thus, we can split the evolution of the entire system into separate evolutions labelled by $m$ and $n$. In other words, we break our problem into that of calculating the evolution of each of the entities $\rho_{nm}(t)\ |\phi_n(\gamma,t)\rangle\langle\phi_m(\gamma,t)|_{\rm m}$ separately. In any small time step $\Delta t$ during which evolution occurs only according to Eq.(B.2), the amplitudes of the coherent states of the mirror change according to

$$\phi_n(\gamma,t) \to (1 - i\Delta t)\phi_n(\gamma,t) + ikn\Delta t, \tag{B.7}$$

while if evolution occurs according to Eq.(B.3), then

$$\phi_n(\gamma,t) \to \phi_n(\gamma,t)(1 - \gamma\Delta t/2). \tag{B.8}$$

Hence we can set up the following differential equation

$$\frac{d\phi_n(\gamma,t)}{dt} = -i\phi_n(\gamma,t) + ikn - \frac{\gamma}{2}\phi_n(\gamma,t), \tag{B.9}$$

the solution for which (with initial condition $\phi_n(\gamma,0) = 0$) is given by

$$\phi_n(\gamma,t) = \frac{ikn}{i+\gamma/2}(1 - e^{-(i+\gamma/2)t}). \tag{B.10}$$

Next let us determine how $\rho_{nm}(t)$ evolves. Following Eq.(B.2) it evolves as

$$\rho_{nm}(t) \to \rho_{nm}(t)\ e^{ik^2(n^2-m^2)\Delta t(1-\cos t)}, \tag{B.11}$$

while Eq.(B.3) transforms

$$\begin{aligned} \rho_{nm}(t) &\to \rho_{nm}(t)\ \langle\phi_n(\gamma,t)|\phi_m(\gamma,t)\rangle^{(1-e^{-\gamma\Delta t})} \\ &= \rho_{nm}(t)e^{-|\phi_n(\gamma,t)-\phi_m(\gamma,t)|^2\gamma\Delta t/2}, \end{aligned} \tag{B.12}$$

where the smallness of $\Delta t$ and the fact that $Im(\phi_n(\gamma,t)\phi_m(\gamma,t)^*) = 0$ (from Eq.(B.10)) have been used. Hence, evolving $\rho_{nm}(0)$ according to Eq.(B.11) and Eq.(B.12) alternately and taking the limit $\Delta t \to 0$ we obtain

$$\begin{aligned} \rho_{nm}(t) &= \rho_{nm}(0) e^{ik^2(n^2-m^2)(t-\sin t)} \\ &\quad \times e^{-\frac{\gamma}{2}\int_0^t |\phi_n(\gamma,t)-\phi_m(\gamma,t)|^2 dt}. \end{aligned} \tag{B.13}$$

Combining Eq.(B.10), Eq.(B.13) and Eq.(B.6), and evaluating the integral in Eq.(B.13) one can obtain Eqs.(2.30)-(2.32) of section 2.7, which constitutes the complete solution for the density matrix of the system at an arbitrary time.

# Bibliography


[1] A. Einstein, B. Podolsky and N. Rosen, Phys. Rev. **47**, 777 (1935).

[2] D. Bohm, *Quantum Theory*, Prentice-Hall, New York (1951), p. 614.

[3] J. S. Bell, Physics **1**, 195 (1964).

[4] J. F. Clauser, M. A. Horne, A. Shimony and R. A. Holt, Phys. Rev. Lett. **23**, 880 (1969).

[5] N. Gisin, Phys. Lett. A **145**, 201 (1991).

[6] S. Popescu and D. Rohrlich, Phys. Lett. A **166**, 293 (1992).

[7] A. Aspect, P. Grangier and G. Roger, Phys. Rev. Lett. **47**, 460 (1981); Z. Y. Ou and L. Mandel, Phys. Rev. Lett. **61**, 50 (1988).

[8] E. Santos, Phys. Lett. A **200**, 1 (1995).

[9] D. M. Greenberger, M. Horne and A. Zeilinger, in *Bell's Theorem, Quantum Theory, and Conceptions of the Universe*, ed. M. Kafatos, Kluwer, Dordrecht (1989), p. 69.

[10] N. D. Mermin, Phys. Today **43**, 9 (1990).

[11] L. Hardy, Phys. Rev. Lett. **71**, 1665 (1993).

[12] J. von Neumann, *Mathematical Foundations of Quantum Mechanics*, pp. 347-445, Princeton University Press, Princeton (1955) (Eng. Trans. by R. T. Beyer).

[13] E. Schrödinger, Naturwissenschaften **23**, 807 (1935); English translation by J. D. Trimmer in Proc. Am. Philos. Soc. **124**, 323 (1980).

[14] E. P. Wigner in *The Scientist Speculates*, I. J. Good, ed., pp. 284-302, Heinemann, London (1961).

[15] H. Everett III, Revs. Mod. Phys. **29**, 454 (1957).

[16] W. H. Zurek, Phys. Today **44**, 36 (1991).

[17] A. K. Ekert, Phys. Rev. Lett. **67**, 661 (1991).

[18] C. H. Bennett and S. J. Wiesner, Phys. Rev. Lett. **69** , 2881 (1992).

[19] C. H. Bennett, G. Brassard, C. Crepeau, R. Jozsa, A. Peres and W. K. Wooters, Phys. Rev. Lett. **70**, 1895 (1993).

[20] W. K. Wootters and W. H. Zurek, Nature **299**, 802 (1982).

[21] D. Deutsch, Proc. Roy. Soc. London A **400**, 97 (1985); D. Deutsch and R. Jozsa, Proc. Roy. Soc. London A **439**, 553 (1992); P. Shor, *Proc. of 35 Annual Symposium on the Foundation of Computer Science*, IEEE Computer Society, Los Alamitos, p. 124; L. Grover, Phys. Rev. Lett. **78**, 325 (1997).

[22] S. L. Braunstein, C. M. Caves, R. Jozsa, N. Linden, S. Popescu and R. Schack, Phys. Rev. Lett. **83**, 1054 (1999); R. Schack and C. M. Caves, LANL e-print quant-ph/9903101; N. Linden and S. Popescu, LANL e-print quant-ph/9906008.

[23] R. F. Werner, Phys. Rev. A **40**, 4277 (1989).

[24] S. Popescu, Phys. Rev. Lett. **72**, 797 (1994).

[25] R. Horodecki, M. Horodecki and P. Horodecki, Phys. Lett. A **222**, 21 (1996).

[26] A. Peres, Phys. Rev. Lett. **77**, 1413 (1996); M. Horodecki, P. Horodecki and R. Horodecki, Phys. Lett A **223**, 1 (1996).

[27] S. Popescu, Phys. Rev. Lett. **74**, 2619 (1995).

[28] C. H. Bennett, H. J. Bernstein, S. Popescu, B. Schumacher, Phys. Rev. A **53**, 2046, (1996)

[29] D. Deutsch, A. Ekert, R. Jozsa, C. Machiavello, S. Popescu, A.Sanpera, Phys. Rev. Lett. **77**, 2818 (1996); C. H. Bennett, G. Brassard, S. Popescu, B. Schumacher, J. A. Smolin and W. K. Wootters, Phys. Rev. Lett. **76**, 722(1996).

[30] C. H. Bennett, D. P. DiVincenzo, J. A. Smolin and W. K. Wootters, Phys. Rev. A **54**, 3824 (1996).

[31] V. Vedral, M. B. Plenio, M. A. Rippin and P. L. Knight, Phys. Rev. Lett. **78**, 2275 (1997).

[32] V. Vedral, M. B. Plenio, K. Jacobs, and P. L. Knight, Phys. Rev. A **56**, 4452 (1997).

[33] V. Vedral and M. B. Plenio, Phys. Rev. A **57**, 1619 (1998).

[34] V. B. Braginsky and Yu. I. Vorontsov, Usp. Fiz. Nauk 114, 41 (1974)[Sov. Phys. Usp. 17, 644(1975).

[35] J. N. Hollenhorst, Phys. Rev. A **19**, 1669 (1979).

[36] C. M. Caves, K. S. Thorne, R. W. P. Drever, V. D. Sandberg, and M. Zimmerman, Rev. Mod. Phys. **52**, 341 (1980).

[37] See for example, R. Weiss, in *Sources of Gravitational Radiation*, edited by L. Smarr (Cambridge Univ. Press, Cambridge, 1979).

[38] C. M. Caves, Phys. Rev. Lett. **45**, 75 (1980); R. Loudon, Phys. Rev. Lett. **47**, 815 (1981); C. M. Caves, Phys. Rev. D **23** 1693 (1981); M. Ley and R. Loudon, J. Mod. Optics **34**, 227 (1987); P. Samphire, R. Loudon and M. Babiker, Phys. Rev. A 51, 2726 (1995).

[39] A. F. Pace, M. J. Collett and D. F. Walls, Phys. Rev. A **47**, 3173 (1993).

[40] G. J. Milburn, K. Jacobs and D. F. Walls, Phys. Rev. A **50**, 5256 (1994).

[41] K. Jacobs, P. Tombesi, M. J. Collett and D. F. Walls, Phys. Rev. A **49**, 1961 (1994).

[42] S. Mancini, P. Tombesi, Phys. Rev. A **49**, 4055 (1994);

[43] M. Pinard, C. Fabre and A. Heidmann, Phys. Rev. A 51, 2443 (1995); A. Heidmann and S. Reynaud, Phys. Rev. A 50, 4237 (1994); C. Fabre, M. Pinard, S. Bourzeix, A. Heidmann, E. Giacobino ans S. Reynaud, Phys. Rev. A 49, 1337 (1994).

[44] S. Mancini, V. I. Manko and P. Tombesi, Phys. Rev. A **55**, 3042 (1997).

[45] C. K. Law, Phys. Rev. A **51**, 2537 (1995).

[46] P. Meystre, E. M. Wright, J. D. McCallen and E. Vignes, J. Opt. Soc. Am. B **2**, 1830 (1985).

[47] A. Dorsel, J. D. McCullen, P. Meystre, E. Vignes, H. Walther, Phys. Rev. Lett. **51**, 1550 (1983); A. Dorsel, J. D. McCullen, P. Meystre, H. Walther, E. Wright, J. Opt. Soc. Am. B **1**, 441 (1984).

[48] G. Drobny, I. Jex and V. Bužek, Phys. Rev. A **48**, 569 (1993).

[49] A. Chefles and S. M. Barnett, J. Mod. Opt. **43**, 709 (1996).

[50] V. Bužek and P. L. Knight in *Progress in Optics XXXIV*, edited by E. Wolf (Elsevier, Amsterdam, 1995); C. C. Gerry and P. L. Knight, Am. J. Phys, **65**, 964 (1997).

[51] R. Schack, A. Breitenbach and A. Schenzle, Phys. Rev. A **45**, 3260 (1992); M. Brune, S. Haroche, V. Lefevre, J. M. Raimond and N. Zagury, Phys. Rev. Lett. **65**, 976 (1990).

[52] K. Wodkiewicz, P. L. Knight, S. J. Buckle and S. M. Barnett, Phys. Rev. A **35**, 2567 (1987).

[53] A. Peres, *Quantum Theory: Concepts and Methods*, Kluwer, Dordrecht (1993).

[54] C. M. Caves, Phys. Rev. Lett. **54**, 2465 (1985).

[55] V. B. Braginsky and F. Ya. Khalili, *Quantum Measurement*, Cambridge Univ. Press, Cambridge (1992).

[56] H. P. Yuen, Phys. Rev. Lett. **51**, 719 (1983); W.-T. Ni, Phys. Rev. A **33**, 2225 (1986); M. Ozawa, Phys. Rev. Lett. **60**, 385 (1988).

[57] W. H. Zurek, Phys. Rev. D **24**, 1516 (1981).

[58] W. H. Zurek, S. Habib, J. P. Paz, Phys. Rev. Lett. **70**, 1187 (1993).

[59] J. P. Paz, S. Habib, W. H. Zurek, Phys. Rev. D **47**, 488 (1993).

[60] D. F. Walls and G. J. Milburn, Phys. Rev. A **31**, 2403 (1985).

[61] B. M. Garraway and P. L. Knight, Opt. Commun. **123**, 517 (1996).

[62] D. F. Walls, M. J. Collett and G. J. Milburn, Phys. Rev. D **32**, 3208 (1985).

[63] T. Quang, P. L. Knight and V. Buzek, Phys. Rev. A **44**, 6092 (1991).

[64] G. Rempe. R. J. Thompson, H. J. Kimble and R. Lalezari, Opt. Lett. **17**, 363 (1992).

[65] I. Tittonen, G. Breitenbach, T. Kalkbrenner, T. Müller, R. Conradt, S. Schiller, E. Steinsland, N. Blanc and N. F. de Rooij, Phys. Rev. A **59**, 1038 (1999).

[66] M. Pinard, Y. Hadjar and A. Heidmann, *Effective mass in quantum effects of radiation pressure*, LANL e-print quant-ph/9901057 (1999).

[67] C. J. Hood, M. S. Chapman, T. W. Lynn, and H. J. Kimble, Phys. Rev. Lett. **80**, 4157 (1998).

[68] A. N. Cleland and M. L. Roukes, Appl. Phys. Lett **69**, 2653 (1996).

[69] L. Davidovich *et al.*, Phys. Rev. A **50**, R895 (1994)

[70] J. I. Cirac and P. Zoller, Phys. Rev. Lett. **74**, 4091 (1995).

[71] C. Monroe, D. M. Meekhof, B. E. King and D. J. Wineland, Science **272**, 1131 (1996).

[72] J. F. Poyatos, J. I. Cirac and P. Zoller, Phys. Rev. Lett. **77**, 4728 (1996).

[73] W. H. Louisell, *Quantum Statistical Properties of Radiation* (John Wiley & Sons, New York, 1990).

[74] A. Caldeira and A. J. Leggett, Physica A **121**, 587 (1983); E. Joos and H. D. Zeh, Z. Physik B **59** 223 (1985); W. G. Unruh, W. H. Zurek, Phys. Rev. D **40**, 1071 (1989).

[75] B. L. Hu, J. P. Paz, and Y. H. Zhang, Phys. Rev. D **47**, 1576 (1993).

[76] P. L. Knight, in "Quantum Fluctuations", Proc. Les Houches Summer School, Session LXIII, 1995, eds. S. Reynaud, and E. Giacobino and J. Zinn-Justin (Elsevier, Amsterdam, 1997).

[77] M. Brune, E. Hagley, J. Dreyer, X. Maître, A. Maali, C. Wunderlich, J. M. Raimond, and S. Haroche, Phys. Rev. Lett. **77**, 4887 (1996).

[78] A. J. Leggett, Contemporary Physics **54**, 583 (1984).

[79] D. Home, and R. Chattopadhyaya, Phys. Rev. Lett. **76**, 2836 (1996).

[80] J. R. Anglin and W. H. Zurek, Phys. Rev. D **53**, 7327 (1996).

[81] G. C. Ghirardi, A. Rimini, and T. Weber, Phys. Rev. D **34** 470 (1986); G. C. Ghirardi, P. Pearle, and A. Rimini, Phys. Rev. A **42**, 78 (1990); I. C. Percival, Proc. Roy. Soc. London A **447** 189(1994); D. I. Fivel, Phys. Rev. A **56** 146 (1997).

[82] R. Penrose, Gen. Rel. Grav. **28**, 581 (1996); L. Diosi, Phys. Rev. A **40**, 1165 (1989).

[83] R. B. Griffiths, J. Stat. Phys. **36** 219 (1984); M. Gell-Mann, and J. B. Hartle, Phys. Rev. D **47**, 3345 (1993); J. J. Halliwell, Ann. NY Acad. Sci. **755**, 726 (1995).

[84] S. W. Hawking, and R. Penrose, *The Nature of Space and Time* (Princeton University Press, New Jersey, 1996); F. Dowker, and A. Kent, J. Stat. Phys. **82**, 1575 (1996); A. Kent, and J. McElwaine, Phys. Rev. A **55**, 1703 (1997).

[85] D. Home, and S. Bose, Phys. Lett. A **217** 209 (1996); D. I. Fivel, LANL Report No: quant-ph/9706002 (1997).

[86] I. C. Percival, and W. Strunz, Proc. Roy. Soc. A **453**, 431 (1997); W. L. Power, *The Interaction of Propagating Spacetime Fluctuations with Wavepackets*, preprint (1997).

[87] P. Pearle, and E. Squires, Phys. Rev. Lett. **73**, 1 (1994).

[88] S. Mancini, D. Vitali and P. Tombesi, Phys. Rev. Lett. **80**, 688 (1998).

[89] A. S. Parkins, P. Marte, P. Zoller and H. J. Kimble, Phys. Rev. Lett. **71**, 3095 (1993).

[90] K. Vogel, V. M. Akulin and W. P. Schleich, Phys. Rev. Lett. **71** 1816 (1993).

[91] C. K. Law and H. J. Kimble, J. Mod. Opt. **44** 2067 (1997).

[92] B. M. Garraway, and P. L. Knight, in *Quantum Communications and Measurement*, ed. V. P. Belavkin *et al* (Plenum Press, New York, 1995).

[93] M. Wilkens, and P. Meystre, Phys. Rev. A **43**, 3832 (1991); S. M. Dutra, P. L. Knight, and H. Moya-Cessa, Phys. Rev. A **48**, 3168 (1993); R. Walser, J. I. Cirac and P. Zoller, Phys. Rev. Lett. **77**, 2658 (1996).

[94] G. Rempe, F. Schmidt-Kaler, and H. Walther, Phys. Rev. Lett **64**, 2783 (1990).

[95] H. Wei, X. Xue and S. D. Morgera, LANL Report No: quant-ph/9807057 (1998).

[96] C. H. Bennett, G. Brassard and N. D. Mermin, Phys. Rev. Lett **68**, 557(1992).

[97] H.-K. Lo and H. F. Chau, Phys. Rev. Lett. **78**, 3410 (1997); D. Mayers, Phys. Rev. Lett. **78**, 3414 (1997).

[98] N. Gisin and A. Peres, Phys.Lett A **162** 15 (1992).

[99] S. L. Braunstein, A. Mann and M. Revzen, Phys. Rev. Lett **68**, 3259(1992).

[100] D. M. Greenberger, M. A. Horne, A. Shimony and A. Zeilinger, Am. J. Phys **58**, 1131 (1990); N. D. Mermin, Am. J. Phys **58**, 731 (1990).

[101] N. D. Mermin, Phys. Rev. Lett **65**, 1838 (1990); D. Home and A. S. Majumdar, Phys. Rev. A **52**, 4959 (1995); A. Chefles and S. M. Barnett, Phys. Rev. A **55**, 1721 (1997).

[102] D. P. DiVincenzo and A. Peres, Phys. Rev. A **55**, 4089 (1997).

[103] H. Buhrman, R. Cleve and W. van Dam, lanl eprint quant-ph/9705033, 1997 ; R. Cleve and H. Buhrman, lanl eprint quant-ph/9704026, 1997 .

[104] L. K. Grover, lanl eprint quant-ph/9704012, 1997.

[105] A. Karlsson, M. Koashi and N. Imoto, Phys. Rev. A **59**, 162 (1999); M. Hillery, V. Buzek and A. Berthiaume, Phys. Rev. A **59**, 1829 (1999); R. Cleve, D. Gottesman and H. K. Lo, Phys. Rev. Lett **83**, 648 (1999).

[106] M.A. Horne, A. Zeilinger and M. Zukowski, in *International Conference on Quantum Electronics* (Technical Digest Series 1992) Vol. 9, p. 162 ; H.Weinfurter , *private communication.*

[107] S. J. D. Phoenix, S. M. Barnett, P. D. Townsend, K. J. Blow, J. Mod. Opt.**42**, 1155(1995); P. D. Townsend, C. Marand, S. J. D. Phoenix, K. J. Blow and S. M. Barnett, Phil. Trans. Roy. Soc London A**354**, 805(1996); P. D. Townsend, Nature 385, 47 (1997).

[108] E. Biham, B. Huttner and T. Mor, Phys. Rev. A **54**, 2651 (1996).

[109] M. Zukowski, A. Zeilinger, M. A. Horne, and A. K. Ekert, Phys. Rev. Lett **71**, 4287 (1993).

[110] B. Yurke and D. Stoler, Phys. Rev. A **46**, 2229 (1992); B. Yurke and D. Stoler, Phys. Rev. Lett. **68**, 1251 (1992).

[111] A. Zeilinger, M. A. Horne, H. Weinfurter, and M. Zukowski, Phys. Rev. Lett **78**, 3031 (1997).

[112] M. Zukowski, A. Zeilinger and H. Weinfurter in *Fundamental Problems in Quantum Theory* vol. 755 Annals of the New York Academy of Sciences (Greenberger and Zeilinger Eds.) p. 91 (1995).

[113] H.-K. Lo and S. Popescu , lanl eprint quant-ph/9707038, 1997.

[114] C. H. Bennett and G. Brassard, in *Proceedings of IEEE International Conference on Computers, Systems and Signal Processing, Bangalore, India* (IEEE, New York, 1984), p. 175 ; C. H. Bennett, Phys. Rev. Lett **68**, 3121(1992); C. H. Bennett, F. Bessette, G. Brassard, L. Salvail and J. Smolin, J. Cryptol. **5**, 3 (1992); B. Huttner, N. Imoto, N. Gisin and T. Mor, Phys. Rev. A **51**, 1863 (1995).

[115] A. Barenco, C. H. Bennett, R. Cleve, D. P. Divincenzo, N. Margolus, P. Shor, T. Sleator, J. A. Smolin and H. Weinfurter, Phys. Rev. A **52**, 3457(1995); A. Barenco, Contemporary Physics **37**, 375(1996).

[116] N. J. Cerf, C. Adami and P. G. Kwiat, lanl eprint quant-ph/9706022, 1997.

[117] J. I. Cirac and P. Zoller, Phys. Rev. Lett. **74**, 4091 (1995).

[118] N. A. Gershenfeld and I. L. Chuang, Science **275**, 350 (1997).

[119] For a review see: M.B. Plenio and V. Vedral, Cont. Phys. **39**, 431 (1998); For a popular account see: A. Zeilinger, Phys. World **11**, 35 (1998).

[120] K. Mattle, H. Weinfurter, P. G. Kwiat and A. Zeilinger, Phys. Rev. Lett. **76**, 4656 (1996).

[121] D. Bouwmeester, J-W. Pan, K. Mattle, M. Eibl, H. Weinfurter, and A. Zeilinger, Nature (London) **390**, 575 (1997).

[122] D. Boschi, S. Branca, F. De Martini, L. Hardy and S. Popescu, Phys. Rev. Lett. **80**, 1121 (1998).

[123] A. Furusawa, *et al*, Science **282**, 706 (1998); S. L. Braunstein and H. J. Kimble, Phys. Rev. Lett. **80**, 869 (1998).

[124] J-W. Pan, D. Bouwmeester, H. Weinfurter, and A. Zeilinger, Phys. Rev. Lett. **80**, 3891 (1998).

[125] P. G. Kwiat, K. Mattle, H. Weinfurter, A. Zeilinger, A. V. Sergienko, and Y. H. Shih, Phys. Rev. Lett. **75**, 4337 (1995).

[126] N. Gisin, Phys. Lett. A **210**, 151 (1996).

[127] P. G. Kwiat, E. Waks, A. G. White, I. Appelbaum, and P. H. Eberhard, LANL eprint quant-ph/9810003.

[128] N. Lutkenhaus, J. Calsamiglia and K-A. Suominen, LANL e-print quant-ph/9809063; L. Vaidman and N. Yoran, LANL e-print quant-ph/9808043.

[129] P. G. Kwiat and H. Weinfurter, Phys. Rev. A **58**, R2623 (1998).

[130] A. Kent, Phys. Rev. Lett. **81**, 2839 (1998); N. Linden, S. Massar, and S. Popescu, Phys. Rev. Lett. **81**, 3279 (1998).

[131] A. Barenco and A. K. Ekert, J. Mod. Opt. **42**, 1253 (1995).

[132] P. Hausladen, R. Jozsa, B. Schumacher, M. Westmoreland and W. K. Wootters, Phys. Rev. A **54**, 1869 (1996).

[133] A. S. Kholevo, Probl. Peredachi Inf **9**, 177 (1973) [A. S. Kholevo, Problems of Information Transmission, **9**, 177 (1973)]; The Holevo bound was first conjectured by: J. P. Gordon, in *Quantum Electronics and Coherent light*, Proceedings of the International School of Physics "Enrico Fermi," Course XXXI, edited by P. A. Miles (Academic, New York, 1964), pp. 156-181; L. B. Levitin, *Information, Complexity and Control in Quantum Physics*, edited by P. A. Miles (Academic, New York, 1964), pp. 111-115.

[134] M. Ohya, Rep. Math. Phys. **27**, 19 (1989); F. Hiai and D. Petz, Comm. Math. Phys. **143**, 99 (1991); M.J. Donald, Comm. Math. Phys. **105**, 13 (1986); M.J. Donald, Math. Proc. Camb. Phil. Soc., **101**, 363 (1987).

[135] A. S. Holevo, IEEE Trans. Info. Th. **44**, 269 (1998); B. Schumacher and M.D. Westmoreland, Phys. Rev. A, **56**, 131 (1997).

[136] S. Popescu and D. Rohrlich, Phys. Rev. A **56**, R3319 (1997).

[137] R. Horodecki, P. Horodecki and M. Horodecki, Phys. Lett. A **200**, 340 (1995).

[138] E. M. Rains, *Entanglement purification via separable superoperators*, LANL e-print quant-ph/9707002.

[139] W. K. Wootters, Phys. Rev. Lett. **80**, 2245 (1998).

[140] M. Horodecki, P. Horodecki and R. Horodecki, Phys. Rev. Lett. **78**, 574 (1997).

[141] M. B. Plenio and P. L. Knight, Phys. Rev. A **53**, 2986 (1996); Proc. Roy. Soc. A **453**, 2017 (1997).

[142] C. Cabrillo *et al.*, Phys. Rev. A **59**, 1025 (1999).

[143] M. B. Plenio *et al.*, Phys. Rev. A **59**, 2468 (1999); See also, G. J. Yang *et al.*, Phys. Rev. A **59**, 4012 (1999).

[144] K. M. Gheri *et al.*, Fortsch. Phys. **46**, 401 (1998).

[145] G. J. Milburn and S. L. Braunstein, LANL e-print quant-ph/9812018; T. C. Ralph and P. K. Lam, Phys. Rev. Lett. **81**, 5668 (1998); C. J. Villas-Bôas *et al.*, LANL e-print quant-ph/9904028; M. S. Zubairy, Phys. Rev. A **58**, 4368 (1998).

[146] J. I. Cirac and A. S. Parkins, Phys. Rev. A **50**, R4441 (1994); M. H. Y. Moussa, Phys. Rev. A **55**, R3287 (1997); S.-B. Zheng and G.-C. Guo, Phys. Lett. A **232**, 171 (1997).

[147] J. I. Cirac *et al.*, Phys. Rev. Lett. **78**, 3221 (1997); S. J. van Enk *et al.*, Phys. Rev. A **59**, 2659 (1999).

[148] T. Pellizzari, Phys. Rev. Lett. **79**, 5242 (1997);

[149] S. J. van Enk *et al.*, Phys. Rev. Lett. **78**, 4293 (1997).

[150] S. J. van Enk *et al.*, Phys. Rev. Lett. **79**, 5178 (1997); Science **279**, 205 (1998); A. Sørensen and K. Mølmer, Phys. Rev. A **58**, 2745 (1998).

[151] A. S. Parkins *et al.*, Phys. Rev. A **51**, 1578 (1995).

[152] M. B. Plenio and P. L. Knight, Rev. Mod. Phys. **70**, 101 (1998).

[153] H.-J. Briegel *et al.*, Phys. Rev. Lett. **81**, 5932 (1998).